

GEMS & GEMOLOGY

VOLUME XXXV

SPRING 1999



THE QUARTERLY JOURNAL OF THE GEMOLOGICAL INSTITUTE OF AMERICA

GEMS & GEMOLOGY

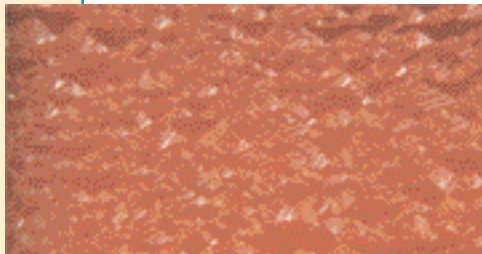
SPRING 1999

VOLUME 35 NO. 1

T A B L E O F C O N T E N T S



pg. 5



pg. 25



pg. 31

pg. 57



EDITORIALS

- 1 **Symposium '99—You Can't Afford to Miss It!**
Alice S. Keller
- 2 **The Dr. Edward J. Gübelin Most Valuable Article Award**

FEATURE ARTICLES

- 4 **The Identification of Zachery-Treated Turquoise**
Emmanuel Fritsch, Shane F. McClure, Mikhail Ostrooumov, Yves Andres, Thomas Moses, John I. Koivula, and Robert C. Kammerling
- 17 **Some Diagnostic Features of Russian Hydrothermal Synthetic Rubies and Sapphires**
Karl Schmetzer and Adolf Peretti
- 30 **The Separation of Natural from Synthetic Colorless Sapphire**
Shane Elen and Emmanuel Fritsch

REGULAR FEATURES

- 42 **Gem Trade Lab Notes**
- 47 **Gem News**
- 61 **Gems & Gemology Challenge**
- 63 **Book Reviews**
- 65 **Gemological Abstracts**
- 77 **Guidelines for Authors**

ABOUT THE COVER: For thousands of years, turquoise has been used in jewelry and other items of adornment. In recent times, much of this material has been treated to improve its appearance and wearability. In particular, a relatively new, proprietary treatment has been used to enhance millions of carats of turquoise for the last decade. Referred to here as the "Zachery treatment," it cannot be detected by standard gemological techniques. The lead article in this issue describes the properties of this treated turquoise and discusses methods to identify it. All of the turquoise shown here, which is from the Sleeping Beauty mine in Arizona, has been treated by this method. The necklace is composed of 12.5 mm turquoise beads separated by diamond rondelles, with a white gold clasp containing 1.65 ct of diamonds. The carving measures 30 × 60 mm. Courtesy of Roben Hagobian, Glendale, California.

Photo © Harold & Erica Van Pelt—Photographers, Los Angeles, California.

Color separations for Gems & Gemology are by Pacific Color, Carlsbad, California. Printing is by Fry Communications, Inc., Mechanicsburg, Pennsylvania.

© 1999 Gemological Institute of America All rights reserved. ISSN 0016-626X

Symposium '99

You Can't Afford to Miss It!

For months now, GIA has been talking about the Third International Gemological Symposium. You've received a brochure.

You've seen ads in this and other publications. You've read the articles and heard about it from your friends. San Diego, June 21-24, 1999, 'Meeting the Millennium.' What is it really, and why am I, as editor of *Gems & Gemology*, urging you to go?

To answer the latter question first: for your own good. GIA has held only two other international symposia in the last 17 years. Each brought together the most important people in the international gem and jewelry community both as participants and attendees. Many of the topics introduced at the 1991 Symposium set the stage for tackling the gemological challenges of the 1990s, such as fracture-filled and synthetic diamonds, jade identification, pearl research, and emerald treatments. The technological advances of the past decade have been mind boggling—and, as a jeweler or gemologist, you are accountable to your customers to know how to address new synthetics, treatments, and deceptive practices as soon as they appear in the market. You also need to know the new marketing practices that work in the U.S. and worldwide, must be able to anticipate periods of economic instability in the diamond and colored stone markets, and must be aware of new and declining localities for gem materials. The 1999 Symposium will give you more of the tools you *must* have to operate successfully in our industry.

So, exactly what is Symposium? The core of the program is a series of concurrent speaker and panelist sessions that will address such topics as sources, production, and economics and manufacturing for both diamonds and colored stones. Also included are sessions on pearls, jewelry design, and estate jewelry, as well as—of course—the

identification of new treatments, synthetics, and simulants. Entering the 21st century, suppliers and retailers alike are looking for new marketing opportunities, both via conventional retail channels and through such electronic media as television and the Internet; all of these will be addressed. New to Symposium this year are the four War Rooms—on appraisals, disclosure, branding, and diamond cut—where attendees and panelists will interact to find solutions to such pressing issues as cut grading and the new L.K.I.-G.E. 'processed' diamonds.

But Symposium offers even more. It offers 70-plus poster sessions with in-depth introductions to specific new techniques, instruments, localities, and the like.

It offers the insight of four prominent nonindustry experts in the areas of marketing, technology, the economy, and ethics for the new millennium. It offers powerful advice from world business leaders such as Peter Ueberroth and the senior statesman of the diamond industry, Maurice Tempelman.

And Symposium is not just about learning. Symposium is also about meeting old friends and making new ones, while enjoying superb food and entertainment in one of the world's most beautiful settings: the Hyatt Regency, on San Diego Bay. The opening reception is at Embarcadero park, right on the water; Tuesday follows with a visit to the 'Nature of Diamonds' exhibit at the San Diego Natural History Museum, and a buffet under the stars. On Wednesday, there will be a pearl reception and fashion show. Symposium closes with Italian cuisine and a unique salute to the history of the Italian jewelry industry, 'Arte in Oro.'

Please, take my word for it. There is nothing like it. And there will be nothing like it for many years to come. The June 1999 International Gemological Symposium is one event you truly can't afford to miss.



Peter Ueberroth

The Dr. Edward J. Gübelin Most Valuable Article Award

The readers of *Gems & Gemology* have voted, and your choices for the Dr. Edward J. Gübelin Most Valuable Article Award for best article published in 1998 reflect the increasing importance of advanced research in the practice of gemology. Receiving first place is "Modeling the Appearance of the Round Brilliant Cut Diamond: An Analysis of Brilliance" (Fall 1998), in which the authors used computer modeling to tackle one of the most complex and controversial issues in the trade, the evaluation of diamond cut. Second place goes to "Characterizing Natural-Color Type IIb Blue Diamonds" (Winter 1998), a comprehensive study of blue diamonds and their color classification. The third-place winner, "Separating Natural and Synthetic Rubies on the Basis of Trace-Element Chemistry" (Summer 1998), used semi-quantitative chemical analysis to address a critical gem identification problem.

The authors of these three articles will share cash prizes of \$1,000, \$500, and \$300, respectively. Following are photographs and brief biographies of the winning authors.

Congratulations also to Ron Lotan of Ramat Gan, Israel, whose ballot was randomly chosen from the many entries to win a five-year subscription to *Gems & Gemology*.



Scott Hemphill



Ilene M. Reinitz



Mary L. Johnson



James E. Shigley

First Place

Modeling the Appearance of the Round Brilliant Cut Diamond: An Analysis of Brilliance

T. Scott Hemphill, Ilene M. Reinitz, Mary L. Johnson, and James E. Shigley

Scott Hemphill, a GIA research associate, has been programming computers for the past 30 years. Mr. Hemphill received a B.Sc. in engineering and an M.Sc. in computer science from the California Institute of Technology. **Ilene Reinitz** is manager of Research and Development at the GIA Gem Trade Laboratory (GIA GTL), New York, and an editor of Gem Trade Lab Notes. Dr. Reinitz, who has co-authored many articles for *G&G* and other publications, received her Ph.D. in geochemistry from Yale University. **Mary Johnson** is manager of Research and Development at GIA GTL, Carlsbad, and editor of the Gem News section. A frequent contributor to *G&G*, she received her Ph.D. in mineralogy and crystallography from Harvard University. **James Shigley** is director of GIA Research in Carlsbad. Dr. Shigley, who has been with GIA since 1982, received his Ph.D. in geology from Stanford University. He has written numerous articles on natural, treated, and synthetic gems.

Second Place

Characterizing Natural-Color Type IIb Blue Diamonds

John M. King, Thomas M. Moses, James E. Shigley, Christopher M. Welbourn, Simon C. Lawson, and Martin Cooper

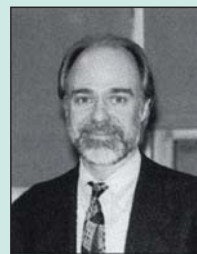
John King is laboratory projects officer at GIA GTL, New York. Mr. King received his M.F.A. from Hunter College, City University of New York. With 20 years of laboratory experience, he frequently lectures on colored diamonds and laboratory grading procedures. **Thomas Moses**, vice president of Identification Services at GIA GTL, New York, attended Bowling Green University in Ohio before he entered the jewelry trade more than 20 years ago. He is a prolific author and an editor of the Gem Trade Lab Notes section. Please see the first-place entry for biographical information on **James Shigley**. **Christopher Welbourn** is head of the Physics and Patents Departments at De Beers DTC Research Centre in Maidenhead, United Kingdom. Dr. Welbourn, who joined the De Beers Research Centre in 1978, holds a Ph.D. in solid state physics from the University of Reading. **Simon Lawson** is a research scientist in the Physics Department of the De Beers DTC Research Centre. He obtained his Ph.D. in optical spectroscopy of diamond at King's College London and has published numerous papers on this topic. **Martin Cooper**, who also joined De Beers more than 20 years ago, is research director at the De Beers DTC Research Centre. Mr. Cooper received his B.Sc. in physics from the University of London and his M.Sc. in materials science from Bristol University.

Third Place

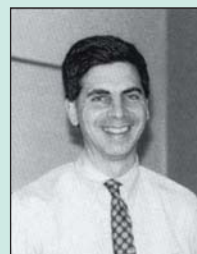
Separating Natural and Synthetic Rubies on the Basis of Trace-Element Chemistry

Sam Muhlmeister, Emmanuel Fritsch, James E. Shigley, Bertrand Devouard, and Brendan M. Laurs.

Sam Muhlmeister is a research associate with GIA GTL, Carlsbad. Born in Germany, Mr. Muhlmeister received bachelor's degrees in physics and mathematics from the University of California at Berkeley. **Emmanuel Fritsch** is professor of physics at Nantes University, France. Dr. Fritsch, who received his Ph.D. from the Sorbonne in Paris, has published numerous articles in *G&G*. **James Shigley** is profiled in the first-place entry. **Bertrand Devouard** is assistant professor of mineralogy at Blaise Pascal University in Clermont-Ferrand, France. Dr. Devouard has a Ph.D. in mineralogy and crystallography from Aix-Marseille University. His research specialties are microstructures and high spatial-resolution analytical techniques in minerals. **Brendan Laurs**, senior editor of *Gems & Gemology*, holds a B.Sc. in geology from the University of California at Santa Barbara and an M.Sc. in geology from Oregon State University. Prior to joining GIA, Mr. Laurs was an exploration geologist specializing in colored gems.



John M. King



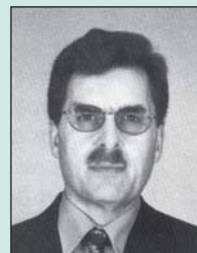
Thomas M. Moses



C.M. Welbourn



Simon C. Lawson



Martin Cooper



Brendan M. Laurs and Sam Muhlmeister



Emmanuel Fritsch Bertrand Devouard

THE IDENTIFICATION OF ZACHERY-TREATED TURQUOISE

By Emmanuel Fritsch, Shane F. McClure, Mikhail Ostrooumov, Yves Andres, Thomas Moses, John I. Koivula, and Robert C. Kammerling

Over the last 10 years, millions of carats of turquoise have been enhanced by a proprietary process called the Zachery treatment. Tests show that this process effectively improves a stone's ability to take a good polish and may or may not improve a stone's color. It also decreases the material's porosity, limiting its tendency to absorb discoloring agents such as skin oils. Examination of numerous samples known to be treated by this process revealed that Zachery-treated turquoise has gemological properties that are similar to those of untreated natural turquoise, and that the treatment does not involve impregnation with a polymer. Most Zachery-treated turquoise can be identified only through chemical analysis—most efficiently, by EDXRF spectroscopy—as it contains significantly more potassium than its untreated counterpart.

ABOUT THE AUTHORS

Dr. Fritsch (fritsch@cirs-immn.fr) is professor of Physics at the University of Nantes, France. Mr. Moses is vice president for Research and Identification at the GIA Gem Trade Laboratory in New York. The late Mr. Kammerling was vice-president for Research and Identification, Mr. McClure is manager of Identification Services, and Mr. Koivula is chief research gemologist at the GIA Gem Trade Laboratory in Carlsbad. Dr. Ostrooumov is professor at the St. Petersburg School of Mines, Russia, and currently professor at the Universidad de Michoacán de San Nicolás de Hidalgo, Michoacán, Mexico. Dr. Andres is assistant professor at the Nantes School of Mines, in Nantes.

Please see acknowledgments at end of article. Gems & Gemology, Vol. 35, No. 1, pp. 4–16 © 1999 Gemological Institute of America

Turquoise is one of the oldest gem materials known. Its use in jewelry and for personal adornment can be traced back 70 centuries, to ancient Egypt (Branson, 1975). Today it is popular in fine jewelry worldwide (see cover and figure 1) as well as in various cultures, most notably among Native American groups of the southwestern United States (figure 2). However, because the supply of high-quality turquoise is limited, and because this material readily accepts many treatments, most turquoise is adulterated (Liddicoat, 1987). Cerville (1985) even states that turquoise *must* be treated, to avoid the change in color caused by absorption of substances such as cosmetics, sweat, or grease into this typically porous material. The most common type of turquoise treatment is impregnation with an organic material. Such treatment can be readily detected by observation with a microscope, use of a hot point (Liddicoat, 1987), or infrared spectroscopy (Dontenville et al., 1986). However, there is a relatively new, proprietary turquoise treatment, commonly known in the trade as “enhanced turquoise” (again, see figures 1 and 2), which cannot be detected by any of these classical methods. The purpose of this article is to describe the properties of this treated turquoise, with the specific intent of offering a method for its identification.

BACKGROUND

At the 1988 Tucson show, one of the authors (RCK) was told that a new type of treated turquoise had been marketed for at least six months under the name “Zacharia-treated turquoise.” This enhancement was reportedly done with chemicals such as copper sulfate (letter from Pat Troutman to RCK, February 24, 1988). Some of the material was being sold through R. H. & Co. Inc. in Glendale, California. Inquiries to R. H. & Co. were answered by Roben Hagobian. He stated that US\$1.5 million had been spent on developing this process, and that the treatment could not be detected. He also specified that it was not called “Zacharia treat-

Figure 1. These pieces illustrate some of the fine turquoise jewelry and fashioned goods that are currently in the marketplace.

All of these pieces have been fashioned from Zachery-treated turquoise from the Sleeping Beauty mine. The beads in the top necklace are 13 mm in diameter; the heart-shaped pendant is 35 mm wide; the cabochons in the earrings each measure 15 × 20 mm; and the larger stones in the rings are about 12 mm in largest dimension. Courtesy of Roben Hagobian; photo © Harold & Erica Van Pelt.



ment;" rather, that name probably referred to a scientist named Zachery who actually developed the procedure. Mr. Hagobian could not provide any details on the method himself, as he only provided the stones to be treated and got them back enhanced. At that time, we were also informed (through a letter dated June 23, 1989, from Pat Troutman to Loretta Bauchiero of GIA) that turquoise that was color-enhanced by this treatment might fade over time. No other information was made available to us, however, and our efforts to obtain additional samples and data were unsuccessful until recently.

At the end of 1996, we inadvertently encountered new information about the treatment in the course of another investigation. While researching polymer-impregnated turquoise, we were told of a company that was treating turquoise by a method that could not be detected. We subsequently learned that the material was being treated and marketed by Sterling Foutz of Sterling Products, Phoenix, Arizona. At the 1997 Tucson show, two of the authors (SFM and EF) met with Mr. Foutz, who agreed to supply a large number of treated samples from known turquoise mines around the world, as well as some untreated natural material from a

number of these localities. Mr. Foutz told us that the process was invented by James E. Zachery, an entrepreneurial electrical engineer who "grew up" in the turquoise trade. It stemmed from a desire to improve the properties of turquoise without using artificial additives such as plastic. The key advantages of this treatment, according to Mr. Foutz, are that the treated stones take a better polish and are more resistant to "oxidation" or discoloration over time, apparently due to a significant decrease in the porosity of the turquoise. They can also apply the same process to produce a greater depth of color in the turquoise. More than 10 million carats of turquoise have been treated by this process since it was first invented in the late 1980s; Roben Hagobian (pers. comm., 1999) noted that in 1998 alone he had 1.2 million carats of turquoise enhanced by the Zachery process.

Mr. Foutz reported that the treatment process takes approximately three to six weeks, and that no organic or inorganic colorants or organic impregnations are used. Because the process is proprietary, Mr. Foutz did not provide specifics of the actual technique and asked us not to use the samples he supplied to research the precise technique. He did add, though, that the process only works on medi-

TABLE 1. Turquoise samples studied by gemological testing and EDXRF analysis.^a

Description	No. of samples	Sample no.	Year acquired	Color	Zachery treated?	FTIR data?	Size (weight or max. dim.)	Comments
Sample Sets								
"Emerald Valley" ^b	2	220a-b	1998	Whitish green; green	No – 1 Yes – 1	No	21 mm 30 mm	Rough, sawn in half; cabochons also made
	2	221a-b	1998	Green	No – 1 Yes – 1	No	34 mm 20 mm	Rough, sawn in half; cabochons also made
	2	222a-b	1998	Green	No – 1 Yes – 1	No	40 mm 34 mm	Rough, sawn in half; cabochons also made
Sleeping Beauty, AZ ^c	4	225a-d	1998	Blue	Yes – 4	No	11.22-18.28 ct	Cabochons, sawn in half; surface treated only (a), throughout (b,c), throughout + surface (d)
Sleeping Beauty, AZ ^d	4	231a-d	1998	Blue	No - 1 Yes - 3	No	18-34 mm	Rough, polished slabs: untreated (a); treated throughout (b), surface treated (c), throughout and surface (d)
Other Samples								
"Blue Bird" ^e	3	164-166	1997	Med. blue	All samples	All samples	18-24 mm	Rough w/ matrix, polished; 166 had a partial blue rim
China	4	362 155-157	GIA 1997	Blue	No – 1 Yes – 3	No – 1 Yes – 3	13 mm 21-23 mm	Rough, sawn and polished Rough w/ matrix, polished
"Emerald Valley"	4	158-160 170	1997	Green	All samples; 2 with no evidence ^g	All samples	23-36 mm	Rough w/ matrix, polished; rough, sawn and polished
Mexico	3	152-154	1997	Blue, sl. gr. blue	All samples	All samples	16-22 mm	Flat fragment w/ matrix, polished; rough, polished
Nevada (unspecified)	1	TQE4B	CRG	Greenish blue	No	Yes	11 mm	Rough, polished
Nevada Fox, NV	3	161-163	1997	Green-blue	All samples	All samples	17-21 mm	Rough w/ matrix, polished; rough, polished
Nevada Smith, NV	3	149-151	1997	Blue	All samples	All samples	22-24 mm	Rough w/ matrix, polished; rough, polished
Persia	1	13925	GIA	Blue	No	No	28.78 ct	Oval cabochon
Sleeping Beauty, AZ	5	141-145	1997	Blue	No – 2 Yes – 3	All samples All samples	15-21 mm	Rough, sawn and polished— all with blue rim, less pronounced on untreated
Sleeping Beauty, AZ	2	229-230	1998	Blue	No	No	5.67, 5.86 ct	Beads
"Thunder Blue" ^f (China)	3	167-169	1997	Blue	All samples	All samples	22-23 mm	Rough w/ matrix, polished
Turquoise Mtn., AZ	3	146-148	1997	Sl. gr. blue	All samples	All samples	21-27 mm	Rough ± matrix, broken; 1 polished, 2 unpolished
U.S. (unspecified)	1	172	EF	Blue	No	Yes	19 mm	Rough, sawn and polished
Utah (unspecified)	1	171	EF	Blue	No	Yes	22 mm	Rough w/ matrix, polished
Uzbekistan	1	OST1	EF	Blue	No	Yes	20 mm	Flat slab w/ matrix, polished
Unspecified locality	6	ZTT1-6	1988-89	Blue	All samples; 1 showed no evidence	Yes – 4 No – 2	0.49-4.39 ct	Cabochons – 5 (1 w/ matrix); bead – 1

^a All samples were tested for refractive index (by the spot method), specific gravity (except Uzbekistan sample OST1, which had too much matrix), long- and short-wave UV radiation, visible spectrum (as seen with a hand-held spectroscope), and response to a thermal reaction tester. EDXRF chemical analysis also was performed on all samples. Abbreviations: max. dim. = maximum dimension, CRG = Centre de Recherches Gemmologiques Jean-Pierre Chenet (University of Nantes) collection, GIA = GIA collection, EF = Emmanuel Fritsch collection, gr. = greenish, sl. = slightly, med. = medium, w/ = with.

^b Refers to distinctly green turquoise from China, Mexico (Baja California), or the U.S. (New Mexico or Crescent Valley, Nevada).

^c One surface-treated cabochon was analyzed by electron microprobe, before and after exposure to oxalic acid solution.

^d All four slabs were analyzed by electron microprobe.

^e Refers to medium blue turquoise from Mexico or the U.S. (Nevada or Arizona–Sleeping Beauty mine).

^f The name given to turquoise from China by a particular supplier.

^g These samples were represented as treated, but they showed no K peak with EDXRF.

um- to high-grade material; low-quality, chalky turquoise will not enhance successfully. Also, several different results are possible with the same basic treatment process, with some adjustments for material from different mines. One is the treatment of the stone throughout without affecting the color of the original material. This approach is usually used on rough, and it is done to decrease the porosity of the turquoise and improve its ability to take a good polish. After a stone has been cut from such rough, it can be treated again to improve its color. This second treatment, which has a relatively shallow penetration, produces a darker, more saturated hue. A third scenario is to treat a previously untreated cut turquoise with the near-surface process both to improve its color and decrease its porosity.

In 1998, we received a letter from Mr. Zachery, who provided additional information regarding the nature of the treatment. According to his letter, "the enhancement process evolved from serious scientific attempts to duplicate the environment that allowed the famous Kingman high-grade turquoise to be deposited amid large potassium feldspar beds. . . . Although wholesale deposition of magnificent specimens did not occur, the microcrystalline structure of almost any specimen could be perfected. . . ." He wrote that "no dyes of any kind, either organic or inorganic, have been used; . . . the normal color producing metallic ions found in natural turquoise, such as copper or iron, have not been added. . . ." and that "any environments wet or dry that may have facilitated the enhancement procedure have not contained any of the aforementioned coloring ions, nor have any electrodes which contain these elements been employed." Moreover, he wrote that this material "has not been impregnated with plastic" or "with any wax, oil or lacquer whether natural or synthetic." He added his belief that "the principles involved in the Zachery process are widely applicable to other porous or penetrable gems such as beryls and opals."

Mr. Zachery recommended the phrase "microcrystalline structurally enhanced by the Zachery process" to describe material treated in this fashion. For the sake of simplicity, we will refer to this product as "Zachery-treated turquoise." For the remainder of this article, this term and the term *treated turquoise* will be used interchangeably to refer to this process.



Figure 2. Turquoise jewelry has long been popular with Native Americans from the Southwestern states. Today, much of this turquoise is also treated by the proprietary Zachery process. Courtesy of Sterling Foutz; photo by Maha DeMaggio.

MATERIALS AND METHODS

We performed comprehensive testing on a total of 58 samples (see table 1): 16 cabochons (four untreated, 12 treated), three beads (two untreated, one treated), two unpolished pieces of rough (both treated), and 37 slabs or polished pieces of rough (eight untreated, 29 treated). The fashioned samples ranged from 0.49 ct to 28.78 ct, and the rough samples ranged up to 4 cm in maximum dimension. The polished surface on the rough samples was flat or slightly rounded.

The samples in table 1 are designated by their geographic origin or color variety (as represented by Mr. Foutz). Untreated samples were from China, Persia, Uzbekistan, and the U.S. (Arizona—Sleeping Beauty mine, Nevada, Utah, and an unspecified locality). Treated samples were from China (including material represented as "Thunder Blue"), Mexico, and the U.S. (Arizona—Sleeping Beauty mine and the Turquoise Mountain mine near Kingman; Nevada—Nevada Fox and Nevada Smith veins at the Fox mine in Crescent Valley). Six treat-

ed samples were from unspecified localities. The color varieties were designated as “Blue Bird” (three treated samples) and “Emerald Valley” (three untreated and seven treated samples). “Blue Bird” refers to medium blue turquoise; these samples could be from Mexico or the U.S. (Nevada or Arizona—Sleeping Beauty mine). “Emerald Valley” refers to turquoise with a distinctly green color; these samples could originate from China, Mexico (Baja California), or the U.S. (New Mexico or Crescent Valley, Nevada).

To test the durability and cutting performance of the treated material, we obtained from Mr. Foutz three rough samples that represented different qualities of “Emerald Valley” turquoise. Each sample was cut in half; one half was treated by the Zachery process (the precise treatment was not specified, but the same type was used on all), and the other was left untreated (figure 3). Subsequently, we had a cabochon fashioned from each half to compare both how well the treated and untreated materials responded to the cutting wheel and the relative quality of their polish. To test the effectiveness of the treatment in decreasing the porosity of the material, we cut fragments of the treated and untreated samples in half, and immersed one half of each in Johnson’s® baby oil for a total of six days. The samples were removed from the oil and examined regularly during this period.

To characterize turquoise with different treatment types, we asked Mr. Foutz to treat a series of slabs from the same piece of rough. A nodule from the Sleeping Beauty mine was cut into four slabs (figure 4), and the following samples were prepared: (1) untreated, (2) surface treated only with the color

enhanced,(3) treated throughout and left natural color, and (4) treated throughout and then surface treated to improve the color. This sample suite allowed us to make direct comparisons between the samples—before and after treatment, and between the different treatments—on a single piece of rough.

Also at our request, Mr. Foutz supplied four cabochons of treated Sleeping Beauty turquoise that we cut in half to observe changes in coloration. Two of these cabochons were treated throughout, one was surface treated only (with the color enhanced), and one was treated throughout and then surface treated to improve the color.

To investigate the color stability of the treated material, we took the three cabochons we had cut from the treated halves of the Emerald Valley treated-and-untreated specimens described above and sawed them in half. We placed one half of each sample in an Oriel 81150 solar simulator with a 300-watt xenon light source. This instrument creates an output emission that approximates the daylight spectrum at two times its normal intensity. We left the cabochons in the solar simulator for 164 hours, checking them at approximately 24 hour intervals. This is equivalent to approximately 328 hours of noon sunlight exposure. The second half of each cabochon was kept in the dark as a control.

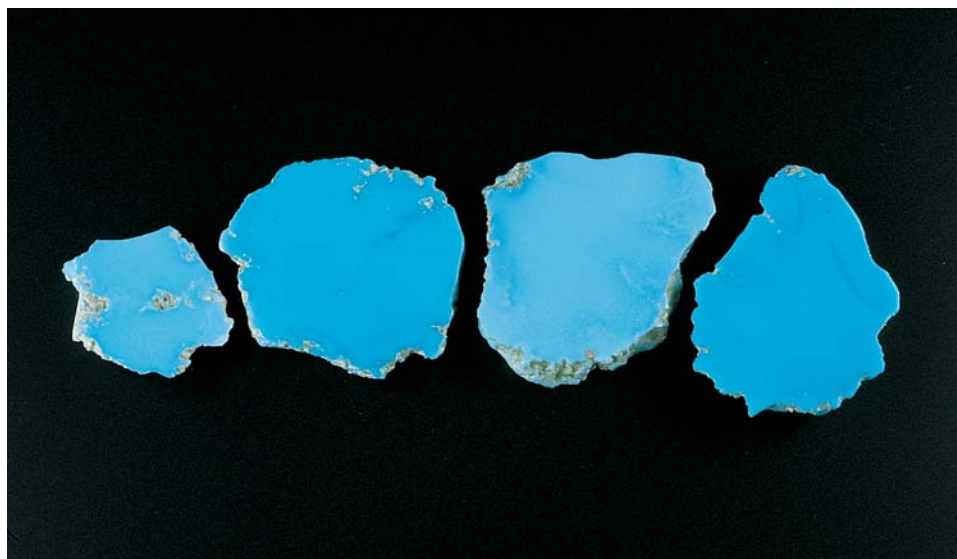
All of the samples were tested by the following methods, with the exception of the one untreated turquoise from Uzbekistan, for which specific-gravity testing would have been meaningless because it contained so much matrix material. Indices of refraction were measured by the spot method with a GIA Gem Instruments Duplex II refractometer. Specific gravity was determined by the hydrostatic

Figure 3. These samples (nos. 220–222a,b; 20–40 mm long) of rough “Emerald Valley” turquoise illustrate the results of treatment on different qualities of material. Half of each sample was treated by the Zachery process, and the other half was left untreated for comparison. Little change is visible in the treated half (top) of the high-quality (low-porosity) material in A. The medium-quality turquoise in B shows distinctly higher color saturation in the treated half (right sample), as does the low-quality material in C (also right). Photos by Maha DeMaggio.



Figure 4. These four slabs (nos. 231a-d; 18–34 mm wide) were cut from the same piece of Sleeping Beauty mine rough. Three of the slabs were treated by the Zachery process to obtain different results.

From left to right: (1) untreated, (2) surface treated only to enhance color, (3) treated throughout and left natural color, and (4) treated throughout and then surface treated to improve the color. Photo by Maha DeMaggio



method. We also observed the samples with a Beck prism spectroscope, and a long-wave (366 nm) and short-wave (254 nm) ultraviolet lamp unit (in a darkened room). We applied a standard thermal reaction tester (TRT) to check for the presence of a polymer.

We performed Fourier-transform infrared spectroscopy (FTIR) on most of the samples (see table 1) using a Nicolet 20 SXC instrument in the specular reflectance mode, at a resolution of 4 cm^{-1} , in the mid-infrared range $4000\text{--}400\text{ cm}^{-1}$. Semi-quantitative chemical analyses by energy-dispersive X-ray fluorescence (EDXRF) were obtained on all the study samples on either of two instruments: a Tracor Spectrace 5000 at GIA or an Oxford Instruments ED2000 at Nantes. The Spectrace 5000 had a rhodium anticathode, whereas the ED2000 had a silver anticathode. Instrumental artifacts caused by the machines, in particular the silver anticathode, were visible in the spectra collected; these could conceal the presence of small amounts of silicon or chlorine. The conditions were chosen to be appropriate for the simultaneous measurement of peaks for light elements (such as aluminum) through the end of the first series of transition elements (copper and zinc). For the Spectrace 5000, the analyses were performed in a vacuum, with no filter, and with a tube voltage of 15 kV and a livetime of 100 seconds. The same conditions were used for the ED2000, except for a tube voltage of 10 kV and a livetime of 120 seconds.

Dr. F. C. Hawthorne at the University of Manitoba, Canada, performed electron microprobe analyses on (1) all four slabs from the Sleeping

Beauty mine and (2) one of the color-treated Sleeping Beauty cabochons that had been cut in half and one half immersed in oxalic acid. Cross-sections of the slabs were analyzed to provide quantitative chemical data near the surface and within the core of each sample. The analyses were performed using a Cameca SX-50 microprobe with an accelerating voltage of 15 kV, sample current of 20 nA, and a beam spot size of 20 microns. Dr. Hawthorne also performed X-ray diffraction analysis, using transmission geometry, on one untreated and two of the treated slabs.

RESULTS

Effectiveness of the Treatment. The three green “Emerald Valley” samples for which one half was treated and the other half was left in its original state illustrate the potential influence of the process on various aspects of appearance, cuttability, and durability. Two of the treated halves were much more saturated than their untreated counterparts, and some areas of matrix were a darker brown. The somewhat chalky appearance of these pieces before treatment disappeared after treatment. The color of the third sample was unaffected by treatment.

As noted above, one of the advantages claimed for Zachery-treated turquoise is that it is easier to cut and takes a better polish. According to the cutter of the six cabochons fashioned from these treated and untreated halves of “Emerald Valley” rough, all of the treated material was easier to work in that it gave a cleaner cut that did not crumble or splinter along the sawn edge. Indeed, the cutter had difficulty keeping the lowest-quality untreated material



Figure 5. Cabochons were fashioned from the treated and untreated rough photographed in figure 3 so that we could compare the cuttability of the material. In each photo, the half fashioned from the treated piece of rough is shown on the right. Note especially the distinct improvement in luster in the treated stones, with the most pronounced difference seen in the lower-quality material (B and C). Photos by Maha DeMaggio.

from breaking up during sawing. The three Zachery-treated turquoise cabochons also took a better polish than the untreated material, with the lowest-quality turquoise showing the most pronounced difference (figure 5). In fact, the unusually high luster was somewhat superior to what one would normally expect from high-quality untreated turquoise.

Another advantage claimed for Zachery treatment is that it reduces the tendency of turquoise to absorb oil and/or grease (by decreasing the porosity). We tested this claim by immersing fragments of these same samples in baby oil (while retaining portions of these fragments as controls). Within a few minutes, we observed that more air bubbles were escaping from the untreated fragments, which indicates that they were more porous than their treated counterparts. After six days of immersion, the three treated fragments did not show any change in appearance, but their untreated counterparts became noticeably darker than the control samples. This illustrates that the treated turquoise has little or no tendency to absorb oil and grease, which would cause it to discolor over time, as does natural turquoise (Bariand and Poirot, 1985).

As noted earlier, some concern was expressed in the trade that Zachery-treated turquoise might fade over time. After exposure for 164 hours in a solar simulator, however, the three treated "Emerald Valley" cabochon halves did not show any fading or other change of appearance when compared to the control samples.

Gemological Properties. The samples ranged from blue through greenish blue to green (again, see table 1). The vast majority were the typical greenish blue color associated with turquoise. However, all of the samples labeled "Emerald Valley" were whitish green to green, as were two samples from Nevada Fox. Most of the rough samples showed various amounts of matrix admixture. On their natural,

unpolished surfaces, the rough samples also revealed the botryoidal morphology typical of turquoise.

In general, the treated samples had darker, more saturated colors than their untreated counterparts. These colors are slightly unnatural in appearance and can be used as an indication of treatment, even though the difference is subtle and would require some experience to discern. Of the four Sleeping Beauty slabs cut from the same piece of rough, the one that was not color treated remained the same color as the untreated slab, whereas the surfaces of the two color-treated samples were darker and slightly more saturated than the underlying material.

To determine if there was a visible penetration of color in the treated material, we sawed in half (and polished the sawn edges) of the four Sleeping Beauty cabochons of known treatment type. The color-treated cabochons showed a layer of darker color that was subtle but clearly visible (figure 6). The penetration depth ranged from approximately 0.2 to 0.5 mm in these specimens.

For all samples—both untreated and treated—the refractive index ranged from 1.60 to 1.62 (spot method). The specific gravity ranged from 2.61 to 2.74. These values are well within those reported for natural, untreated turquoise.

When examined with the hand spectroscope, all samples—again, both treated and untreated—showed the band at about 430 nm that is characteristic of turquoise. In addition, all samples luminesced a weak to moderate whitish blue to long-wave UV radiation and were inert to short-wave UV. None of the samples, whether natural or Zachery treated, showed any response to the thermal reaction tester.

When viewed with the gemological microscope, all samples revealed a typical turquoise structure with minor cavities and occasional pyrite and calcite inclusions. The treated samples did not reveal

any of the characteristics that are common to turquoise treated by more traditional methods (such as evidence of filler materials in surface-reaching fractures and cavities). We did not observe fillers in any of the Zachery-treated samples we examined.

In fact, there was only one distinctive difference visible in any of the treated samples—concentrations of color along fractures—and it was only visible in some of them. This was best illustrated in the treated slabs from Sleeping Beauty that were cut from the same piece of rough and then processed differently. We did not see any color concentrations along fractures in the untreated slab or two of the treated slabs. However, the slab that was first treated all the way through and then surface treated to improve its color showed distinct concentrations of dark blue along fractures (figure 7). The color concentrations were not confined to the fracture itself, but rather they also penetrated the turquoise on either side of the break. This is an important observation, since low-quality turquoise that is impregnated and dyed will often show concentrations of color along fractures, but those concentrations consist of a colored filler material and are confined to the fracture itself (figure 8). Either type of color concentration is unnatural and, in our experience, does not occur in untreated turquoise.

Infrared Spectroscopy. Reflectance infrared spectroscopy of natural and treated samples in the mid-infrared range produced similar spectra for both groups. Both showed major peaks at approximately 1125, 1050, and 1000 cm^{-1} , which represent vibrations of the PO_4 units; they did not show the peaks expected for polymer impregnation or organic compounds (for details, see Dontenville et al., 1986). These spectra also confirm that the samples tested were indeed natural, and not synthetic turquoise. The width of the peak, which was similar for both the untreated and Zachery-treated turquoise,



Figure 6. This cross section of a cabochon that was surface treated to improve color shows a narrow rim of more saturated color. The depth of this rim ranged from 0.2 to 0.5 mm in the samples we examined. Photomicrograph by Shane F. McClure; magnified 14 \times .

demonstrates that the crystallite size is within the same range for both products (see Fritsch and Stockton, 1987).

Energy-Dispersive X-ray Fluorescence Spectrometry. EDXRF analyses of all the untreated and treated samples demonstrated, as expected, the presence of all the major constituents of turquoise [$\text{CuAl}_6(\text{PO}_4)_4(\text{OH})_8 \cdot 5\text{H}_2\text{O}$] that could be detected with our instruments (figure 9): aluminum (Al), phosphorus (P), and copper (Cu). Iron (Fe), a common impurity in turquoise, was also detected in all samples. The height of the Fe peak correlated to the green component of the color (in pyrite- and iron-oxide-free samples); that is, the green samples showed the most intense Fe peaks. This is consistent with the report by Cervelle et al. (1985) that Fe^{3+} produces the yellow component of green turquoise. Sulfur (S) was occasionally detected; its signal was stronger in pieces with pyrite (FeS) inclusions. Traces of the common transition elements titanium, chromium, and vanadium were also pre-

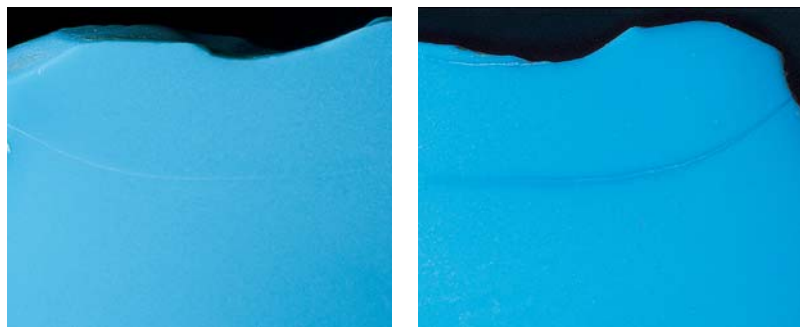


Figure 7. Blue color concentrations along fractures were seen in some of the color-treated samples. In these two slabs shown in figure 4, the sample that was treated but not color enhanced (left) shows no change in coloration along the fracture. However, the same fracture in the adjacent slab, which was color enhanced, shows an obvious color concentration (right). Photomicrographs by Shane F. McClure; magnified 10 \times .

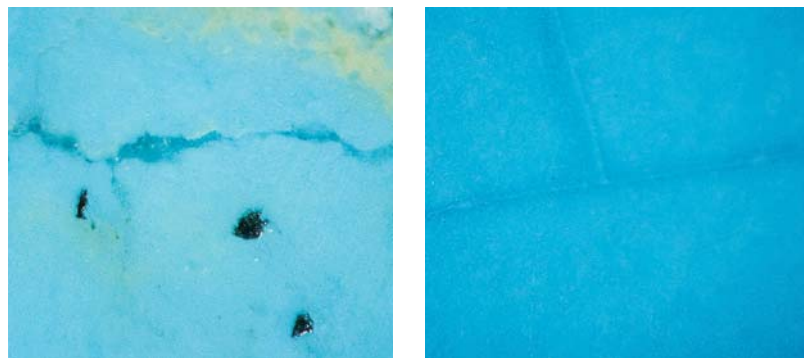


Figure 8. Color concentrations in Zachery-treated material look very different from those seen in turquoise impregnated with colored polymers. The color concentrations in the blue-polymer-filled stone (left) are restricted to the fractures. In the Zachery-treated stone (right) the color concentrations appear to diffuse into the stone adjacent to the fractures. Photomicrographs by Shane F. McClure; magnified 35 \times .

sent in some samples (both natural and treated). A small calcium (Ca) signal was present in all the natural, untreated samples; this Ca peak was sometimes accompanied by a separate potassium (K) peak, which was always smaller.

In general, the EDXRF spectra of the treated and untreated samples were similar, with one important exception: The potassium peak was much stronger in most of the treated samples than in the untreated ones, when this peak was compared to that of an element that is intrinsic to turquoise (such as phosphorus; figure 10). Although the height of the potassium peak varied from one treated piece to the next, in the vast majority of instances the amount of potassium in the treated turquoise was significantly greater than that recorded in the untreated samples.

EDXRF analyses of the four slabs cut from the same piece of Sleeping Beauty rough gave particularly interesting results in this regard. As originally recorded, the potassium contents of the untreated sample as well as the two samples that had been color treated were strong when compared to the phosphorus peak. Yet the slab that had been treated without changing its color did not show elevated potassium. Closer inspection of the untreated sample revealed a cavity in the center of the slab, which must have contained some potassium-bearing compound. When the untreated sample was analyzed in an area away from the cavity, the potassium content was much smaller. Electron microprobe analyses of these four slabs were consistent with the later EDXRF results. In addition, systematic variations in the total wt.% oxides measured by microprobe analysis in these four slabs indicated a decrease in porosity with increasing intensity of treatment.

EDXRF analyses were also performed on the four Sleeping Beauty cabochons that were cut in half, with one half treated for a specific result and the other half left untreated. As was the case with the slabs, the two stones that were color treated showed elevated potassium, and the two cabochons that

were treated without producing any effect on their color did not.

Because the three non-color-treated samples described above (the slab and the two cabochons) lacked elevated potassium contents, we decided to test some additional samples that we knew were similarly treated (i.e., for durability only, not for color) to determine if the increase in potassium occurred only in color-treated stones. Mr. Foutz loaned us 13 samples of irregular slabs from China, Mexico, and Arizona that he had treated specifically for durability/porosity but not for color. These irregular slabs ranged from green to blue to very light blue (a color the turquoise trade sometimes calls "white" turquoise) and had various amounts of matrix present. We specifically requested specimens of varying qualities and localities different from those of the three stones described earlier, which were all high-quality material from the Sleeping Beauty mine. Of these 13 treated samples, 10 showed significantly elevated potassium levels. The other three showed much smaller K peaks, but these peaks were still slightly stronger than those in the untreated turquoise we have tested. These results suggest that the porosity of the starting material helps determine whether or not a piece of treated turquoise will show elevated potassium with EDXRF. It was primarily the high-quality treated material that lacked elevated potassium levels, possibly because such material is less porous.

Three of the treated samples in table 1 (one high quality, and the other two medium quality) also lacked the K peak in their EDXRF spectra.

X-Ray Diffraction. Analyses of the one untreated and two of the treated Sleeping Beauty slabs revealed no significant differences among the three samples. This proves that no new minerals (other than, possibly, turquoise) were precipitated in the treated turquoise, and the cell dimensions remained unchanged.

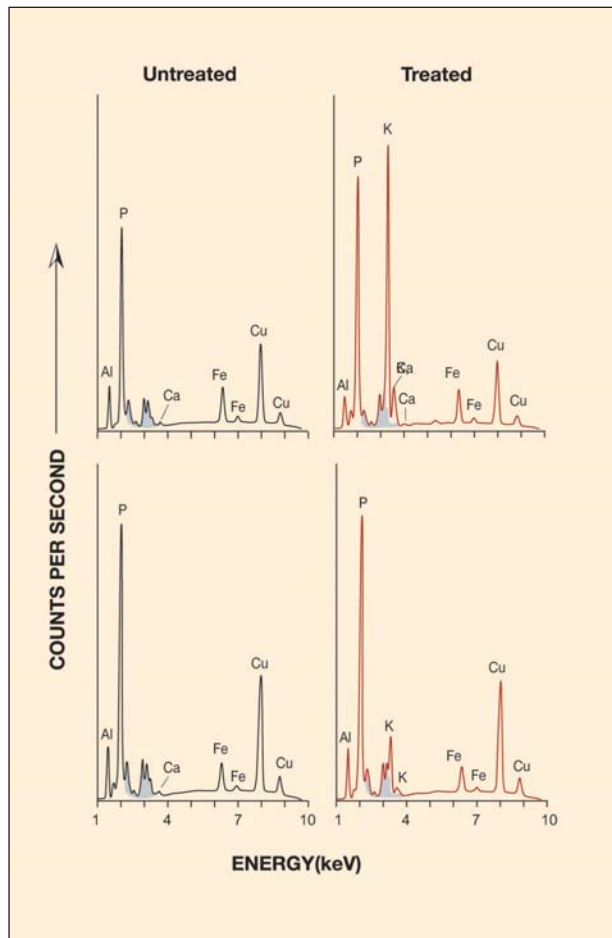
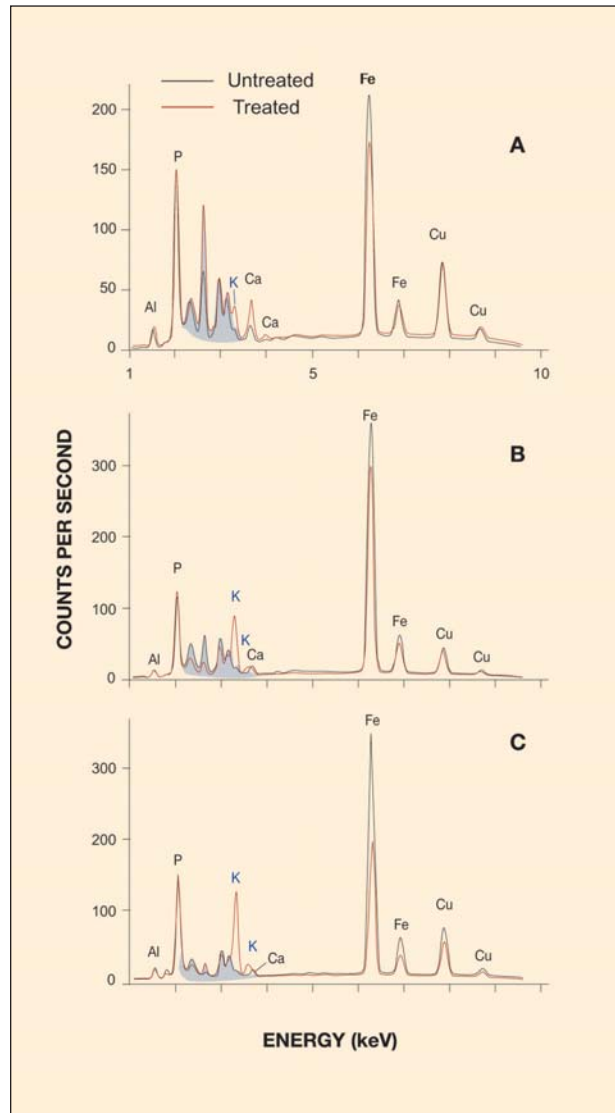


Figure 9. The EDXRF spectra for untreated turquoise from various deposits were very similar; those shown here (left) are from the Nevada Smith mine (top) and the Sleeping Beauty mine (bottom). A small potassium peak is sometimes present in the untreated material, but it is always smaller than the calcium (Ca) peak. In contrast, the Zachery-treated turquoise (right) usually shows potassium peaks, which are much higher than in the untreated turquoise. The highest and lowest potassium peaks that we detected in the treated material are shown at the top and bottom, respectively. Note: The shaded peaks are artifacts of the instrumentation, and should be ignored.

Oxalic Acid. Mr. Foutz (pers. comm., 1998) told us about a simple—but destructive—test that may distinguish untreated from Zachery-treated turquoise. A small amount of oxalic acid solution is applied to the sample; if the material has been Zachery treated, a white skin usually will form on the surface. Mr. Foutz noted that this test works best on stones that have received color treatment and may not show on stones that have been treated for durability/porosity only.

To investigate this, we prepared a 20% solution of oxalic acid, into which we immersed one half of each of the three Sleeping Beauty cabochons treated by the different methods. We also tested an untreated-

Figure 10. These EDXRF spectra of the “Emerald Valley” samples shown in figure 3 demonstrate the potassium enrichment in the treated halves (red line) compared to their untreated counterparts (black line). To facilitate comparison, the spectra have been normalized according to the height of their phosphorus (P) peaks. For the treated samples, the potassium (K) peak is small in the high-quality sample (A), and becomes progressively larger in the medium- (B) and low-quality (C) samples. Note: The shaded peaks are artifacts of the instrumentation, and should be ignored.



ed turquoise bead. For comparison purposes, we retained the other half of each cabochon and set aside another untreated bead of like color. After the stones had been in the solution for four hours, we rinsed them off and allowed them to dry. The untreated bead showed no apparent change, and the stone that was treated throughout but not color treated showed only a very slight whitishness. However, the stone that was treated throughout and then color treated showed a definite lightening of the blue color, and the stone that was only color treated showed a dramatic change to pale blue (figure 11). The porosity of all of the treated stones was also increased, proportional to the amount of visible reaction to the acid. This was evidenced by the fact that the stones were now sticky to the touch. These results are consistent with the information we received from Mr. Foutz. Microprobe analyses performed on one of the color-treated Sleeping Beauty cabochons revealed that the enriched potassium at the surface of the treated control half was absent from the half that was immersed in oxalic acid. They also confirmed that the immersed half showed an increase in porosity.

We performed another variation of this test by placing a small drop of solution on several polished slabs of treated turquoise. Minutes to hours were required for a reaction, and the acid left a mark that was considerably larger than the original spot of acid applied because the liquid spread on the surface of the sample. Note that it is very difficult to perform this test on curved surfaces, since the acid runs off before it has time to react with the turquoise. The white film that forms as a result of this procedure does not wipe off, and repolishing is required to return the stone to its original condition. Therefore, this test is destructive and should be used only with that limitation in mind.

DISCUSSION

Identification by Gemological Tests. Zachery-treated turquoise cannot be identified using classical gemological methods. Its gemological properties completely overlap those of natural turquoise.

The only gemological clues to the presence of this treatment are visual in nature and quite subtle. These include a slightly unnatural color (in those stones that have been color treated) and a very high-quality polish. These clues are not proof of treatment, but they are indications that the average gemologist might see in the course of a visual examination. The presence of blue color concentrations

along fractures and into the adjacent turquoise is another indication of Zachery treatment.

Identification by Advanced Testing. The mid-infrared spectra of untreated and Zachery-treated turquoise showed no significant differences. The most effective method of identifying Zachery-treated turquoise is chemical analysis. Specifically, EDXRF revealed that the vast majority of the Zachery-treated samples in this study contained significantly more potassium than natural, untreated turquoise (again, see figure 10). These results confirm observations made by the senior author (EF) after examining the original samples in 1990. Only six of the 55 Zachery-treated stones tested by EDXRF (including the 13 samples not shown in table 1 because they were not fully characterized) did not show a higher potassium content than that seen in the untreated turquoise. We know from Mr. Foutz that three of these exceptions were treated without improving their color. We do not know the intended effect of the treatment on the other three samples. What is most important is that all the stones that revealed a high potassium content were indeed Zachery treated.

Porosity and the Treatment Process. In his 1998 letter to the authors, Mr. Zachery stated that the treated material "has not been impregnated with any wax, oil or lacquer." Our studies support this statement. However, this does not exclude the possibility that the treatment might be adding other components, which affect the porosity of the turquoise.

To understand how the filling of pores in a mineral can affect its appearance, it is necessary to understand how light reflects off materials of differing porosities. The visual appearance of porosity in materials such as turquoise is equivalent to that of a material containing small bubbles of air (of much lower R.I.) scattering light. If the voids are larger than the wavelength of visible light (i.e., a micron or more on average), then the white light that is scattered will recombine, giving a white, cloudy, or milky cast to the stone (Fritsch and Rossman, 1988). This is indeed what we observe in all natural, untreated turquoise. The same phenomenon gives rise to the white color in milky quartz (scattering by microscopic fluid inclusions). Even if the material is strongly colored, scattering will produce a lighter color. Hence, a dark brown beer has a very light-colored foam, because the myriad microscopic air bubbles scatter light efficiently, and the walls of the

bubbles are very thin. Conversely, if the voids are filled, a significantly darker and more saturated color will be observed. A similar phenomenon is seen when a piece of colored fabric is partially immersed in water: The wet area becomes much darker and more saturated than the dry area, because the voids in the weave (its "porosity") are filled with water, thus considerably reducing the light scattering. This is what we believe we are seeing in Zachery-treated turquoise, and what is known to happen in polymer-impregnated turquoise.

One scenario that would be consistent with our observations is that turquoise is being grown in situ within the porous areas during treatment, with potassium being an aid to or by-product of the process. Alternately, the treatment may use the natural porosity of untreated turquoise to introduce a substance that helps make the material more cohesive. These scenarios would reduce the porosity of the turquoise and thus might improve the color in some specimens, much in the same way that the filling of porous chalky turquoise with polymers improves its color. These theories are best supported by the fact that the treated turquoise no longer accepts contaminants such as oils, and that the quality of the polish is improved.

The lack of potassium in some treated samples may be due to the low porosity of the starting material. If the turquoise has little or no porosity before treatment, then it will be more difficult to introduce a foreign substance. Hence, even if such a piece has undergone the full treatment process, it may not show the presence of potassium.

Another explanation is that turquoise that is nonporous or only slightly porous will not allow the potassium to penetrate until the treatment is concentrated enough to improve the stone's color. This would be consistent with the fact that three of the stones that did not show an increased potassium content were known to have been treated without improving their color. These stones were all high-quality material and demonstrated the reduced porosity characteristic of this treatment.

Gemological Nomenclature. This type of treatment presents some nomenclature problems for gemologists. In the colored stone trade, treatments that affect color are often perceived more negatively than those that affect clarity or other characteristics. The problem with material treated by the Zachery process is that, while in the vast majority



Figure 11. An oxalic acid solution can be used to detect some of the Zachery-treated turquoise. For each pair, the sample on the right was immersed in oxalic acid for four hours. Shown clockwise from the lower left, the samples are: untreated (beads); treated throughout and left natural color; treated throughout and then color treated; and color treated only. Photo by Maha DeMaggio.

of cases we can tell by chemical analysis that a stone has been treated, at this time there is no definitive way to determine whether its color has been affected. One can usually assume that stones that show blue concentrations in and near fractures have been color treated, but not all of the turquoise that has been color treated by the Zachery process shows these concentrations.

Mr. Foutz sells his material as "enhanced" turquoise, to differentiate it from treated material that is referred to as "stabilized." Unfortunately, as discussed above, we do not know exactly what is happening to the turquoise when it is treated by this process. In fact, Mr. Foutz admits that he and Mr. Zachery do not know the exact mechanism that is taking place. This creates a nomenclature problem for gemological laboratories, where concise descriptions of treatments are essential. Until more is known about the process involved, the GIA Gem Trade Laboratory will continue to call this material "Treated Natural Turquoise."

CONCLUSION

Zachery-treated turquoise cannot be detected by standard gemological techniques, although a slightly unnatural color and blue color concentrations in and around fractures are indications. Bleaching after

exposure to oxalic acid may also indicate treatment, but this is a destructive test. On the basis of the large number of samples we tested from various localities, we have demonstrated that the vast majority of Zachery-treated turquoise can be identified by relatively high potassium levels. However, chemical analysis requires access to advanced technology such as EDXRF spectrometry or microprobe analysis; such instrumentation is available in only the most sophisticated gemological laboratories. The presence of potassium as the only detectable additive is unique among gem treatments.

Acknowledgments: The authors thank the late Pat Troutman of the Hope Franklin company, Prescott, Arizona, for first bringing this material to their attention. Special thanks go to Sterling Foutz (sfoutz@earthlink.net) of Sterling Products, Prescott, for providing numerous samples and valuable information. We are also grateful to Phil Owens, of the GIA Gem Trade Laboratory in Carlsbad, for his assistance and information regarding the cutting and polishing of this material; and to Shane Elen, of GIA

Research, for gathering EDXRF data. Dr. Frank Hawthorne, at the University of Manitoba, kindly provided electron microprobe analyses and X-ray diffraction data.

This article is dedicated to the memory of the late Bob Kammerling, our friend and colleague.

REFERENCES

- Bariand P., Poirot J.-P. (1985) *Larousse des Pierres Précieuses*. Larousse, Paris, France, pp. 242–249.
- Branson O. (1975) *Turquoise, the Gem of the Centuries*. Treasure Chest Publications, Santa Fe, NM.
- Cervelle B. (1985) Turquoises: les bonnes, les brutes et les traitées. *La Recherche*, No. 163, pp. 244–247.
- Dontenville S., Calas G., Cervelle B. (1986) Etude spectroscopique des turquoises naturelles et traitées. *Revue de Gemmologie a.f.g.*, No. 85, pp. 8–10; No. 86, pp. 3–4.
- Fritsch E. (1990) "Zacharia" treated turquoise. Internal GIA Research memo, April 19, 1990.
- Fritsch E., Stockton C.M. (1987) Infrared spectroscopy in gem identification. *Gems & Gemology*, Vol. 23, No. 1, pp. 18–26.
- Fritsch E., Rossman G.R. (1988) An update on color in gems. Part 3: Colors caused by band gaps and physical phenomena. *Gems & Gemology*, Vol. 24, No. 2, pp. 81–102.
- Liddicoat R.T. Jr. (1987) *Handbook of Gem Identification*, 12th ed. Gemological Institute of America, Santa Monica, CA.

Get Your Complete Set of 1998 Issues

That's more than 320 pages of cutting-edge trade news and scientific research from some of the world's keenest gemological minds!



SAVE 20%

Off the Single-Issue Price



ONLY \$40*

For all Four Issues

* \$48 in Canada, \$60 elsewhere

TO ORDER: Call Toll Free 800-421-7250, ext. 7138 or 760-603-4000, ext 7138



SOME DIAGNOSTIC FEATURES OF RUSSIAN HYDROTHERMAL SYNTHETIC RUBIES AND SAPPHIRES

By Karl Schmetzer and Adolf Peretti

Most Russian hydrothermal synthetic rubies and pink, orange, green, blue, and violet sapphires—colored by chromium and/or nickel—reveal diagnostic zigzag or mosaic-like growth structures associated with color zoning. When the samples are properly oriented, these internal patterns are easily recognized using a standard gemological microscope in conjunction with immersion or fiber-optic illumination.

Pleochroism is also useful to separate chromium-free blue-to-green synthetic sapphires from their natural counterparts. Samples colored by a combination of chromium, nickel, and iron are also described.

ABOUT THE AUTHORS

Dr. Schmetzer is a research scientist residing in Petershausen, near Munich, Germany. Dr. Peretti (aperetti@gemresearch.ch) is director of GRS Gemresearch Swisslab AG, Lucerne, Switzerland.

Acknowledgments: The authors are grateful to the following people for supplying some of the samples used in this study: Fred Mouawad, Bangkok, Thailand; Christopher P. Smith and Dr. Dietmar Schwarz, both of the Gübelin Gemmological Laboratory, Lucerne, Switzerland; Dr. James E. Shigley, GIA Research, Carlsbad, California; and the Siberian Gemological Center, the United Institute of Geology, Geophysics and Mineralogy, and the joint venture Taurus, all of Novosibirsk, Russia.

Gems & Gemology, Vol. 35, No. 1, pp. 17–28

© 1999 Gemological Institute of America

Hydrothermal synthetic ruby of Russian production first appeared on the international market in 1993 (Peretti and Smith, 1993, 1994). Subsequently, in 1995, yellow, orange, blue-green, and blue synthetic sapphires from Novosibirsk became available (figure 1). Recently, these sapphires were described in detail (Peretti et al., 1997; Thomas et al., 1997). As those authors reported, infrared and visible-range spectroscopy, as well as trace-element chemistry, are useful to separate these synthetic sapphires from their natural counterparts. Microscopic examination has also revealed features of diagnostic value, such as copper-bearing particles and flake-like aggregates, as well as various types of fluid and multi-phase inclusions. However, the gemologist does not always have access to sophisticated analytical equipment, and characteristic inclusions are not always present. Therefore the authors decided to investigate the internal growth patterns of this material in an effort to identify distinctive characteristics that might be readily seen in most samples.

Growth patterns in hydrothermal synthetic emeralds, such as those of Russian production, generally are known to gemologists (see Schmetzer, 1988), and irregular growth features in Russian hydrothermal synthetic rubies and sapphires also have been mentioned briefly (Sechos, 1997; Thomas et al., 1997). However, these publications described no specific orientation of the synthetic rubies and sapphires during examination for these features. In the experience of the present authors, the observation of growth features in unoriented samples is sufficient to identify only some hydrothermally grown samples; that is, only heavily disturbed, strongly roiled growth patterns can be observed without a specific orientation (figure 2; see also figure 16 in Thomas et al., 1997, p. 200). These patterns can also be mistaken for growth features seen in natural rubies and sapphires. For oriented samples, however, a diagnostic growth



Figure 1. Russian crystal-growth laboratories are now producing hydrothermal synthetic ruby as well as sapphires in a range of colors. The blue-green sapphire in the center (9.2 × 7.0 mm) weighs 2.65 ct. Photo by Maha DeMaggio.

pattern can be seen in most of the synthetic rubies, as well as in a major portion of the synthetic sapphires. Yet few of these growth patterns have been illustrated to date. The present study gives a detailed description of the diagnostic growth features, and describes a method to position a sample so that these features can be readily seen in commercially available Russian hydrothermal synthetic rubies and sapphires (i.e., those colored by chromium and/or nickel).

Differences in pleochroism have been mentioned as being useful to separate some Taurus greenish blue synthetic sapphires from their natural counterparts (Thomas et al., 1997). A pleochroism of weak to strong green-blue to blue was indicated for some of the Taurus samples; however, this is also found in basaltic-type bluish green to blue natural sapphire (see, e.g., Schmetzer and Bank, 1980, 1981). Consequently, we also re-evaluated the applicability of pleochroism to the identification of synthetic Russian hydrothermal rubies and sapphires.

MATERIALS AND METHODS

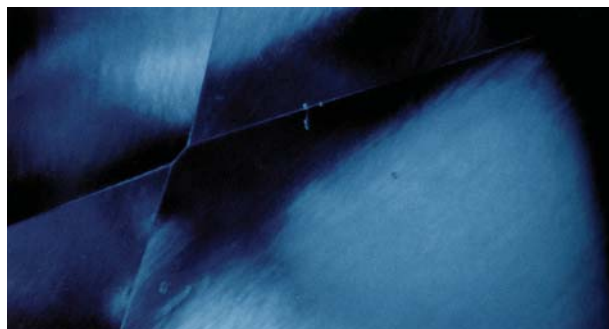
The 83 samples studied were reportedly produced either at the United Institute of Geology, Geophysics and Mineralogy, Novosibirsk, Russia, or at the hydrothermal growth facilities of Taurus Co., also in Novosibirsk. Forty-two samples were acquired between 1993 and 1996 by one of the authors (AP) during various stays in Bangkok and Novosibirsk (see Peretti et al., 1997). Two additional synthetic rubies were purchased in 1998 at Taurus Co., Bangkok, Thailand; and a collection of 17 samples, loaned by C. P. Smith, contained hydrothermal

synthetic rubies and sapphires obtained from 1993 to 1998 in Novosibirsk and Bangkok. A set of 22 faceted samples from the GIA research collection originated directly from Taurus Co., Novosibirsk; 18 of these were used in the report by Thomas et al. (1997).

The samples included six complete synthetic ruby (2) and synthetic sapphire (4) crystals grown on tabular seeds (see, e.g., figure 3), as well as two crystals that were grown on spherical (Verneuil) seeds specifically for the study of crystal growth. The eight crystals ranged from about 6 to 59 ct. Twenty-two of the samples were irregular pieces that had been sawn from larger crystals, and 12 samples were plates that had been polished on both sides. Most of these 34 irregular pieces and plates contained a portion of a colorless tabular seed. A polished window was prepared on about 15 of the crystal fragments (the largest of which was 41 ct) for microscopic examination. The remaining 41 synthetic rubies and sapphires of various colors were faceted and ranged from 0.22 to 4.72 ct (see, e.g., figure 1).

To characterize the samples according to their cause of color and trace-element contents, we obtained ultraviolet-visible (UV-Vis) spectra for about half the 41 synthetic rubies and pink sapphires, and all the 42 synthetic sapphires, by means of a Leitz-Unicam SP 800 UV-Vis spectrophotometer. We performed trace-element analysis by energy-dispersive X-ray fluorescence (EDXRF), using a Tracor Northern TN 5000 system, for 32 samples that included each color variety and/or each type of absorption spectrum.

Figure 2. If a hydrothermal synthetic sapphire or ruby is not oriented in a specific direction when it is examined with magnification and fiber-optic illumination, as seen in this Russian synthetic sapphire, the growth patterns are difficult to resolve and may mimic those seen occasionally in natural corundum. Magnified 40x.



To document a possible color change by gamma-irradiation, we exposed one intense blue-green synthetic sapphire to ^{60}Co in a commercial irradiation facility.

Morphological characteristics of the complete crystals were measured with a goniometer. The external faces of the smaller sawn pieces, the polished plates, and the internal growth patterns of all 83 samples were examined with a Schneider horizontal (immersion) microscope with a specially designed sample holder and specially designed eye-pieces (to measure angles: Schmetzer, 1986, and Kiefert and Schmetzer, 1991; see also Smith, 1996). We also examined many of the samples with an Eickhorst gemological microscope (without immersion) using fiber-optic illumination.

Most of the faceted samples were cut with their table facets at various oblique angles to the *c*-axis of the original crystal. Consequently, we determined the pleochroism of all the faceted samples in immersion with the following three-step procedure: (1) using crossed polarizers, we oriented the *c*-axis parallel to the direction of view by observation of the variation in interference rings as the sample was rotated (see Kiefert and Schmetzer, 1991); (2) we rotated the sample through 90° about the vertical axis of the sample holder to orient the *c*-axis in the east-west direction of the microscope, and then removed one polarizer; and (3) we determined both pleochroic colors by rotating the remaining polarizer.

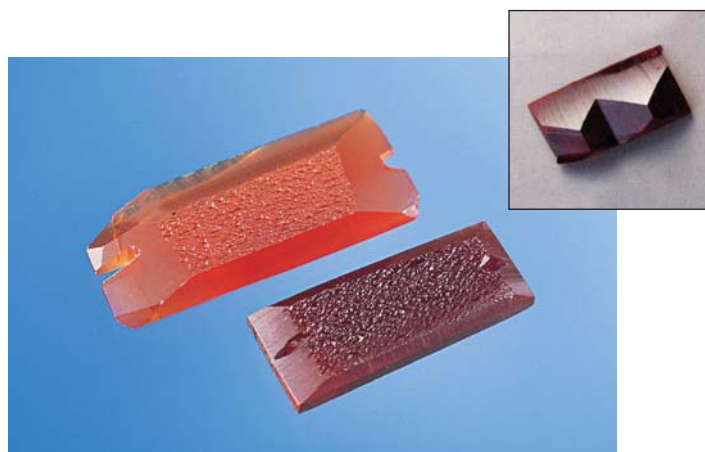


Figure 3. These three samples are representative of the Russian hydrothermal synthetic ruby and sapphire crystals grown on tabular seeds. Two standard seed orientations are used: The 31×13 mm synthetic ruby on the bottom was grown with a seed parallel to a prism $b \{10\bar{1}0\}$, whereas the orange synthetic sapphire (40×18 mm) and the synthetic ruby in the inset (35×18 mm) were grown with seeds parallel to a negative rhombohedron $-r \{01\bar{1}1\}$. The rough, uneven faces of two of the crystals are oriented parallel to the seed; by contrast, the crystal in the inset reveals alternating hexagonal dipyramids $n \{2\bar{2}43\}$. Photo © GIA and Tino Hammid; inset by M. Glas.

RESULTS AND DISCUSSION

Characterization of Samples According to Color and Cause of Color. On the basis of color, absorption

TABLE 1. Properties of Russian hydrothermal synthetic ruby and sapphire samples colored by chromium and/or nickel.

Color	Cause of color	Pleochroism <i>c</i> -axis	Pleochroism \perp <i>c</i> -axis	Samples ^a
Ruby and pink sapphire	Cr^{3+}	Yellowish red to orange	Red to purplish red	15 pieces, 14 faceted, 8 plates, 2 crystals, 2 crystals with spherical seeds
Reddish orange to orange-pink sapphire	Cr^{3+} , Ni^{3+}	Light reddish yellow	Intense reddish orange	5 faceted
Orange sapphire	Cr^{3+} , Ni^{3+}	Light yellowish orange	Intense orange	2 crystals, 1 faceted
Yellow sapphire	Ni^{3+}	Yellow	Yellow	4 faceted
Green sapphire	Ni^{2+} , Ni^{3+}	Yellowish orange	Yellowish green	1 piece, 1 faceted
Bluish green sapphire	Ni^{2+} , Ni^{3+}	Orange	Green	2 faceted
Blue-green sapphire	Ni^{2+} , Ni^{3+}	Reddish orange	Bluish green	1 piece, 2 faceted
Blue sapphire	Ni^{2+}	Reddish violet	Blue-green	1 plate, 3 faceted
Blue-violet sapphire	Ni^{2+} , Cr^{3+}	Reddish violet	Blue	1 piece, 2 faceted
Bluish violet sapphire	Ni^{2+} , Cr^{3+}	Violetish red	Bluish violet	3 faceted
Violet sapphire	Ni^{2+} , Cr^{3+}	Violetish red	Violet	1 faceted

^a "Crystals" were complete, and grown on tabular seeds; rough "pieces" were sawn from crystals grown on tabular seeds; and thin "plates" were polished on both sides.

BOX A: CHARACTERIZATION OF RUSSIAN HYDROTHERMAL SYNTHETIC SAPPHIRES COLORED BY CHROMIUM, NICKEL, AND IRON

The three synthetic corundum samples that were found to contain a combination of chromium, nickel, and iron consisted of two color-change synthetic sapphires (one rough and one faceted) and one bluish violet synthetic sapphire crystal.

Color-Change Samples. The seed in this crystal was oriented differently from those in the crystals from the main sample. This crystal showed an uneven face that was oriented perpendicular to a large r face; consequently, the seed must have been cut perpendicular to r . The internal growth patterns of the faceted color-change sample indicate the same seed orientation. Such a seed orientation has not been observed in other chromium- and/or nickel-bearing Russian synthetic rubies or sapphires.

The color-change synthetic sapphires (figure A-1) were bluish green in day (or fluorescent) light and reddish violet in incandescent light. There was only a weak change in these colors when the samples



Figure A-1. These color-change synthetic sapphires are colored by iron, chromium, and nickel. The faceted sample weighs 2.89 ct. Incandescent light; photo by M. Glas.

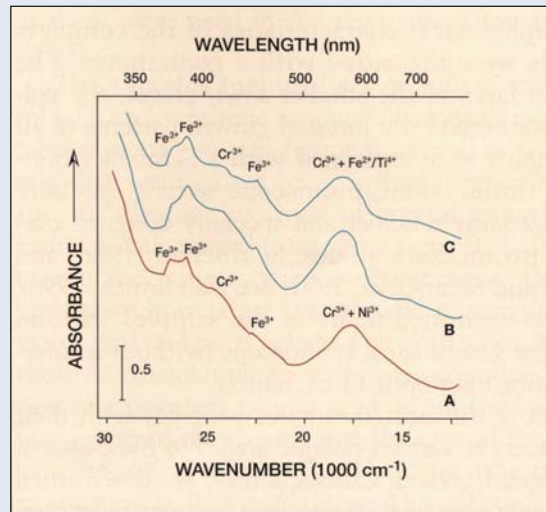


Figure A-2. The absorption spectrum of this color-change hydrothermal synthetic sapphire (A) is very similar to the spectra (B and C) of natural color-change sapphires (in this case, from Mercaderes, Colombia). The synthetic sapphire reveals absorption bands of Fe^{3+} , Cr^{3+} , and Ni^{2+} , whereas the natural samples are colored by Fe^{3+} , Cr^{3+} , and $\text{Fe}^{2+}/\text{Ti}^{4+}$ pairs. The maximum caused by Cr^{3+} and Ni^{2+} (A) is slightly shifted to higher wavelengths compared to the peak caused by Cr^{3+} and $\text{Fe}^{2+}/\text{Ti}^{4+}$ (B and C).

spectroscopy, and trace-element analysis, we found that 71 of the 83 samples were colored predominantly by chromium and/or nickel (table 1). Synthetic ruby and sapphires containing these elements are now commercially produced by Tairus Co. at Novosibirsk. Three of the remaining 12 samples are described in Box A; these samples are colored by chromium, nickel, and iron. The remaining nine synthetic sapphires did not contain chromium and/or nickel as color-causing trace elements. Therefore, these samples are not described here.

On the basis of their color, absorption spectra, and trace-element contents, we separated the 71 commercially available samples into six color "varieties:" ruby-pink sapphire and reddish orange to orange, yellow, green to blue-green, blue, and blue-

violet to violet sapphire (again, see table 1). Although traces of iron were detected by EDXRF in these samples, no Fe^{3+} absorption bands were observed. Consequently, the influence of iron on their color is negligible. EDXRF analyses revealed various amounts of chromium—but no nickel—in the synthetic rubies and pink sapphires. In the yellow, green, blue-green, and blue samples, traces of nickel only were present as color-causing elements, whereas the blue-violet to violet and the orange to reddish orange synthetic sapphires contained traces of both chromium and nickel. These chemical properties are comparable to analytical data published by Thomas et al. (1997).

The absorption spectra were consistent with our chemical data as well as with the interpretation of

were viewed parallel and perpendicular to the *c*-axis; that is, the colors were more intense parallel to *c*. These samples were found to be heavily iron-doped members of the chromium-nickel series. Their absorption spectra showed the dominant Ni²⁺ absorption band of blue synthetic sapphire superimposed on minor Cr³⁺ and Fe³⁺ absorption bands (figure A-2). With an absorption maximum in the yellow and minima in the red and blue-green areas of the visible region, this spectrum reveals all the features associated with color change in a mineral (see, e.g., Schmetzer et al., 1980; Hänni, 1983). In natural color-change sapphire (e.g., from Mercaderes, Colombia), this particular spectrum is caused by Fe²⁺/Ti⁴⁺ absorption bands of blue sapphire superimposed on Cr³⁺ and Fe³⁺ absorption bands (figure A-2; Schmetzer et al., 1980; see also Keller et al., 1985). In the authors' experience, natural color-change samples from Sri Lanka and Tanzania (Umba and Tunduru-Songea areas) have almost identical spectra.

The growth patterns of both samples (figure A-3) were comparable to the patterns seen in samples

of the chromium-nickel series (see, e.g., figures 13 and 15), with subparallel striations and subgrain boundaries between microcrystals observed in both. However, unlike the color zoning seen in samples grown with one of the two standard seed orientations (see, e.g., figure 8), these two samples revealed color zoning at an inclination to the dominant subgrain boundaries.

Bluish Violet Sample. This crystal consists of a thin overgrowth of synthetic corundum over a tabular seed with an orientation parallel to *-r*. Typical irregular surface features representing subindividuals were seen on both *-r* faces parallel to the seed plate. The pleochroic colors were violet perpendicular to the *c*-axis, and yellow parallel to the *c*-axis. The color of the crystal is a complex function of superimposed Cr³⁺, Ni²⁺, and Fe³⁺ absorption bands; the absorption spectrum is comparable to that of bluish violet sapphires of the chromium-nickel series, with additional subordinate Fe³⁺ absorption bands. This sample was higher in chromium than the two color-change synthetic sapphires.

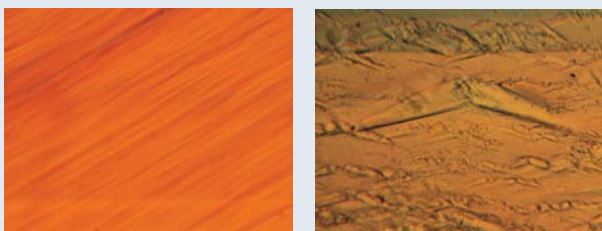


Figure A-3. The growth patterns in the color-change synthetic sapphires were similar to those seen in the synthetic samples of the series. Subparallel striations (left) were observed in the faceted sample at 70× magnification. A zigzag pattern (right) was visible in the crystal in a view parallel to the striations at 50× magnification (both with immersion).

color causes by Thomas et al. (1997).^{*} Our samples are represented in a triangular diagram (figure 4), with basic colors caused predominantly by Cr³⁺ (rubies and pink sapphires), Ni³⁺ (yellow sapphires), and Ni²⁺ (blue sapphires). Intermediate synthetic sapphires colored by a combination of Cr³⁺ and Ni³⁺ (reddish orange to orange), Ni³⁺ and Ni²⁺ (green to blue-green), and Ni²⁺ and Cr³⁺ (blue-violet to violet) are arranged along the edges of the triangle. Thomas et al. (1997) described all samples of the Ni²⁺-Cr³⁺ series as greenish blue. However, we feel that samples of this series are better described as blue, blue-violet, bluish violet, and violet (see figure 4 and table 1). Intermediate samples with high chromium and small Ni²⁺ contents, as well as samples with high amounts of Ni³⁺ and smaller Ni²⁺ contents,

were not observed in this study. An intense blue-green sample, however, turned intense yellowish green on γ -irradiation, which can be explained by conversion of part of the Ni²⁺ to Ni³⁺ (see Thomas et al., 1997).

For comparison, the natural counterparts of these synthetic rubies and sapphires are represented in another triangular diagram, with red to pink, yellow, and blue to blue-violet in the three corners (figure 5). This diagram is based on several thousand absorption spectra recorded over a 25 year period by one of the authors (KS; mostly unpublished), from

^{*}The polarization of the spectrum of a greenish blue synthetic sapphire is erroneously reversed in figure 5A in the Thomas et al. (1997) article.

Coloration of Hydrothermal Synthetic Corundum

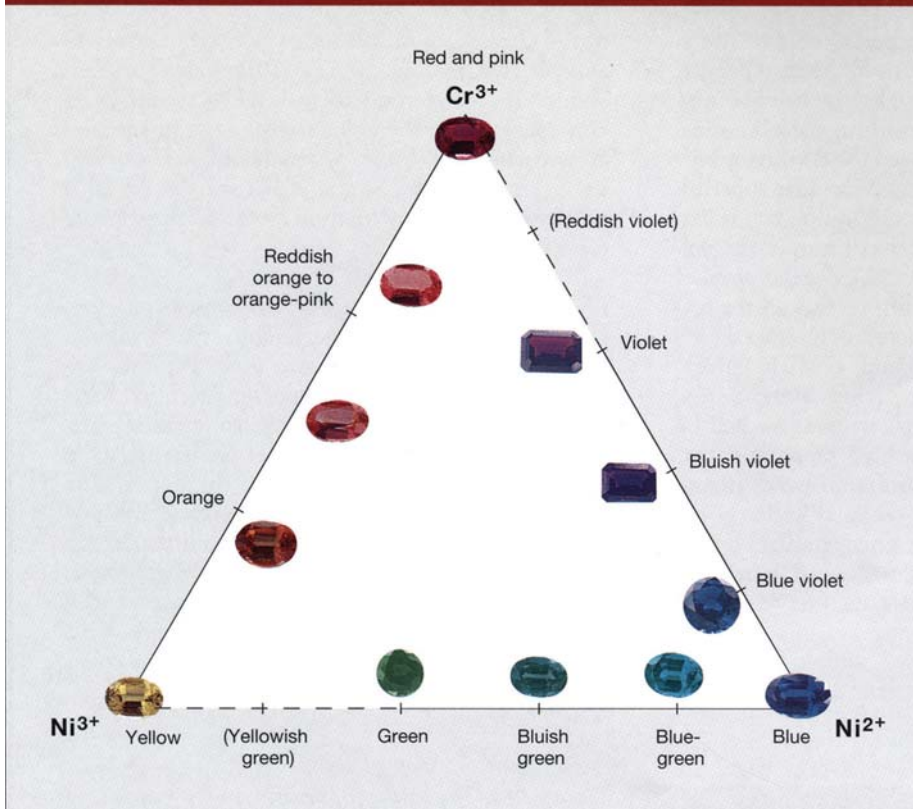


Figure 4. This triangular diagram shows the varieties of Russian hydrothermal synthetic corundum that are colored by chromium and nickel. The three basic chromophores are labeled at the corners of the triangle, namely Cr^{3+} (red to pink), Ni^{3+} (yellow), and Ni^{2+} (blue). Solid lines represent intermediate color varieties observed by the authors, and broken lines represent possible intermediate samples which were not available for this investigation. Samples containing Ni^{3+} and Ni^{2+} are green to blue-green; Cr^{3+} with Ni^{3+} produces reddish orange to orange; and Ni^{2+} with Cr^{3+} causes blue-violet to violet. The yellow sample (1.09 ct) measures 7.1×5.2 mm, and the blue sample (2.70 ct) measures 9.5×6.8 mm. Photos by M. Glas.

all major commercial sources of natural ruby and sapphire. There are two basic types of natural yellow sapphire, which are caused predominantly by color centers or by Fe^{3+} . Intermediate between red and yellow are chromium-bearing "padparadscha" sapphires. Blue to blue-violet natural sapphires are colored predominantly by $\text{Fe}^{2+}/\text{Ti}^{4+}$ ion pairs (metamorphic type) or by $\text{Fe}^{2+}/\text{Ti}^{4+}$ and $\text{Fe}^{2+}/\text{Fe}^{3+}$ ion pairs (basaltic type). Sapphires with intermediate colors exist in the blue-to-yellow (Fe^{3+}) and blue-to-red (Cr^{3+}) series (again, see figure 5).

Figure 5. This triangular diagram shows the colors of natural ruby and sapphires that are equivalent to the synthetic samples illustrated in figure 4. The three principal causes of color in natural corundum are Cr^{3+} (red to pink), color centers or Fe^{3+} (yellow), and $\text{Fe}^{2+}/\text{Ti}^{4+}$ ion pairs with or without additional $\text{Fe}^{2+}/\text{Fe}^{3+}$ pairs (blue to blue-violet). All intermediate colors are seen in natural corundum. Adapted from Schmetzer and Bank (1981).

Pleochroism. The pleochroism of both natural and synthetic corundum is identical for samples in the yellow-orange-red color range, including "padparad-

Coloration of Natural Gem Corundum

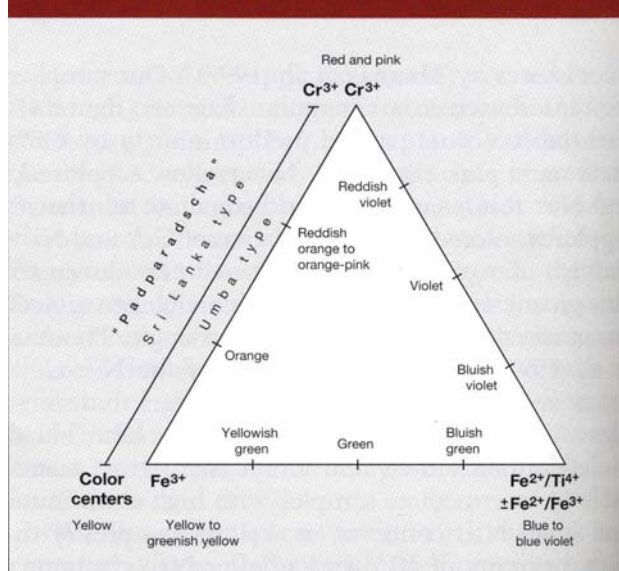
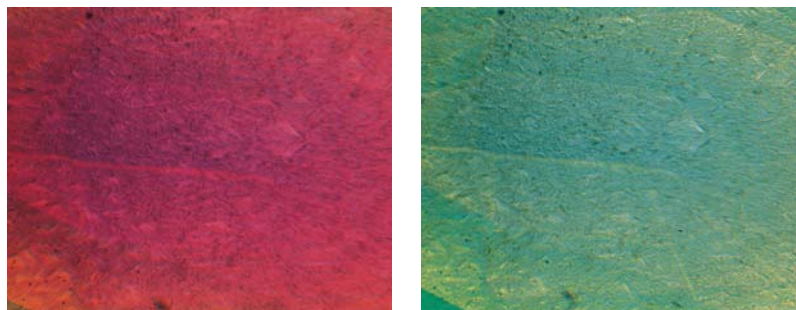


Figure 6. The blue synthetic sapphires showed diagnostic pleochroism that is the opposite of that seen in natural blue sapphire. In the Russian hydrothermal synthetics, we saw reddish violet parallel to the c-axis and blue-green perpendicular to it. Immersion, polarized light, magnified 40 \times .



scha." Likewise, natural and synthetic reddish violet to bluish violet sapphires cannot be separated routinely by their pleochroism. However, pleochroism is a diagnostic feature of blue-to-green natural and synthetic sapphires.

Natural blue sapphire is predominantly colored by ion pairs of Fe²⁺ and Ti⁴⁺, with additional influence from Fe³⁺ or Fe²⁺/Fe³⁺ (or both) absorptions. All natural blue to blue-violet sapphires colored by the Fe²⁺/Ti⁴⁺ ion pair reveal distinct pleochroism: light blue or greenish blue, green, and yellowish green parallel to the c-axis, and intense blue, bluish violet, or violet perpendicular to the c-axis (Schmetzer and Bank, 1980, 1981; Schmetzer, 1987; Kiefert and Schmetzer, 1987).

The blue hydrothermal synthetic sapphires in the chromium-nickel series are colored predominantly by Ni²⁺. These sapphires revealed a distinct pleochroism of reddish violet *parallel* to the c-axis and blue-green *perpendicular* to the c-axis (figure 6)—the opposite of that seen in natural blue sapphire. Consequently, this difference in pleochroism is useful to separate natural and synthetic blue sapphire.

The pleochroism of the Ni²⁺- and Ni³⁺-bearing blue-green to green synthetic sapphires (table 1) also differs from that of natural blue-green, bluish green, or green sapphires. Natural samples of this series contain relatively high amounts of Fe³⁺ (again, see figure 5); their pleochroism is yellowish green, green, or bluish green parallel to the c-axis and bluish green to blue perpendicular to the c-axis (Schmetzer and Bank, 1980, 1981; Schmetzer, 1987; Kiefert and Schmetzer, 1987). Using the techniques described above, we observed in their hydrothermal synthetic counterparts reddish orange to yellowish orange *parallel* to the c-axis and bluish green to yellowish green *perpendicular* to the c-axis (figure 7).** Consequently, pleochroism is also useful to distinguish hydrothermal synthetic sapphires in the blue-green to green series from their natural counterparts.

Orientation of Seeds and Morphology of the Rough.

The morphology of the two rubies that were grown on spherical seeds is consistent with the description in Thomas et al. (1997).

As reported by Thomas et al. (1997) for the Tairus hydrothermal synthetic sapphires, the seed plates in the samples we examined were cut from Czochralski-grown colorless synthetic sapphire. In the complete crystals, the seed plates measured 30–40 mm in their longest dimension. Examination of these complete crystals, as well as of the sawn pieces, polished plates, and faceted stones that contained residual parts of the seed, revealed that the seed plates were cut in two different standard orientations: (1) parallel to the c-axis, that is, parallel to a first-order hexagonal prism b {10 $\bar{1}$ 0} (figure 8); and (2) at an inclination of about 32° to the c-axis, that is, parallel to a negative rhombohedron $-r$ {01 $\bar{1}$ 1} (figure 9). Seed plates cut in the latter orientation were not mentioned by Thomas et al. (1997), but they were seen in about half the samples we examined.

The crystals grown with seeds cut parallel to the prism b revealed two large rough, uneven faces (see, e.g., figure 10) parallel to the seed, and two elongated faces each of the following forms: basal pinacoid c {0001}, positive rhombohedron r {10 $\bar{1}$ 1}, and positive rhombohedron ϕ {10 $\bar{1}$ 4} (figure 11A). In addition, these samples showed six smaller second-order hexagonal prism faces a {11 $\bar{2}$ 0}. Occasionally, smaller r faces and hexagonal dipyrramids n {2243} were also observed (figure 11B).

**Note that Thomas et al. (1997, p. 196) reported a strong violetish blue to blue-green pleochroism in the Ni²⁺/Ni³⁺-doped samples that they describe as blue-green. According to S. Z. Smirnov (pers. comm., 1999), the dichroism given in the Thomas et al. (1997) article represents colors seen in daylight in samples that were not crystallographically oriented. These colors are not identical to those determined parallel and perpendicular to the c-axis for oriented samples (see also table 1 of the present article). Note also that a small color shift is always observed between daylight and incandescent light with the immersion microscope (see the Materials and Methods section).

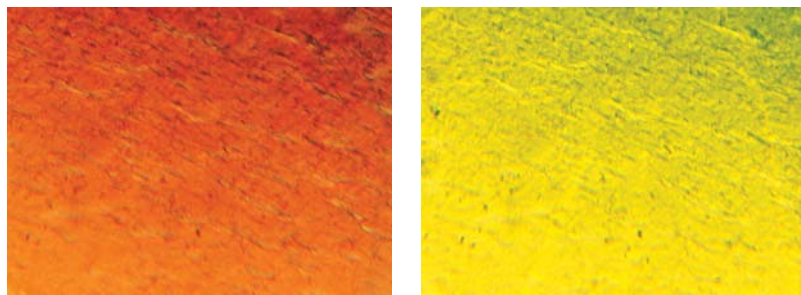


Figure 7. The pleochroism observed in the Ni^{2+} - and Ni^{3+} -bearing blue-green to green synthetic sapphires also appears to be distinctive: reddish orange parallel to the c -axis, and yellowish green perpendicular to it. Immersion, polarized light, magnified 50 \times .

Most of the crystals grown with 30–40 mm seeds cut parallel to the negative rhombohedron $-r$ $\{01\bar{1}1\}$ showed two large uneven faces parallel to $-r$, two relatively large, elongated faces parallel to a positive rhombohedron r , and striated, somewhat curved faces parallel to the basal pinacoid c (figure 11C). In some samples, another elongated positive rhombohedron ϕ was also present (figures 11C and D). Adjacent to the uneven $-r$ faces were two large hexagonal dipyramids n ; two smaller n faces were developed adjacent to the positive rhombohedron r . In most cases, two smaller faces of the prism a were observed perpendicular to the seed plane (figure 11D). Occasionally, smaller r , ϕ , and n faces also were present (figure 11C).

We do not know of any natural ruby or sapphire crystals with this morphology, especially with dominant b or $-r$ faces. Consequently, crystals with this

morphology can be easily recognized as synthetic.

In those samples grown with seed plates 30–40 mm long, the two large uneven faces parallel to the seed dominated the morphology of the crystals (see, e.g., figures 3 and 11). In one relatively thick crystal, instead of an uneven face parallel to $-r$, alternating n faces were seen (see figure 3, inset). Where smaller seeds (i.e., 10–15 mm long) were used for the crystal growth, no external faces parallel to the seed were observed (figure 9). Therefore, crystals grown on smaller seed plates may not have *either* b or $-r$ faces; synthetic crystals with such a morphology *could* be confused with natural ruby or sapphire.

Internal Growth Structures. Color Zoning. A difference in color from one growth sector to another, or in subsequent growth regions, was observed in some of the polished plates (see, e.g., figure 9). A

Figure 8. This thin plate (approximately 1.2 mm thick) of a hydrothermal synthetic ruby crystal has been cut perpendicular to the colorless seed (visible at the bottom of the photo) to show characteristic growth zoning. The seed is oriented parallel to the c -axis. Three generations of synthetic ruby are revealed by the irregular boundaries that parallel the surface of the seed, which is oriented parallel to a hexagonal prism b $\{10\bar{1}0\}$. Numerous subindividuals—long, thin microcrystals—are also visible; color zoning is seen between different growth sectors of adjacent subindividuals. Immersion, magnified 30 \times .

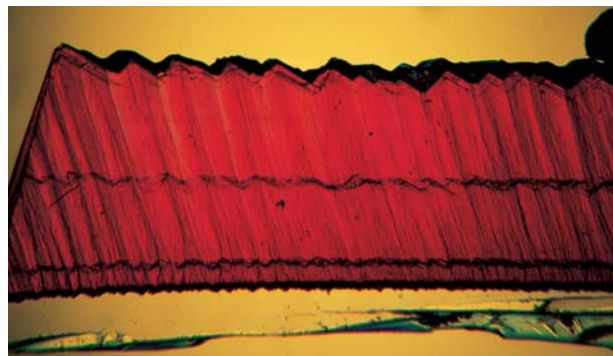
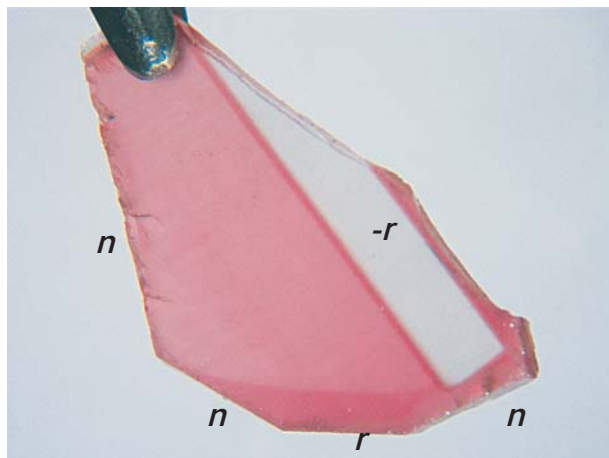


Figure 9. This 11.5 \times 6.5 mm plate (0.8 mm thick) of a hydrothermal synthetic ruby, cut at an inclination of 30 $^\circ$ to the optic axis, shows the relationship of the crystal faces to the seed. The colorless seed is oriented parallel to a negative rhombohedron $-r$ $\{01\bar{1}1\}$. The synthetic ruby shows three hexagonal dipyramids n $\{22\bar{4}3\}$ and one face of the positive rhombohedron r $\{10\bar{1}1\}$. A color zoning is also seen between subsequent growth regions.



similar color distribution is frequently seen on a macroscopic scale in natural as well as flux-grown synthetic ruby and sapphire crystals. In the rough and faceted Russian hydrothermal synthetic rubies and sapphires, we did not observe any macroscopic color distribution in different growth sectors or regions that could be useful to distinguish these samples.

Growth Boundaries. Tairus hydrothermal synthetic corundum is routinely grown in a single autoclave run, rather than in several successive runs (S. Z. Smirnov, pers. comm., 1998). However, some of our samples revealed one or more distinct growth planes parallel to the seed (again, see figure 8). These planes represent boundaries between layers of synthetic corundum and indicate that these specimens grew in several intervals. They suggest that there were "interruptions" during the formation of these particular crystals, probably due to unintentional brief fluctuations in the power supply of the growth facility.

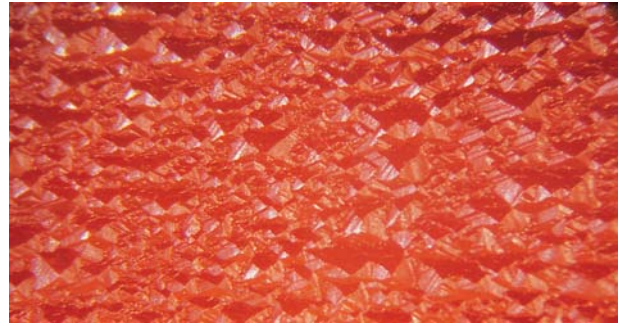
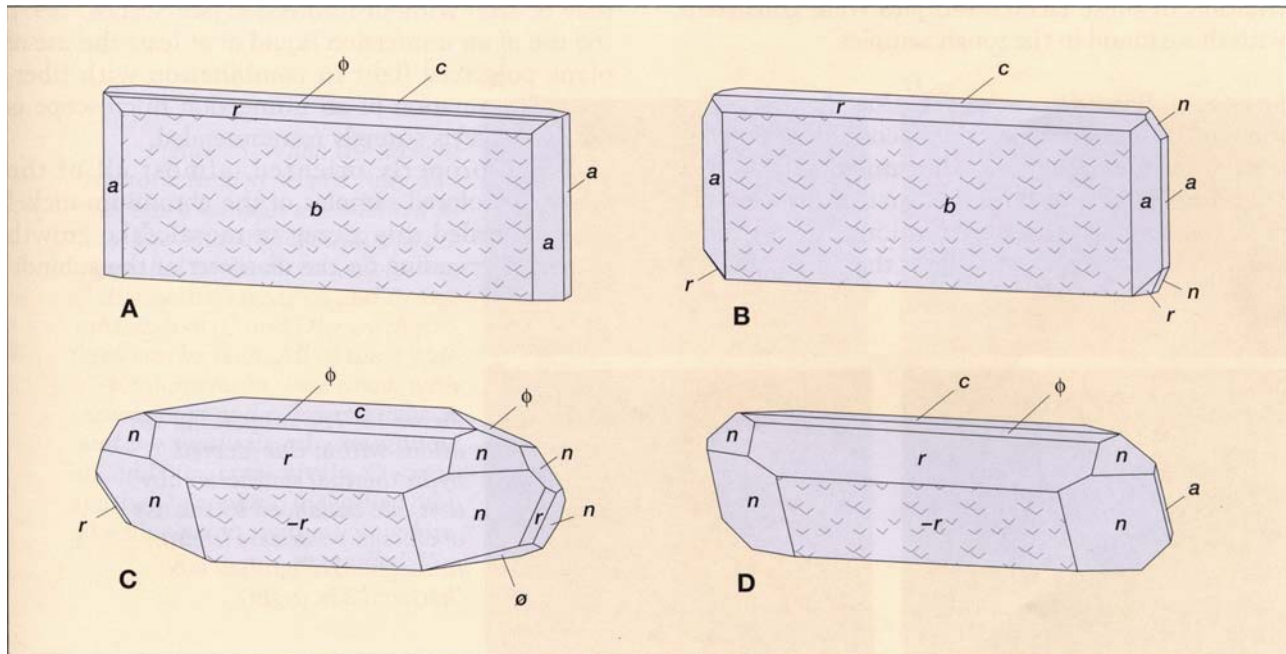


Figure 10. The rough surface texture of this orange hydrothermal synthetic sapphire crystal is formed by a distinct microstructure consisting of numerous long, thin microcrystals, as illustrated in figure 8. Magnified 20x.

Specific boundaries were also noted in all eight faceted samples (two synthetic rubies and six variously colored synthetic sapphires) that contained parts of the seed (see, e.g., figure 12). In general, these boundaries were associated with tiny copper-bearing particles, as previously described by Peretti and Smith (1993) and Peretti et al. (1997). The cop-

Figure 11. The morphology of the synthetic ruby and sapphire crystals is controlled by the orientation of their seed plates. Crystals A and B were grown with tabular seeds cut parallel to a prism $b \{10\bar{1}0\}$. On these crystals, uneven faces are developed parallel to b ; also present are the basal pinacoid $c \{0001\}$, the prism $a \{11\bar{2}0\}$, positive rhombohedra $r \{10\bar{1}1\}$ and $\phi \{10\bar{1}4\}$, and (in some cases) the hexagonal dipyrmaid $n \{22\bar{4}3\}$. Crystals C and D were grown with tabular seeds cut parallel to a negative rhombohedron $-r \{01\bar{1}1\}$. Uneven faces are developed parallel to $-r$; also shown are the basal pinacoid $c \{0001\}$, the prism $a \{11\bar{2}0\}$ (in D), positive rhombohedra $r \{10\bar{1}1\}$ and $\phi \{10\bar{1}4\}$, and the hexagonal dipyrmaid $n \{22\bar{4}3\}$.



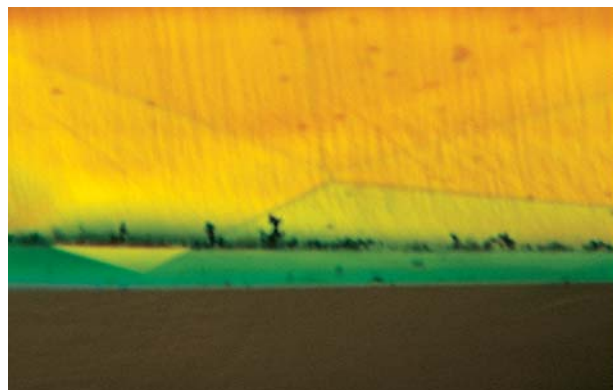


Figure 12. A portion of the seed is present along the table facet (flat lower surface) of this yellow hydrothermal synthetic sapphire. Adjacent to the seed are tiny copper-bearing particles. The faint striations oriented nearly perpendicular to the seed represent subgrain boundaries between long, thin microcrystals within the larger crystal. (The area around the table facet appears green because of dispersion.) Immersion, magnified 50 \times .

per in these inclusions originates from the wires used to mount the seed plates, from the seals of the autoclave, and/or from the buffers used during crystal growth (see also Thomas et al., 1997). In some of these faceted samples, the boundaries between seed and overgrowth were oriented parallel to a prism face; in the others, they were parallel to a rhombohedral face. Consequently, the two types of seed orientation in these faceted samples were consistent with those found in the rough samples.

Subgrain Boundaries and Color Zoning. The Russian hydrothermal synthetic corundum crystals consist of numerous long, thin microcrystals that are observed at a specific inclination to the seed plate, depending on its orientation. The terminations of these microcrystals form the rough, uneven

surfaces that are parallel to the seed plate on the crystals (again, see figures 8 and 10). This growth pattern has been described by Voitsekhovskii et al. (1970) for hydrothermally grown synthetic corundum as a “microblock” structure that consists of an assemblage of fine (0.05 to 0.5 mm in diameter) elongated crystals that are disoriented relative to one another by not more than 1–3 minutes of arc.

These long, thin microcrystals form a diagnostic growth pattern that is associated with a distinct type of fine-scale color zoning observable in immersion. In thin (1–2 mm) plates cut perpendicular to the seed, the variable intensity in color between growth sectors of adjacent subindividuals is clearly visible (figure 8). In thicker plates, or in faceted samples, in the same orientation, only the boundaries between the differently colored growth sectors can be seen, in the form of subparallel (i.e., not perfectly parallel) striations (figure 13). The use of crossed polarizers often can enhance the contrast between growth sectors (figures 13 and 14).

An even more characteristic internal growth pattern is seen in a view parallel to these striations. To find the best—that is, most diagnostic—direction of view in faceted samples, search first for the presence of the subparallel striations, then turn the faceted stone to a direction in which the striations are parallel to the direction of view. Only in this orientation is it possible to see the zigzag or mosaic-like growth pattern that is most distinctive of this material (figure 15). Although this growth pattern sometimes may be seen without immersion (see Sechos, 1997), the use of an immersion liquid or at least the use of plane polarized light in combination with fiber-optic illumination (if an immersion microscope is not available) is strongly recommended.

When properly oriented, almost all of the intensely colored samples of the chromium-nickel series revealed this zigzag or mosaic-like growth pattern. Depending on the diameter of the subindi-

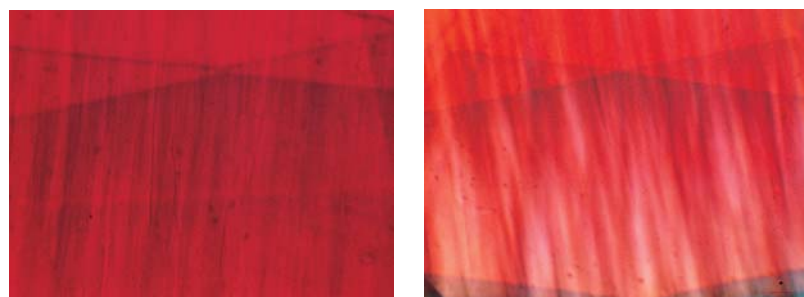


Figure 13. The subparallel striations within this faceted hydrothermal synthetic ruby (left) are enhanced by the use of crossed polarizers (right). Immersion; magnified 40 \times (left) and 35 \times (right).

viduals that form the synthetic corundum crystal, the color zoning may vary from fine to coarse in texture. With training, however, the gemologist can recognize the striations and zigzag or mosaic-like patterns in synthetic rubies and sapphires that have sufficient color saturation, with the exception of yellow synthetic sapphires colored by Ni^{3+} alone. In only one of the four yellow samples with no evidence of Cr^{3+} in the absorption spectrum did we observe extremely weak striations (figure 12). In addition, no diagnostic growth pattern was found in two light blue, almost colorless, samples in which Ni^{2+} was the predominant cause of color as proved by absorption spectroscopy and EDXRF analysis.

Although growth patterns associated with color zoning are also observed frequently in natural rubies and sapphires (figure 16), these patterns are very different from those seen in the synthetic samples. In general, natural rubies and sapphires are not composed of numerous long, thin microcrystals with slightly different orientations. Thus, growth patterns in natural samples are mainly caused by color zoning due to growth fluctuations within a single crystal. The mosaic-like pattern in hydrothermal synthetic rubies and sapphires is strongly diagnostic, and no chemical or spectroscopic examination is necessary when it is present. However, UV-Vis or infrared spectroscopy in combination with trace-element analysis may be necessary to identify the yellow synthetic sapphires, as well as extremely pale samples of other hues.

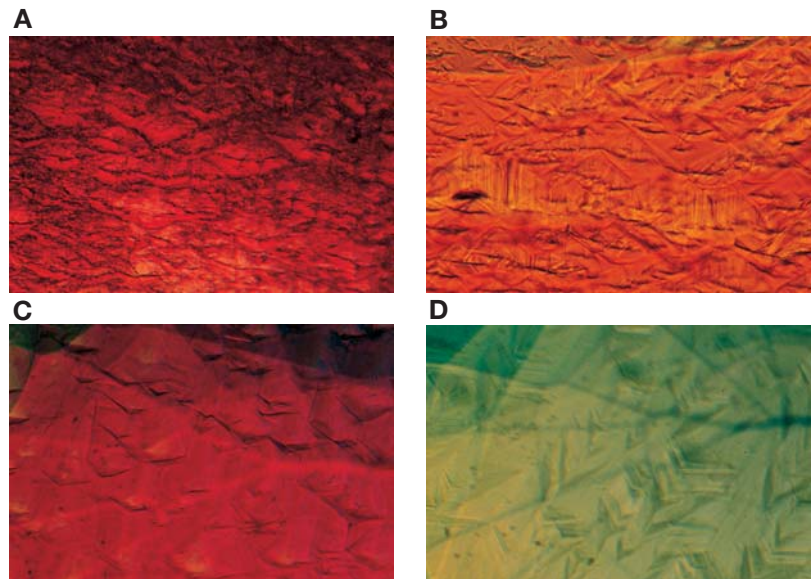


Figure 14. In this faceted blue-green synthetic sapphire, as in the synthetic ruby in figure 13, one can see striations representing oriented subgrain boundaries between the long, thin microcrystals. Immersion, crossed polarizers, magnified 70x.

CONCLUSION

The hydrothermally grown nickel- and/or chromium-doped Russian synthetic rubies and sapphires examined revealed an external morphology and internal growth features that reflect their formation conditions. The identification of characteristic growth patterns is a relatively straightforward method to distinguish most of these synthetics from their natural counterparts. A horizontal microscope with immersion or a standard gemological microscope with fiber-optic illumination in combination with polarizing filters is all that is needed to carry out this investigation.

Figure 15. When the faceted hydrothermal synthetic ruby and sapphire samples are oriented so that the subparallel striations are parallel to the direction of view, distinctive zigzag (A and B) and mosaic-like (C and D) growth patterns can be seen. All of these photomicrographs were taken with immersion and polarized light. A and B = synthetic ruby, magnified 50x and 60x, respectively; C = pink synthetic sapphire, magnified 40x; D = blue-green synthetic sapphire, magnified 45x.



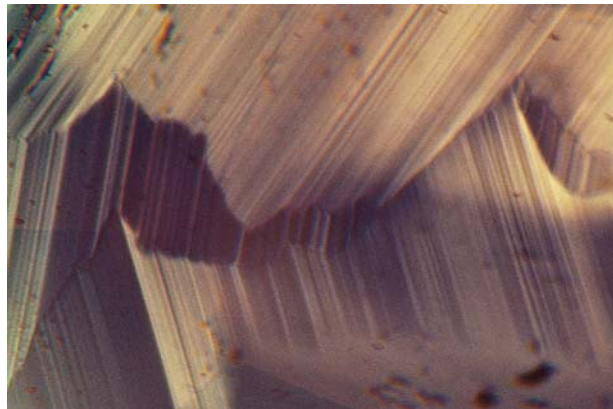


Figure 16. Growth patterns are frequently seen in natural rubies and sapphires, as in this blue sapphire from Andranondambo, Madagascar. This pattern is not related to microstructures consisting of subindividuals that reveal color zoning between various growth sectors. In this case, the pattern consists of growth planes parallel to one and two n faces. Adjacent growth sectors show changes in size and color intensity. Immersion, magnified 50 \times .

The characteristic internal features of these hydrothermal synthetic rubies and sapphires are: (1) subparallel striations; and (2) a distinct zigzag or mosaic-like growth structure, associated with color zoning between different growth sectors of adjacent subindividuals. The latter can be seen only when the sample is viewed in a direction parallel to the striations. Only the yellow hydrothermal synthetic sapphires and extremely light blue samples did not show any of these diagnostic internal growth characteristics. In the absence of other distinctive inclusions, such corundums will require additional testing by spectroscopic or analytical techniques such as UV-visible absorption spectroscopy or EDXRF.

Pleochroism is also useful to identify some hydrothermal synthetic sapphires, particularly to distinguish chromium-free samples of the blue-to-green series from their natural counterparts. To perform this test, the orientation of the optic axis in a faceted sample must first be determined.

REFERENCES

- Hänni H.A. (1983) Weitere Untersuchungen an einigen farbwechselnden Edelsteinen. *Zeitschrift der Deutschen Gemmologischen Gesellschaft*, Vol. 32, No. 2/3, pp. 99–106.
- Keller P.C., Koivula J.I., Jara G. (1985) Sapphire from the Mercaderes-Río Maya area, Cauca, Colombia. *Gems & Gemology*, Vol. 21, No. 1, pp. 20–25.
- Kiefert L., Schmetzer K. (1987) Blue and yellow sapphire from Kaduna Province, Nigeria. *Journal of Gemmology*, Vol. 20, No. 7/8, pp. 427–442.
- Kiefert L., Schmetzer K. (1991) The microscopic determination of structural properties for the characterization of optical uniaxial natural and synthetic gemstones, part 1: General considerations and description of the methods. *Journal of Gemmology*, Vol. 22, No. 6, pp. 344–354.
- Peretti A., Mullis J., Mouawad F., Guggenheim R. (1997) Inclusions in synthetic rubies and synthetic sapphires produced by hydrothermal methods (TAIRUS, Novosibirsk, Russia). *Journal of Gemmology*, Vol. 25, No. 8, pp. 540–561.
- Peretti A., Smith C.P. (1993) A new type of synthetic ruby on the market: Offered as hydrothermal rubies from Novosibirsk. *Australian Gemmologist*, Vol. 18, No. 5, pp. 149–157.
- Peretti A., Smith C.P. (1994) Letter to the Editor. *Journal of Gemmology*, Vol. 24, No. 1, pp. 61–63.
- Schmetzer K. (1986) An improved sample holder and its use in the distinction of natural and synthetic ruby as well as natural and synthetic amethyst. *Journal of Gemmology*, Vol. 20, No. 1, pp. 20–33.
- Schmetzer K. (1987) Zur Deutung der Farbursache blauer Sapphire—eine Diskussion. *Neues Jahrbuch für Mineralogie Monatshefte*, Vol. 1987, No. 8, pp. 337–343.
- Schmetzer K. (1988) Characterization of Russian hydrothermally-grown synthetic emeralds. *Journal of Gemmology*, Vol. 21, No. 3, pp. 145–164.
- Schmetzer K., Bank H. (1980) Explanations of the absorption spectra of natural and synthetic Fe- and Ti-containing corundums. *Neues Jahrbuch für Mineralogie Abhandlungen*, Vol. 139, No. 2, pp. 216–225.
- Schmetzer K., Bank H. (1981) The colour of natural corundum. *Neues Jahrbuch für Mineralogie Monatshefte*, Vol. 1981, No. 2, pp. 59–68.
- Schmetzer K., Bank H., Gübelin E. (1980) The alexandrite effect in minerals: Chrysoberyl, garnet, corundum, fluorite. *Neues Jahrbuch für Mineralogie Abhandlungen*, Vol. 138, No. 2, pp. 147–164.
- Sechos B. (1997) Identifying characteristics of hydrothermal synthetics. *Australian Gemmologist*, Vol. 19, No. 9, pp. 383–388.
- Smith C.P. (1996) Introduction to analyzing internal growth structures: Identification of the negative d plane in natural ruby. *Gems & Gemology*, Vol. 32, No. 3, pp. 170–184.
- Thomas V.G., Mashkovtsev R.I., Smirnov S.Z., Maltsev V.S. (1997) Tairus hydrothermal synthetic sapphires doped with nickel and chromium. *Gems & Gemology*, Vol. 33, No. 3, pp. 188–202.
- Voitsekhovskii V.N., Nikitichev P.I., Smirnova Z.F., Furmakova L.N. (1970) The microblock structure of hydrothermal crystals of corundum. *Soviet Physics-Crystallography*, Vol. 14, No. 5, pp. 733–735.

THE SEPARATION OF NATURAL FROM SYNTHETIC COLORLESS SAPPHIRE

By Shane Elen and Emmanuel Fritsch

Greater amounts of colorless sapphire—promoted primarily as diamond substitutes, but also as natural gemstones—have been seen in the gem market during the past decade. In the absence of inclusions or readily identifiable growth structures, natural colorless sapphires can be separated from their synthetic counterparts by their trace-element composition and short-wave ultraviolet (SWUV) transparency. Energy-dispersive X-ray fluorescence (EDXRF) analysis shows higher concentrations of trace elements (i.e., Fe, Ti, Ca, and Ga) in natural sapphires. These impurities cause a reduction in SWUV transparency that can be detected by UV-visible spectrophotometry (i.e., a total absorption in the UV region below 280–300 nm, which is not seen in their synthetic counterparts). This article describes a SWUV transparency tester that can rapidly identify parcels of colorless sapphires.

ABOUT THE AUTHORS

Mr. Elen (selen@gia.edu) is a research gemologist at GIA Research, Carlsbad, California, and Dr. Fritsch is professor of physics at Nantes University, France.

The authors thank Sam Muhlmeister and Dino DeGhionno of the GIA Gem Trade Laboratory in Carlsbad for recording some of the EDXRF spectra and measuring gemological properties, respectively. Some of the samples were loaned by Dave Ward of Optimagem, San Luis Obispo, California; Michael Schramm of Michael Schramm Imports, Boulder, Colorado; and Shane F. McClure of the GIA Gem Trade Laboratory in Carlsbad. Dr. James E. Shigley of GIA Research provided constructive review of the manuscript.

Gems & Gemology, Vol. 35, No. 1, pp. 30–41
© 1999 Gemological Institute of America

Hundreds of millions of carats of colorless synthetic sapphire are manufactured annually (all growth techniques combined), according to B. Mudry of Djvahirdjian in Monthey, Switzerland, a leading producer of Verneuil synthetics (pers. comm., 1997). He estimates that about 5%–10% of this production (50–100 million carats) is used by the jewelry industry. Distinguishing natural from synthetic colorless sapphire can often, but not always, be accomplished by standard gemological testing (see below). However, this distinction is time consuming for large parcels, and it is difficult to impossible for melee-size stones.

As first described more than 50 years ago (Wild and Biegel, 1947), natural colorless corundum can be separated from flame-fusion synthetic colorless corundum (only Verneuil material was being produced at that time) by a difference in transparency to short-wave ultraviolet (SWUV) radiation. The present study shows that the difference in SWUV transparency is a result of the difference in trace-element chemistry between natural and synthetic colorless sapphire. We also demonstrate that SWUV transparency testing is valid for Czochralski-grown synthetic colorless sapphire, too. Therefore, this technique can help meet the need for a simple, cost-effective method to mass screen this relatively inexpensive gem material.

BACKGROUND

Natural Colorless Sapphire. Colorless sapphire is a relatively pure form of aluminum oxide (Al_2O_3); it is often inaccurately called “white sapphire.” Truly colorless sapphire is quite uncommon, and most “colorless” sapphire is actually near-colorless, with traces of gray, yellow, brown, or blue. For the purposes of this article, both colorless and near-colorless sapphires will be referred to as “colorless.” The primary source for this material has been, and remains, Sri Lanka.

Colorless sapphire was a common diamond simulant in

Figure 1. Colorless sapphire continues to be popular in jewelry, especially for items such as tennis bracelets, but also as single stones. The larger loose sapphire is 4.44 ct; the tennis bracelet contains a total weight of 4.33 ct; the stone in the pendant is 8.56 ct and the sapphire in the ring is 5.17 ct. Courtesy of Sapphire Gallery, Philipsburg, Montana; photo © Harold & Erica Van Pelt.



the late 19th and early 20th centuries. In the early 1970s, it first began to be used as an inexpensive starting material for blue diffusion-treated sapphires (Kane et al., 1990). At around the same time, large quantities of colorless sapphire were heat treated to produce yellow sapphire (Keller, 1982). The demand for colorless sapphire increased significantly in the late 1980s to early 1990s. This was a result of the greater interest in blue diffusion-treated sapphires (Koivula et al., 1992), and colorless sapphire's increasing popularity in jewelry as an affordable alternative to diamond that could be used as melee, for tennis bracelets, or attractively set as a center stone (Federman, 1994).

From 1993 through the first half of 1994, a steady demand for faceted colorless sapphire caused the per-carat price to almost double, to US\$70 per carat retail ("White sapphire sales up 172%," 1994). Colorless sapphire jewelry (figure 1) has remained

popular ("Demand strong for white sapphires," 1996; M. Schramm, pers. comm., 1999), and has fueled a market for synthetic colorless sapphire.

Synthetic Colorless Sapphire. Synthetic sapphire has been produced by several growth techniques—in particular, flux, hydrothermal, flame-fusion, and Czochralski. However, because of manufacturing costs, only two types of synthetic colorless sapphire are typically used as gems: flame-fusion (Verneuil, 1904) and Czochralski "pulled" (Rubin and Van Uitert, 1966). Early in the 20th century, flame-fusion synthetic colorless sapphire was the first synthetic gem material to be used as a diamond simulant (Nassau, 1980, p. 210). However, other synthetic gem materials have since surpassed colorless synthetic sapphire for this purpose because of the significantly lower refractive index and dispersion of corundum as compared to diamond.



Figure 2. These stones (0.32 ct to 3.08 ct) formed part of the sample set used in this study. The colorless sapphires on the left are synthetic, and those on the right are natural. Photo © Tino Hammid and GIA.

Early synthetic sapphire produced by the Verneuil method often contained characteristic growth defects, such as striations and inclusions. These defects were unacceptable to the industrial market, which required extremely high (“optical”) quality synthetic sapphire. This led to the development of several new growth techniques, including the Czochralski method, which provides the highest-quality single crystals for application in high-performance optics, sapphire semiconductor substrates, watches, and bearings (Nassau, 1980, p. 84). With these refinements, the characteristics that were previously used to separate natural from synthetic colorless sapphire became less obvious or were eliminated, and the separation became considerably more difficult.

Review of Identification Techniques. In many instances, larger natural and synthetic colorless sapphires (see, e.g., figure 2) can be separated by standard gemological methods, such as microscopy (for the identification of inclusions and the study of growth structures visible with immersion) or UV-induced fluorescence (see below). However, smaller,

melee-size sapphires may not exhibit any characteristic inclusions or growth structures. R.I. and S.G. values are of no help, as they are identical for synthetic and natural stones (Liddicoat, 1987, p. 338).

Inclusions. Natural colorless sapphire contains the same distinctive inclusions encountered in other color varieties of corundum: silk (fine, needle-like rutile or boehmite crystals), groups of rutile needles intersecting in three directions at 60° to one another, zircon crystals surrounded by stress fractures, and well-defined “fingerprint” inclusions (figure 3) that consist of large networks of irregular fluid-filled cavities (Gübelin, 1942a and b, 1943; Kane, 1990). Two- and three-phase inclusions may be encountered, as well as small crystals of spinel, uraninite, mica, pyrite, apatite, plagioclase, albite, and dolomite (Gübelin and Koivula, 1992; Schmetzer and Medenbach, 1988).

Colorless synthetic sapphire may exhibit growth-induced inclusions, typically small gas bubbles (figure 4) or unmelted aluminum oxide particles that occur individually, in strings, or in “clouds.” Gas bubbles may appear round or elongated in a flask or tadpole shape (figure 5). The gas bubbles may follow curved trajectories, allowing indirect observation of the curved striae that are otherwise invisible in colorless synthetic sapphire (Webster, 1994).

The irregularly shaped gas bubbles in synthetic corundum could be mistaken for natural crystal inclusions with partially dissolved crystal faces. Occasionally, undissolved alumina may take on the appearance of a natural inclusion (Webster, 1994). As noted above, however, recent production tech-

Figure 3. This “fingerprint” is actually a partially healed fracture that exhibits a network of fluid inclusions; it is typical of natural colorless sapphire. Photomicrograph by Shane Elen; magnified 20×.

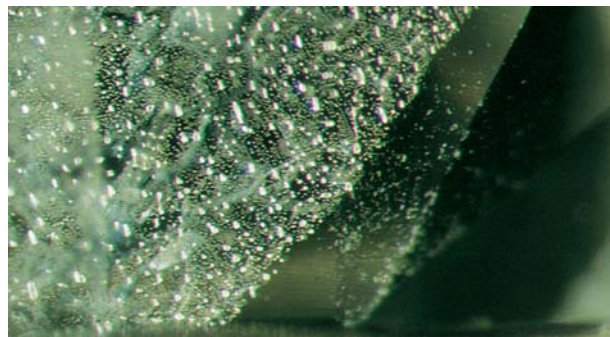




Figure 4. This group of gas bubbles is typical of Verneuil synthetic sapphire. Photomicrograph by Shane Elen; magnified 20 \times .

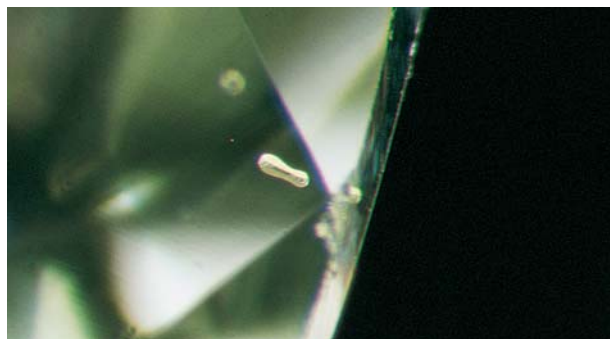


Figure 5. Although bubbles are uncommon in Czochralski-grown synthetic sapphires, this flask-shaped bubble was noted in one of the samples. Photomicrograph by Shane Elen; magnified 20 \times .

niques have almost entirely eliminated any characteristic inclusions, especially in the case of Czochralski-grown synthetic corundum, which has a strictly controlled growth environment.

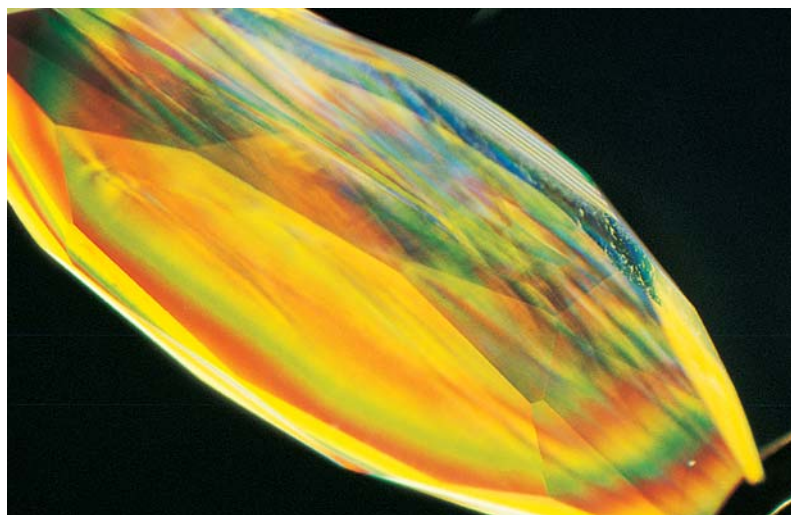
Growth Structures. Immersion microscopy often can reveal internal growth features such as twinning or growth planes in corundum (Smith, 1996). The detection of Plato lines (Plato, 1952; figure 6) may identify Verneuil synthetic sapphire, which does not always exhibit visible growth features. However, heat treatment of colorless flame-fusion synthetic sapphire can make growth structures even less apparent (Kammerling and Koivula, 1995), and we have never observed Plato lines in colorless synthetic sapphire grown by the Czochralski method. Furthermore, observation of growth structures by immersion microscopy is not easy, and requires some practice and understanding of crystallography.

Other Techniques. Energy-dispersive X-ray fluorescence (EDXRF) spectrometry has been used for the chemical analysis of many different gemstones (Stern and Hänni, 1982), most recently for the separation of natural from synthetic ruby (Muhlmeister et al., 1998). This semi-quantitative method used to identify trace elements is particularly suited for gemstones such as colorless sapphire that may not exhibit inclusions or growth features. However, the technique requires expensive equipment and a trained operator, and it can test only one stone at a time.

In addition, natural and synthetic colorless sapphires may exhibit different luminescence reactions to UV radiation, cathode rays (electron beam), and X-rays (Anderson, 1990; Webster, 1994). Some gemologists have used UV luminescence (figure 7)

as a first step in separating batches of natural and synthetic colorless sapphire: Stones that show chalky blue fluorescence to SWUV radiation are considered synthetic, but those that are inert could be either natural or synthetic, so they must be individually evaluated for other distinguishing characteristics (C. Carmona, pers. comm., 1999). However, because the intensity and color of the luminescence is not consistent within each group (i.e., natural or synthetic), luminescence is not a conclusive test. UV fluorescence or cathodoluminescence can be used for positive identification of colorless sapphire only when characteristic growth features—such as the angular growth zoning typical of natural stones

Figure 6. Plato lines may be observed in some Verneuil synthetic sapphire by viewing the sample (while it is immersed in methylene iodide) down the optic axis with cross-polarized light. Photomicrograph by Shane Elen; magnified 3 \times .



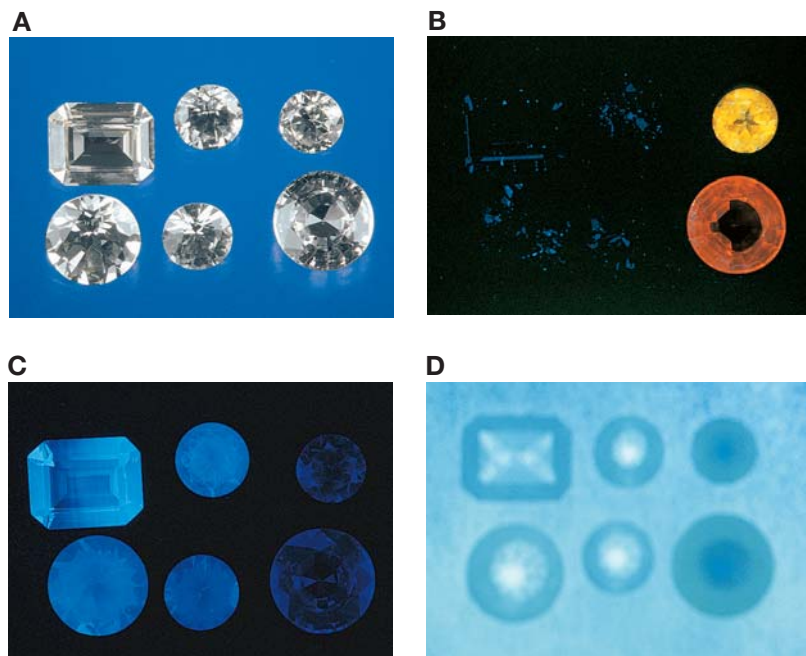


Figure 7. These six samples of natural (two on the far right) and synthetic (the Czochralski, the two in the middle; Verneuil, the two on the far left) sapphires range from 0.78 to 2.75 ct. They were photographed with: (A) natural light, (B) long-wave (LW) UV, (C) SWUV, and (D) in the SWUV transparency tester. Here, the synthetic samples are inert to LWUV, while the natural stones fluoresce strongly yellow and orange; all the synthetics fluoresce chalky blue to SWUV, but the natural stones are inert (the slight blue is due to reflection from the synthetics). Although these fluorescence colors are typical, they are not consistent. The natural sapphires appear dark in the SWUV transparency tester because they absorb SWUV; the synthetic sapphires appear transparent. Photo A by Maha DeMaggio; B–D by Shane Elen.

(figure 8) and the curved striae seen in synthetic sapphires (figure 9)—are observed in the luminescence patterns (Ponahlo, 1995; Kammerling et al., 1994). However, these features may be difficult to resolve, and magnification is frequently required.

More than 50 years ago, Wild and Biegel (1947) noted that natural and synthetic (Verneuil) colorless sapphires differed in their transparency to short-wave UV radiation (again, see figure 7). Colorless synthetic corundum subsequently was found to exhibit transparency down to 224 nm, whereas colorless natural corundum did not transmit below 288 nm (Anderson and Payne, 1948). Theoretically, pure corundum is extremely transparent to short-wave UV because of its lack of impurities, and should exhibit transparency down to 141 nm (French, 1990). As the level of impurities increases, the transparency to SWUV decreases. Although transparency to SWUV may be decreased in stones that are heavily flawed, the colorless sapphire in the jewelry market is typically “eye clean.”

Yu and Healey (1980) applied these SWUV transparency differences to the separation of natural from synthetic *colored* corundum by means of an instrument called a *phosphoroscope* (Yu and Healey, 1980). Its use for this purpose was limited, though, because colored synthetic corundum grown by the hydrothermal and flux methods often exhibited SWUV absorption similar to that of natural corundum of comparable color. However, hydrothermal

and flux synthetic sapphires are not commercially available in colorless form, so we felt this technique could be useful for this separation.

MATERIALS AND METHODS

A total of 112 colorless natural and synthetic sapphires were characterized for this study. The 72 natural samples were all faceted stones. They ranged

Figure 8. Although cathodoluminescence has been used to reveal the characteristic straight growth bands in this natural colorless sapphire, these bands often can be observed with long-wave UV radiation or immersion microscopy. Photomicrograph by Shane Elen; magnified 3.5x.



from 0.05 to 3.08 ct (2.0–8.4 mm) and originated from Sri Lanka (66), Montana (1), Myanmar (1), Umba (1), and unknown sources (3). The synthetic sapphires consisted of 39 faceted samples (0.05–3.82 ct, 2.0–9.5 mm) and one Verneuil-grown half boule (18.3 ct). The faceted synthetic sapphires included five flame-fusion and four Czochralski-grown samples of known growth method. The 30 remaining faceted synthetic samples were of unknown growth method. In addition, a single 8 mm round brilliant hydrothermal colorless sapphire, which had been grown for experimental purposes (Walter Barshai, pers. comm., 1997), was obtained from Tairus.

Of the 112 samples, the origin of 43 natural and 22 synthetic faceted sapphires was confirmed by the presence of characteristic inclusions or growth structures observed using immersion microscopy or luminescence patterns. The remainder, generally the smaller samples, exhibited no readily identifiable features, so we accepted their origins as represented by the reliable sources who supplied them.

We performed EDXRF analysis on 26 natural and 19 synthetic samples of known origin with a Tracor Spectrace 5000 X-ray system, using conditions established for ruby analysis (see Muhlmeister et al., 1998). The purpose was twofold: to determine the usefulness of this technique to separate natural from synthetic colorless sapphires, and to provide more information about how trace-element content affects the SWUV transparency. EDXRF analysis was restricted to samples greater than 4 mm in diameter (approximately 0.3 ct) because of limitations imposed by the X-ray spot size of this equipment. Absorption spectra were obtained on all 112 samples at room temperature with a Hitachi U4001 spectrophotometer. Spectra for a few of the samples were collected from 250 nm to 750 nm; however, since data above 350 nm were not important for this study, the remaining analyses were collected in the UV range from 250 nm to 350 nm.

At the request of GIA, John Schnurer of Physics Engineering (Yellow Springs, Ohio) constructed a SWUV transparency instrument for the separation of natural from synthetic colorless sapphire (see Box A). This instrument was based on the phosphoroscope originally proposed by Yu and Healey (1980), and was constructed to provide a relatively simple, rapid, and cost-effective means of separation.

RESULTS

Chemical Composition. The natural sapphire samples typically contained three or more trace ele-



Figure 9. Curved striae cannot be detected in colorless synthetic sapphires with standard visible lighting. However, some flame-fusion synthetic sapphires may reveal this feature when exposed to SWUV radiation. Photomicrograph by Shane Elen; magnified 6x.

ments (table 1; figure 10). The most significant was iron (Fe); other elements recorded include titanium (Ti), calcium (Ca), and gallium (Ga). Vanadium (V) and chromium (Cr) were only detected at concentrations just exceeding the detection limit of the instrument. In general, no trace elements were detected in the flame-fusion and Czochralski-grown synthetic sapphires, although some samples showed very small amounts of Ca, Ti, and Fe—again, just exceeding the detection limit. The iron content was much greater in the natural sapphires (0.021–0.748 wt.% FeO) than in the synthetic sapphires (up to 0.007 wt.% FeO; table 1). Qualitative analyses of the hydrothermal synthetic sapphire showed significant amounts of Fe, Ga, cobalt (Co), and copper (Cu).

UV-Visible Spectrophotometry. Table 1 lists the wavelengths for the absorption cutoff of all the samples analyzed by EDXRF. The natural colorless sapphires typically showed a sharp absorption cutoff (i.e., complete absorption) below 280–300 nm, whereas the synthetic sapphires showed at most only a slight increase in absorption at around 250 nm (see, e.g., figure 11). Note that three of the small (about 2 mm) colorless natural sapphires exhibited a gentle increase in absorption, only slightly greater than that of the synthetic samples. The hydrothermal synthetic sapphire exhibited a sharp absorption cutoff at 280 nm, similar to natural sapphire.

SWUV Transparency. All 72 natural colorless sapphires tested with the modified phosphoroscope were opaque to SWUV, and all 40 flame-fusion and Czochralski-grown synthetics were transparent to SWUV. The single hydrothermal synthetic sapphire

BOX A: THE MODIFIED PHOSPHORSCOPE TO TEST SHORT-WAVE UV TRANSPARENCY

The modified phosphoroscope (after Yu and Healey, 1980; figures A-1 and A-2) we constructed for this study consists of a glass plate that has been coated with a specially selected (proprietary) nontoxic phosphor, an overhead short-wave ultraviolet (SWUV) lamp, and a mirror positioned at a 45° angle below the glass plate. To reduce glare, the glass plate and mirror were placed inside a box, with the UV lamp mounted externally. The phosphor-coated glass plate fluoresces when exposed to SWUV radiation (254 nm wavelength), creating a brightfield background.

For testing, we placed the samples table-down on the glass plate, one or more at a time, and observed their transparency to SWUV in the mirror (figure A-3). Samples that are opaque to SWUV (i.e., natural colorless sapphires) do not allow the radiation to pass through the stone to the phosphor-coated plate, so there is no fluorescence where the stone contacts the plate. Consequently, natural colorless

sapphires appear in the mirror as dark spots on a brightfield background. Conversely, samples that are transparent to SWUV (such as melt-grown synthetic colorless sapphires) allow UV radiation to pass through the stone to the phosphor-coated plate. So the Verneuil- and Czochralski-grown synthetic colorless sapphires typically appear in the

Figure A-1. The SWUV transparency tester was constructed with simple materials: wood, a mirror, a glass plate, and drafting vellum. A Gem Instruments long-wave/short-wave UV lamp is positioned over an opening at the top of the box.

The samples are loaded into the upper part of the unit through a door on the back. The number of stones that can be tested depends on the size of the fluorescent plate, which in turn is governed by the size and intensity of the SWUV source; 100 melee-size stones can easily be accommodated in this particular unit. Photo by Maha DeMaggio.



appeared opaque to SWUV. Some of the natural and synthetic colorless sapphires acquired a slight brown bodycolor as a result of their exposure to SWUV radiation. However, they returned to their original color after gentle heating under the bulb of an incandescent desk lamp (Kammerling and McClure, 1995).

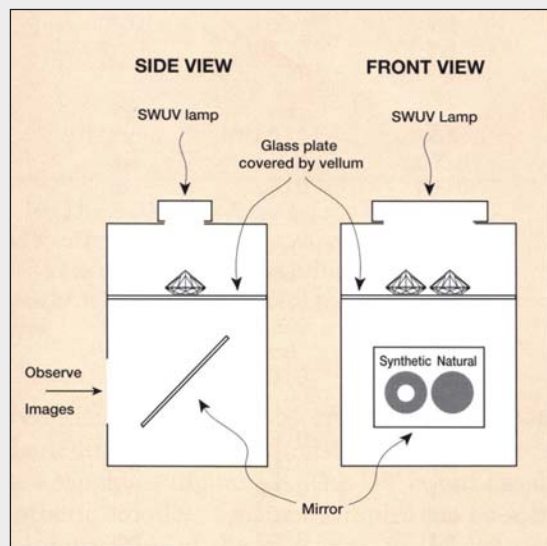
DISCUSSION

The higher concentrations of Fe, Ti, and Ga aid in distinguishing natural colorless sapphire from the synthetic material. However, Fe is the dominant impurity in natural colorless sapphire, where it is present in quantities typically 10 to 100 times greater than in its synthetic counterpart. The

mirror as light spots, each of which is surrounded by a dark perimeter, imposed on the brightfield background. The dark perimeter results from total internal reflection of the incident radiation as it passes through the pavilion and strikes the bezel facets. Therefore, it is important when testing the transparency to observe only the response in the central part of the gem (Yu and Healey, 1980).

Following the lead provided by Yu and Healey (1980), one of the authors (SE) subsequently modified this unit by replacing the proprietary phosphor with a readily available translucent paper product (drafting vellum) that has all the necessary fluorescence characteristics described above. This product

Figure A-2. This schematic diagram of the SWUV transparency unit shows how the image of the samples that have been illuminated by the UV lamp is reflected toward the viewer. This also illustrates the appearance, observed in the mirror, of a natural sapphire (right) as compared to its synthetic counterpart (left).

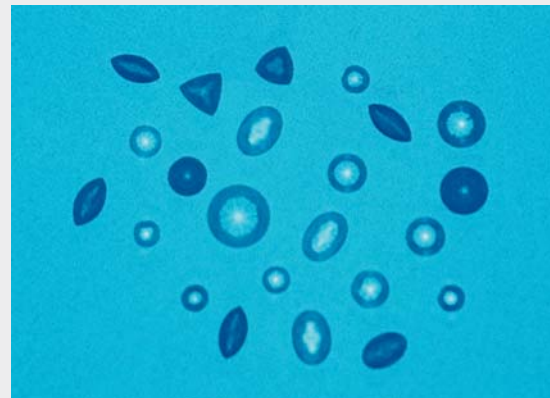


is more uniform than the proprietary phosphor, and it has brighter fluorescence characteristics; it is also inexpensive, clean, and nontoxic.

The modified phosphoroscope is simple to construct from inexpensive materials (about \$30 excluding the UV source). Those interested in constructing a SWUV transparency tester should review the limitations listed in the Discussion and note the following recommendations:

1. Wear UV-protective glasses, and take precautions not to expose unprotected skin to the SWUV radiation when the gems are sorted by hand.
2. Use known samples of natural and synthetic colorless sapphires as standards for evaluating the reactions of the unknown stones. These "control" samples should be 3 to 4 mm in diameter and free from abundant eye-visible inclusions. These may also be useful in selecting the appropriate paper product for the luminescent screen when constructing a phosphoroscope.

Figure A-3. When viewed with the SWUV transparency tester, the natural colorless sapphires appear opaque, while the synthetic samples are transparent, resulting in a bright spot in their central regions. These samples range from 0.20 to 2.12 ct. Photo by Shane Elen.



hydrothermal synthetic sapphire also contained Fe and Ga, but it showed distinctive Co and Cu, too—neither of which was detected in any of the other samples. The impurities detected in natural sapphires (i.e., Fe, Ti, Ca, and Ga) are present essentially as transition metal ions, so their absorptions affect the ultraviolet transparency of the colorless sapphires as measured by UV-visible spectropho-

tometry. The absorption is due to charge-transfer processes, as well as to electronic transitions of isolated metal ions (McClure, 1962). Although all the transition impurities induce absorption in the UV, iron is the primary cause because its absorption is situated closer to the visible range and it is the dominant impurity in the natural material. Consequently, we plotted the relationship between

TABLE 1. Semi-quantitative EDXRF data and UV absorption maxima for natural and synthetic colorless sapphires.

Sample no.	Weight (ct)	Oxide (wt.%)						UV abs. ^a (nm)
		CaO	TiO ₂	V ₂ O ₃	Cr ₂ O ₃	FeO	Ga ₂ O ₃	
Natural								
1433	3.08	bdl ^b	0.006	bdl	bdl	0.066	0.033	292
1447 ^c	2.10	0.061	0.030	bdl	bdl	0.090	0.055	300
2190	0.78	0.047	0.036	0.003	bdl	0.116	0.012	292
2191	1.10	bdl	0.032	0.004	0.002	0.246	0.019	298
2336	1.84	bdl	0.018	bdl	bdl	0.117	0.003	293
2348 ^c	0.33	0.045	0.048	0.004	bdl	0.099	0.005	293
2349 ^c	0.19	0.069	0.049	bdl	bdl	0.091	0.008	290
2885	0.84	0.021	0.016	0.005	0.015	0.748	bdl	310
2886	2.75	bdl	0.018	0.002	bdl	0.058	0.013	290
4009	0.98	0.011	0.033	0.005	0.002	0.046	0.018	290
4010	0.94	bdl	0.018	bdl	bdl	0.079	0.005	292
4011	0.59	0.029	0.031	bdl	bdl	0.097	0.014	290
4012	0.64	0.039	0.026	bdl	bdl	0.122	0.011	292
4013	0.76	0.016	0.022	0.003	0.006	0.096	0.014	288
4014	0.75	bdl	0.013	bdl	bdl	0.042	0.005	284
4015	0.49	0.039	0.065	bdl	bdl	0.048	0.016	282
4016	0.42	0.041	0.028	bdl	bdl	0.134	0.015	291
4017	0.60	0.039	0.024	bdl	bdl	0.021	0.014	280
4018	0.33	0.048	0.043	0.004	bdl	0.091	0.011	290
4019	0.33	0.029	0.028	bdl	bdl	0.148	0.013	292
4020	0.47	0.037	0.011	bdl	bdl	0.179	0.013	291
4021	0.42	0.060	0.010	bdl	0.003	0.108	0.012	292
4022	0.32	0.066	0.017	bdl	bdl	0.276	bdl	296
4023	0.61	0.029	0.028	0.005	bdl	0.055	0.023	288
4024	0.74	0.017	0.036	0.006	bdl	0.059	0.020	291
4025	0.57	0.017	0.024	0.004	bdl	0.070	0.017	292
Synthetic – Czochralski								
1635	0.89	0.022	bdl	bdl	bdl	bdl	bdl	<250
2334	0.91	0.017	bdl	bdl	bdl	0.003	bdl	<250
2352	0.98	0.027	0.009	bdl	0.003	0.004	bdl	<250
2353	1.01	0.024	bdl	bdl	0.004	0.002	bdl	<250
Synthetic – Flame Fusion								
2335	2.81	bdl	0.005	bdl	bdl	bdl	bdl	<250
2509	18.30	bdl	bdl	bdl	bdl	bdl	bdl	<250
2887	2.44	0.016	0.009	bdl	bdl	0.002	bdl	<250
2888	2.12	bdl	0.005	bdl	bdl	0.002	bdl	<250
2889	2.49	bdl	bdl	bdl	bdl	bdl	bdl	<250
2890	1.45	bdl	bdl	bdl	0.003	0.002	bdl	<250
Synthetic – Unspecified Method of Synthesis								
3931a	1.12	0.019	0.009	bdl	bdl	0.003	bdl	<250
3931b	1.06	0.028	bdl	bdl	bdl	0.005	bdl	<250
3931c	0.99	0.015	bdl	bdl	bdl	0.002	bdl	<250
3931d	1.06	0.018	0.006	0.003	bdl	0.004	bdl	<250
3932a	0.66	bdl	0.006	bdl	bdl	0.003	bdl	<250
3932b	0.64	0.024	bdl	bdl	bdl	bdl	bdl	<250
3932c	0.61	0.038	bdl	bdl	bdl	0.007	bdl	<250
3933	3.82	bdl	bdl	bdl	bdl	bdl	bdl	<250
3934	1.10	0.014	bdl	bdl	bdl	0.003	bdl	<250
Detection Limits^d								
	0.3	0.019	0.009	0.004	0.004	0.004	0.005	
	0.6	0.013	0.005	0.003	0.003	0.003	0.003	
	1.0	0.009	0.005	0.003	0.002	0.002	0.002	

^aFor the synthetic samples, the absorption cutoff did not occur in the measured region above 250 nm, so we infer <250 nm.

^bbdl = below detection limit. MnO was looked for, but not detected in any of the samples.

^cThree samples also contained traces of Si, probably due to the presence of silicate inclusions: 1447 = 0.251 wt.% SiO₂, 2348 = 0.396 wt.% SiO₂, and 2349 = 0.428 wt.% SiO₂.

^dDetection limits vary according to the weight of the sample. Calculated after Jenkins (1980).

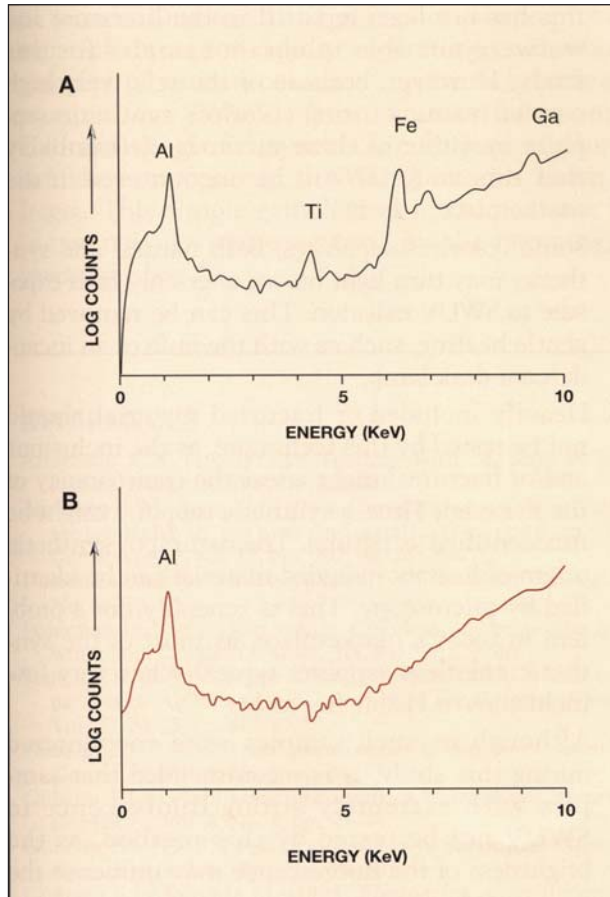


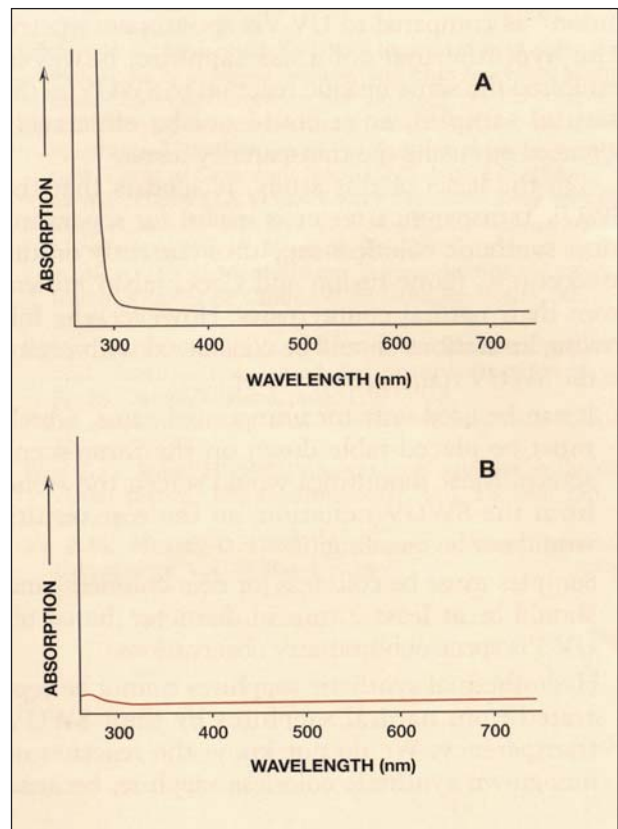
Figure 10. The EDXRF spectra typical of natural (A) and synthetic (B) colorless sapphires are distinct. The natural sapphires exhibit more trace-element peaks (e.g., Fe, Ti, and Ga) than the synthetic sapphires.

the Fe content and the UV absorption cutoff for natural, flame-fusion, and Czochralski-grown synthetic colorless sapphires (figure 12). The UV cutoff for all the synthetic colorless sapphire samples can be seen at the intersection of the two axes, in the bottom left corner of the plot (at 250 nm). In reality, this point only represents a slight increase in absorption, and the true cutoff occurs below 250 nm (i.e., below the wavelength range of the UV-Vis spectrophotometer used for this study). Together, the EDXRF and the UV-Vis data illustrate the effect of trace-metal impurity concentrations on SWUV transparency; in particular, they show how the increase in iron content results in a decrease in SWUV transparency.

For the natural colorless sapphires, the sharp increase (or cutoff) in SWUV absorption below

280–300 nm indicates complete absorption, and therefore the point at which they become opaque to SWUV radiation. With the exception of the hydrothermal sample—which showed an absorption cutoff at 280 nm, and therefore could not be separated from natural sapphire using UV-Vis spectrophotometry—the synthetic colorless sapphires exhibited only a slight increase in SWUV absorption around 250 nm, which indicates that they are relatively transparent to SWUV. Although most of the small (2 mm) natural sapphires exhibited a sharp absorption edge, a few did not. Certainly, some natural colorless sapphires with low impurity concentrations may be thin enough to allow some transmission of SWUV. In our sample, this appeared to be the case particularly for the few melee stones

Figure 11. These UV-Vis spectra are representative of natural (A) and synthetic (B) colorless sapphires. The natural samples show a sharp absorption cutoff below 280–300 nm, whereas no cutoff is evident in this region for the synthetic sapphires. Therefore, the natural sapphires were opaque to SWUV radiation (at 254 nm), but the synthetic samples were transparent.



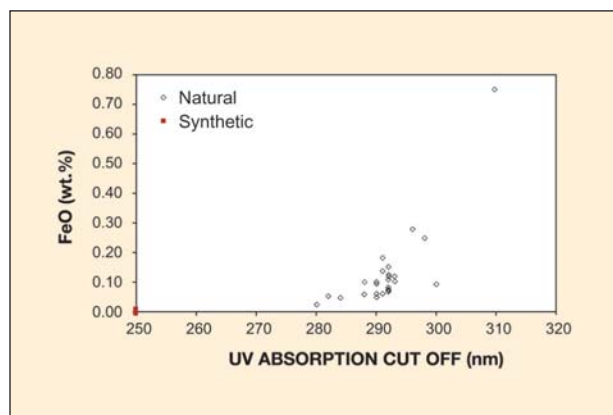


Figure 12. Iron is the primary cause of absorption in colorless sapphire. In general, the natural sapphires analyzed in this study showed higher UV absorption values with increasing iron content. The synthetic sapphires (19 represented here) all showed very low iron contents (<0.007 wt.% FeO), and had UV cutoffs below the wavelength for SWUV radiation (~250 nm).

that were cut with shallow pavilions. Nevertheless, these samples appeared opaque in the SWUV transparency tester, perhaps because of the lower “resolution” as compared to UV-Vis spectrophotometry. The hydrothermal colorless sapphire, however, exhibited the same opaque reaction to SWUV as the natural samples, so it could not be effectively screened out using the transparency tester.

On the basis of this study, it appears that the SWUV transparency tester is useful for separating most synthetic colorless sapphires currently on the market (i.e., flame-fusion and Czochralski grown) from their natural counterparts. However, the following limitations should be considered with regard to the SWUV transparency tester:

1. It can be used only for unmounted gems, which must be placed table down on the fluorescent screen. Most mountings would screen the stone from the SWUV radiation, so the test results would not be meaningful.
2. Samples must be colorless (or near-colorless) and should be at least 2 mm in diameter (based on UV-Vis spectrophotometry observations).
3. Hydrothermal synthetic sapphires cannot be separated from natural sapphires by their SWUV transparency. We do not know the reaction of flux-grown synthetic colorless sapphire, because

this has not been reported in the literature and we were not able to obtain samples for this study. However, because of the relatively high cost of manufacturing colorless synthetic sapphire by either of these methods, it is unlikely that this material will be encountered in the marketplace.

4. Some colorless sapphires, both natural and synthetic, may turn light brown after only brief exposure to SWUV radiation. This can be removed by gentle heating, such as with the bulb of an incandescent desk lamp.
5. Heavily included or fractured material should not be tested by this technique, as the inclusions and/or fractures might affect the transparency of the material. Thus, a synthetic sapphire might be misidentified as natural. The natural or synthetic origin of heavily included material can be identified by microscopy. This is generally not a problem in today’s marketplace, as most of the synthetic colorless sapphire typically has very few inclusions or visible fractures.
6. Although no such samples were encountered during this study, it is recommended that samples with extremely strong fluorescence to SWUV not be tested by this method, as the brightness of the fluorescence may influence the “apparent” opacity of the sample and result in an incorrect identification.

CONCLUSION

With standard gemological techniques, only one colorless sapphire at a time can be investigated. In addition, it is usually more difficult to identify smaller stones, because they commonly do not show any diagnostic features. The advanced techniques of EDXRF analysis and UV-Vis spectrophotometry are also useful to separate most natural and synthetic colorless sapphires. Our trace-element data illustrate that, in general, natural colorless sapphires contain greater amounts of Fe, Ti, Ca, and Ga than do their synthetic counterparts. UV-Vis data further confirm that synthetic colorless sapphires are more transparent to SWUV, because they exhibit only a small increase in absorption at approximately 250 nm. By comparison, natural colorless sapphires typically exhibit total absorption below 280–300 nm.

However, EDXRF and UV-Vis spectrophotometry are not readily available to most gemologists; nor are they economical for testing large quantities

of stones. Our modified phosphoroscope proved most effective for rapidly separating unmounted samples of natural colorless sapphires (which are opaque to SWUV) from flame-fusion and Czochralski-grown synthetic colorless sapphires (which are transparent to SWUV), in sizes 2 mm or larger. This simple gemological instrument can be inexpensively manufactured by the gemologist (again, see box A).

The SWUV transparency tester cannot be used to separate natural sapphire from hydrothermal synthetic sapphire. However, the relatively high cost of producing colorless hydrothermal synthetic sapphire (Walter Barshai, pers. comm., 1997) precludes its widespread use by the jewelry industry. If necessary, in most cases results from the SWUV transparency test can be confirmed with a gemological microscope.

REFERENCES

- Anderson B.W. (1990) *Gem Testing*, 10th ed. Rev. by E.A. Jobbins, Butterworth & Co., London.
- Anderson B.W., Payne C.J. (1948) Absorption of visible and ultraviolet light in natural and artificial corundum. *The Gemmologist*, Vol. 17, No. 207, pp. 243–247.
- Demand strong for white sapphires (1996) *Jewellery News Asia*, No. 147, p. 84.
- Federman D. (1994) Gem profile: Colorless sapphire—The great white hope. *Modern Jeweler*, Vol. 93, No. 8, p. 44.
- French R.H. (1990) Electronic band structure of Al_2O_3 with comparison to AlON and AlN. *Journal of the Ceramic Society*, Vol. 73, No. 3, pp. 477–489.
- Gübelin E.J. (1942a) Local peculiarities of sapphires. *Gems & Gemology*, Vol. 4, No. 3, pp. 34–39.
- Gübelin E.J. (1942b) Local peculiarities of sapphires. *Gems & Gemology*, Vol. 4, No. 4, pp. 50–54.
- Gübelin E.J. (1943) Local peculiarities of sapphires. *Gems & Gemology*, Vol. 4, No. 5, pp. 66–69.
- Gübelin E.J., Koivula J.I. (1992) *Photoatlas of Inclusions in Gemstones*. ABC Edition, Zurich, Switzerland.
- Jenkins R. (1980) *An Introduction to X-ray Spectrometry*. Heyden, Philadelphia.
- Kammerling R.C., DeGhionno D., Madison P. (1994) Gem Trade Lab notes: Synthetic sapphire, another striae resolution technique. *Gems & Gemology*, Vol. 30, No. 4, p. 270.
- Kammerling R.C., Koivula J.I. (1995) Microscope lighting techniques for identifying melt-grown synthetics. *Bangkok Gems and Jewellery*, Vol. 8, No. 7, pp. 88–94.
- Kammerling R.C., McClure S.F. (1995) Gem Trade Lab notes: Synthetic sapphire, with color changed by UV radiation. *Gems & Gemology*, Vol. 31, No. 4, p. 271.
- Kane R.E., Kammerling R.C., Koivula J.I., Shigley J.E., Fritsch E. (1990) The identification of blue diffusion-treated sapphires. *Gems & Gemology*, Vol. 26, No. 2, pp. 115–133.
- Kane R.E. (1990) Gem Trade Lab notes: Sapphire—Large colorless. *Gems & Gemology*, Vol. 26, No. 3, pp. 225–226.
- Keller P.C. (1982) The Chanthaburi-Trat gem field, Thailand. *Gems & Gemology*, Vol. 18, No. 4, pp. 186–196.
- Koivula J.I., Kammerling R.C., Fritsch E. (1992) Gem news: Update on diffusion-treated sapphires. *Gems & Gemology*, Vol. 28, No. 1, pp. 62–63.
- Liddicoat R.T. Jr. (1987) *Handbook of Gem Identification*, 12th ed. Gemological Institute of America, Santa Monica, CA.
- McClure D.S. (1962) Optical spectra of transition-metal ions in corundum. *Journal of Chemical Physics*, Vol. 36, No. 10, pp. 2757–2779.
- Muhlmeister S., Fritsch E., Shigley J.E., Devouard B., Laurs B.M. (1998) Separating natural and synthetic rubies on the basis of trace element chemistry. *Gems & Gemology*, Vol. 34, No. 2, pp. 80–101.
- Nassau K. (1980) *Gems Made By Man*. Chilton Book Co., Radnor, PA.
- Plato W. (1952) Oriented lines in synthetic corundum. *Gems & Gemology*, Vol. 7, No. 7, pp. 223–224.
- Ponahlo J. (1995) Cathodoluminescence (CL) of gemstones and ornamental stones. *Analisis*, Vol. 23, No. 1, pp. M30–M33.
- Rubin J.J., Van Uitert L.G. (1966) Growth of sapphire and ruby by the Czochralski technique. *Materials Research Bulletin*, Vol. 1, pp. 211–214.
- Schmetzer K., Medenbach O. (1988) Examination of three-phase inclusions in colorless, yellow, and blue sapphires from Sri Lanka. *Gems & Gemology*, Vol. 24, No. 2, pp. 107–111.
- Smith C.P. (1996) Introduction to analyzing internal growth structures: Identification of the negative *d* plane in natural ruby. *Gems & Gemology*, Vol. 32, No. 3, pp. 170–184.
- Stern W.B., Hänni H.A. (1982) Energy dispersive X-ray spectrometry: A non-destructive tool in gemmology. *Journal of Gemmology*, Vol. 18, No. 4, pp. 285–296.
- Verneuil A. (1904) Memoire sur la reproduction du rubis par fusion. *Annales de Chimie et de Physique*, Ser. 8, No. 3, pp. 20–48.
- Webster R., Read P.G. (1994) *Gems: Their Sources, Descriptions and Identification*, 5th ed. Butterworth-Heinemann Gem Books, Oxford, England, pp. 851, 931–933.
- White sapphire sales up 172% (1994) *Jewellery News Asia*, No. 120, pp. 92–94.
- Wild G.O., Biegel H. (1947) Absorption of sapphire in the ultraviolet region. *The Gemmologist*, Vol. 16, No. 195, pp. 279–280.
- Yu R.M., Healey D. (1980) A phosphoroscope. *Journal of Gemmology*, Vol. 17, No. 4, p. 250.

Editors

Thomas Moses ♦ Ilene Reinitz

Shane F. McClure

GIA Gem Trade Laboratory

Contributing Editors

GIA Gem Trade Laboratory, East Coast

G. Robert Crowningshield

GIA Gem Trade Laboratory, West Coast

Karin Hurwit ♦ Mary L. Johnson

Cheryl Y. Wentzell

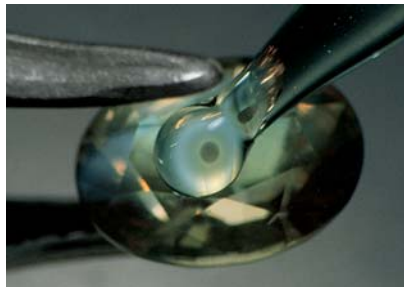
**ALEXANDRITE,
With a Fish-Eye Effect**

The West Coast Gem Trade Laboratory recently examined an oval mixed cut that proved to be somewhat unusual. We identified the 2.93 ct stone as a natural alexandrite chrysoberyl; it appeared red-brown in incandescent light, with a slight change of color toward green in fluorescent light.

The identification as chrysoberyl was a relatively routine gemological matter. However, while looking for a biaxial interference figure using a small glass ball as a condensing lens and cross-polarized light, we noted a fish-eye type of optical effect (figure 1). Further examination of the stone at different levels of magnification revealed a slightly milky cloud that appeared to be composed of extremely fine, submicroscopic particles.

The "fish-eye" could only be resolved in one particular direction

Figure 1. This unusual fish-eye effect was noted in a 2.93 ct alexandrite when it was observed in one particular direction through a condensing lens with cross-polarized light.



through the stone. Since this did not coincide with an optic axis in the chrysoberyl, we did not suspect that it was an odd interference phenomenon.

A similar optical effect—although not as well defined—can be seen when cat's-eye imitations made from fiber-optic glass are examined with a condensing lens down the length of their fibers. If the submicroscopic inclusions in the natural chrysoberyl are aligned in the same manner as the glass fibers in the imitation cat's-eyes, the effect shown might be due to a tunneling of light through the lens. If this is indeed the cause of the optical effect shown in figure 1, then an important question remains unanswered: Why is cross-polarized light necessary to resolve the "fish-eye"? This is the first time that we have seen such an optical effect in any natural gemstone, and we have many questions. More detailed optical examination, probably including the study of a thin section under high magnification, would be required to find a more complete answer.

John I. Koivula

DIAMOND, with a Stellate Cloud

During the course of diamond quality grading, graders occasionally encounter unusual internal features. Even though such features can reduce the overall clarity of their host, and consequently the assigned clarity grade, they can be interesting from a scientific standpoint. Such was the case with the stellate "cloud" in a near-colorless round-brilliant-cut diamond shown in figure 2.

Because of the extent and translucency of this cloud, together with its prominent position centered under the table facet, the assigned clarity grade was understandably low. Nevertheless, the exotic hexagonal, star-like appearance of this cloud gave the interior of the diamond an attractive geometric character. While geometric clouds are occasionally seen in diamonds, most of these are cubic or octahedral in shape; a hexagonal form is considerably rarer.

The cloud shown here appears to be a phantom of either a hextetrahedron or hexoctahedron diamond crystal. In these two crystal forms, the triangular faces are divided into six sections each. As shown in figure 3, this division changes a four-sided tetrahedron to a 24-sided hextetrahedron, or an eight-sided octahedron to a 48-sided hexoctahedron.

When one looks perpendicular to a hextetrahedral or hexoctahedral crystal face, one sees a form composed of six pie-shaped faces divided by six interfacial ridges. This gives the appearance of a six-rayed star. A phantom formed in a diamond crystal with this habit might show a stellate cloud in a cut stone. If the cutter oriented the rough so that a hextetrahedral or hexoctahedral face was nearly parallel to the plane of the table facet, then the star-shaped cloud would be readily visible through the table facet.

Editors' note: The initials at the end of each item identify the editor(s) or contributing editor(s) who provided that item.

Gems & Gemology, Vol. 35, No. 1, pp. 42-46

©1999 Gemological Institute of America



Figure 2. The hexagonal star-shaped cloud in this diamond appears to represent a phantom with a rare crystal form. The riblike extensions possibly follow previous growth steps. Magnified 10 \times .

The view of this cloud was distorted by reflection and refraction from the facets, so no firm conclusion could be drawn as to which crystal form it represented. Suffice it to say that this is a most unusual inclusion in a diamond, and in this writer's opinion it is also quite beautiful.

John I. Koivula

EMERALD, The Case of the Invisible Filler

The use of organic compounds to fill surface-reaching fractures and fracture systems in emeralds has been a standard practice for many years. It is often said that virtually all emeralds today are "oiled," and this generalization has been borne out by our experience in the laboratory. The visibility of surface-reaching fractures is reduced by replacing the air that normally fills those openings with an organic compound that has a refractive index similar to that of the host emerald. The treatment effectively reduces the mirror-like reflective quality of any cracks and, in the process, improves the apparent color intensity of the emerald. This method of emerald enhancement was thoroughly addressed by R. Ringsrud in the Fall 1983 issue of *Gems & Gemology* ("The oil treatment of emeralds in Bogotá, Colombia," pp. 149–156), and by R. Kammerling et al.

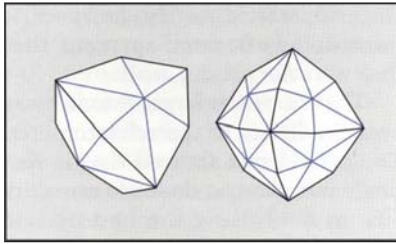


Figure 3. These line drawings illustrate two rare forms found among isometric crystals such as diamond. The hextetrahedron at left has 24 faces, formed by dividing each of the four triangular faces of a tetrahedron into six parts. The hexoctahedron at right exhibits 48 faces.

in the Summer 1991 issue ("Fracture filling of emeralds: Opticon and traditional 'oils,'" pp. 70–85).

Occasionally, a surface-reaching fracture will intersect an included crystal or a larger primary fluid-inclusion chamber (a negative crystal), thereby exposing the inclusion to the surface. Some of these mineral inclusions are very vulnerable to attack by acidic solutions. Most notable are carbonates, such as calcite and dolomite. If exposed to the surface, these inclusions are often dissolved away, sometimes during the cleaning processes used on rough crystals to remove iron oxide and hydroxide stains and other undesirable debris. This leaves a comparatively large void, with the shape of the original mineral inclusion, in the emerald. Fluid inclusions simply drain out once they have been intersected by a fracture, also leaving a void.

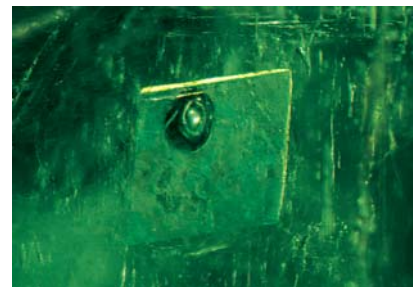
When such voids are filled with an organic compound, the result is never perfect. The refractive indices of the fillers we have encountered to date do not exactly match that of the surrounding emerald. (In particular, they cannot match *both* refractive indices of an emerald.) The relief caused by this difference in refractive indices makes the filled voids visible. Gas bubbles trapped in the filler within these relatively large voids often make the treatment even more obvious (see, e.g., figure 4). As a result,

such voids often provide the first indications of treatment when the emerald is examined with magnification.

Therefore, staff members in the West Coast lab were somewhat surprised to encounter a treated natural emerald with a filled void that was essentially invisible. This lack of relief indicated that the R.I. of the filling agent was nearly identical to those of the emerald—more so than any other filler we had previously examined. The only reason this void was recognized at all was because it contained three gas bubbles. As can be seen in figure 5, the bubbles appear to be enclosed within the emerald itself; the chamber surrounding them is virtually invisible. No form of microscopic manipulation or creative illumination, including an attempt at the Becke line test, adequately resolved the complete outline of the void. Nor did we see any flash-effect colors in the "invisible" fractures that must have been intersecting it. The refractive index of the emerald was 1.576–1.581, so the filler must have had an R.I. between those two readings.

Although there is no doubt that a filler was present, the combined limitations of nondestructive testing and the short time available for examination prevented us from determining

Figure 4. Note the prominent gas bubble and yellowish liquid filling in this rhombohedral void. As is typical of most large voids in such treated emeralds, the chamber is readily visible because the refractive index of the filler is sufficiently different from one or both of those of the surrounding emerald. Magnified 15 \times .



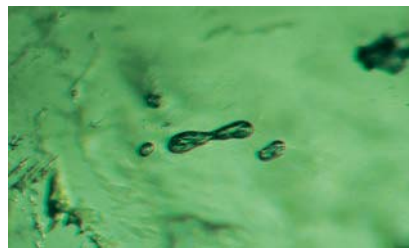


Figure 5. These three trapped gas bubbles provide the only evidence of a filled void in this emerald; the filler itself is virtually invisible, probably because its refractive index is very close to both those of the host emerald. Magnified 30 \times .

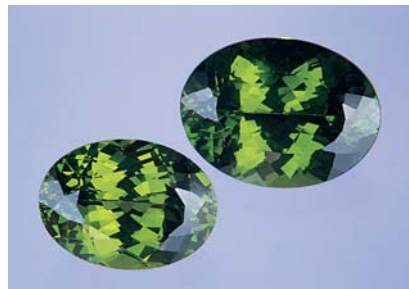
its precise nature. We did observe that the filling material was either solid or highly viscous. It is possible that a mixture of substances yielded the very close match in optical properties that made this filling invisible. However, because natural emeralds exhibit a range of refractive indices, we think it unlikely that such "invisible" treatment will become the norm.

John I. Koivula

GLASS Imitation of Peridot

Two green oval faceted gems were recently sent to the West Coast laboratory (figure 6). An identification was requested for the larger of the two (26.28 ct). When they were examined face up, both looked very much like the peridot that has been coming out of Pakistan for the last several years.

Figure 6. These green ovals look like peridot, but they were identified as glass. The sample on the right weighs 26.82 ct.



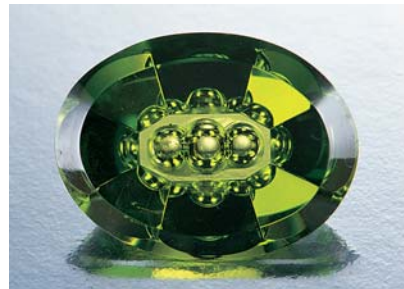
Once we started testing, however, it immediately became apparent that they were not peridot at all.

The R.I. of the larger "stone" was over the limits of the refractometer. The polariscope showed that it was singly refractive, and we measured its S.G. at 4.43 using the hydrostatic method. These properties indicate a high-property glass. Microscopic examination revealed parallel flow lines, confirming this conclusion.

We subsequently learned that these two samples had been purchased at the 1998 Tucson gem show as Chinese peridot by renowned American gem cutter Arthur Anderson. He acquired a few of these pieces in their faceted shape, intending to recut them into some of his own designs. As he started to cut the first one (figure 7), he noticed that the material did not react to the cutting wheel like peridot, at which point he sent the two pieces to the GIA Gem Trade Laboratory for identification.

Glass has been used to imitate a multitude of gemstones for centuries. In recent years, it has been found in salted parcels of amethyst, aquamarine, and Mexican fire opal, to name just a few examples. Careful manipulation of the color makes it impossible to distinguish these glasses from the stones they imitate by visual appearance alone. Of course, any number of gemological tests (e.g., optic character) can separate these

Figure 7. The behavior during carving of a third sample, similar to those shown in figure 6, made the cutter suspicious that the material was not peridot. This glass imitation weighs 18.81 ct.



imitations quickly in most instances, but it is easy to forget that any stone could potentially be glass.

This is the first instance we have encountered of material sold as Chinese peridot turning out to be glass. This should, however, serve as a warning for anyone in the market for such peridot to be wary of this imitation.

SFM and IR

JADEITE with Unusual Evidence of Enhancement

The identification of treated jadeite has been a persistent problem for gemologists and jewelers for many years. The methods of treatment most commonly used historically, such as dyeing and waxing, are intended to enhance the outward appearance of lower-quality, or poorly polished, material. More recently, there has been a proliferation of jadeite objects treated throughout by a multi-step process that involves heating, acid "bleaching," and impregnation with an organic polymer (see, e.g., E. Fritsch et al., "Identification of bleached and polymer-impregnated jadeite," *Gems & Gemology*, Fall 1992, pp. 176–187). The jadeite gems, jewelry, and carvings enhanced by this process are widely known as "bleached jade" or "B-jade."

Because the vast majority of the surface-reaching fissures filled by this process are extremely fine, there is usually no visible evidence of treatment even with a microscope. Today, most laboratory gemologists rely primarily on Fourier-transform infrared spectrometry (FTIR) to detect B-jade. So, while it is relatively easy for a gemologist to identify a material as jadeite, detection of bleaching and impregnation almost always requires advanced testing with FTIR.

On rare occasions, however, a large surface pit or wider fissure will contain visual evidence of this treatment in the form of polymer residue and/or trapped gas bubbles. Such was the case for a mottled bright green-and-white jadeite bangle that was recently submitted to the West

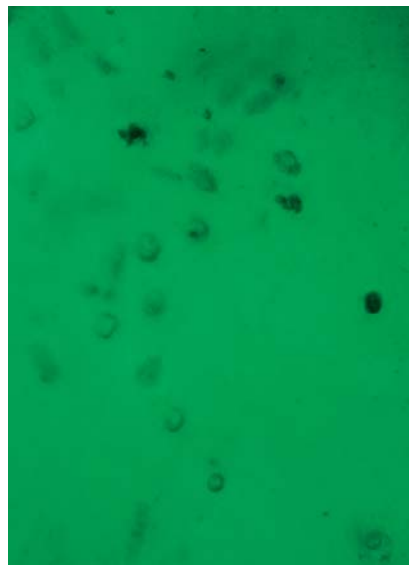


Figure 8. Subsurface bubbles provide evidence of enhancement in a bangle bracelet of "B-jade." Some of the bubbles are badly distorted, while others are nearly spherical. Their reduced visibility is caused by the translucency of the overlying jadeite. Magnified 40x.

Coast laboratory for identification and testing for possible enhancement. Without magnification, this bracelet looked like many other jadeite objects we receive in the laboratory. When we examined it with a microscope at even 10x magnification, however, numerous small gas bubbles (figure 8) were easily seen. Some of the bubbles were almost per-

Figure 9. The suture lines in this natural-color black cultured pearl are readily visible with magnification and reflected light. Magnified 30x.



fectly spherical, while others were quite distorted. They were individually contained in small voids in the jadeite that we speculated must have been formed during the acid bleaching.

It is possible that acid-dissolvable inclusions of some mineral, such as a carbonate, may have been removed from the jadeite by the acid treatment. The resulting voids were then only partially filled with the polymer during the impregnation step, leaving a gas bubble as proof of enhancement.

John I. Koivula

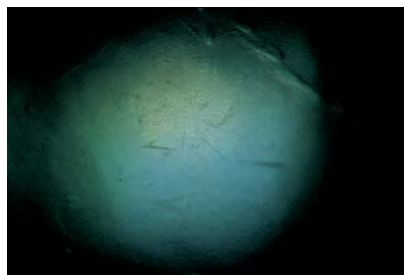
CULTURED PEARLS

Black, Surface Enhanced

Suspecting that a strand of 11 mm black circled pearls had been treated to enhance their appearance, a client submitted them to our West Coast lab for identification. All the pearls had an extremely high luster and showed pronounced purplish pink and green overtones. While handling them, the client had noticed a peculiar smoothness on the pearls' surface and that they were somewhat sticky to the touch.

Gemological tests verified that they were indeed cultured pearls of natural color, and microscopic examination with reflected overhead illumination showed a highly reflective surface, with a top nacre layer that was very transparent. Pearls (both natural and cultured) normally show a pattern of fine lines (figure 9), called suture lines, that are a characteristic growth feature in the nacre. However,

Figure 10. Suture lines are much more difficult to resolve in this coated black cultured pearl. Magnified 30x.



the suture lines in these black cultured pearls were barely visible (figure 10). We did see some fine polishing lines, but they appeared to be located slightly underneath the surface rather than on it. The needle probe left a smooth indentation, similar to that left on plastic-coated materials, which raised more doubts regarding the surface condition. Without using destructive testing methods, though, we could not verify the type of treatment. Therefore, we obtained the client's permission to remove one cultured pearl (figure 11) for further testing.

We checked this sample with a thermal reaction tester. The hot needle initially left only a chalked groove, as would be expected for a soft carbonate. However, with continued application of heat, the chalked material began to coagulate. This change proved that some foreign material was present on the surface. We sent the cultured pearl to a laboratory that specializes in polymer analysis to identify the surface material. The laboratory reported that this foreign material was a poly-dimethyl siloxane, a form of silicone that is occasionally applied to pearls to enhance their appearance. KH

Imitation Tahitian Pearls

The occurrence of gray-to-black natural pearls is rare (see, e.g., M. Goebel and D. M. Dirlam, "Polynesian black pearls," *Gems & Gemology*, Fall 1989, pp. 130-148). Throughout the trade, dark-colored pearls are presumed to be cultured, but a laboratory

Figure 11. The coating on this black cultured pearl greatly enhances all aspects of its appearance.





Figure 12. The grayish green spheres (10.15–10.25 mm in diameter) in these ear studs make convincing imitations of Tahitian black pearls.

report is often desired to determine whether the color is natural or the result of treatment. Less frequent is the need to determine whether the material itself is genuine (that is, natural/cultured or imitation). A recent example of such a submission, examined in the West Coast lab, are the ear studs shown in figure 12.

To the unaided eye, these grayish green spheres (which measured 10.15–10.25 mm in diameter) have the appearance of “pistachio” colored Tahitian cultured pearls. However, magnification revealed several sub-surface features that were typical for glass or plastic, but unlike any we have ever seen in a pearl: swirl marks, flow lines, and gas bubbles beneath a smooth, transparent coating (figure 13). We obtained a refractive index of

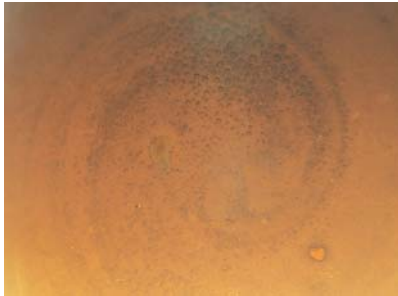


Figure 13. With 10× magnification, the imitation pearls shown in figure 12 exhibit gas bubbles and swirl marks below a smooth coating.

1.50 by the spot method, and determined that the optic character was isotropic. We saw no lines with a desk-model spectroscope, and we observed weak, chalky green fluorescence to both long- and short-wave UV radiation. These properties proved these items to be imitation pearls.

A strand of silvery gray to black imitation pearls was seen in the West Coast lab a few years ago (Fall 1995 Gem Trade Lab Notes, pp. 202–203). Those beads had an odd, rubbery surface texture, and a layered construction was visible at the drill holes. We determined that one of the layers was bismoclite (a bismuth oxide chloride used as a coating material), which gave those imitation pearls their color. Unfortunately, the mounting of each of the recently examined ear studs

Figure 14. This 1.44 ct chatoyant purplish brown cabochon was identified as the rare mineral taaffeite.



Figure 15. A group of parallel reflective planar inclusions with striations was responsible for the cat's-eye effect in this taaffeite. Magnified 30×.



prevented observation of a drill hole or determination of their composition.

CYW and IR

Cat's-Eye TAAFFEITE

Some gems commonly exhibit phenomena, such as change of color (alexandrite), chatoyancy (chrysoberyl), and asterism (sapphire). Occasionally we are reminded that any gem material potentially can show a phenomenon, even if such a phenomenon was not seen in that material before.

Such was the case with a 1.44 ct chatoyant cabochon recently submitted to the West Coast lab for identification. The purplish brown stone had a fairly well developed “eye” (figure 14). We determined an R.I. of 1.72 by the spot method, and an S.G. of 3.68 by the hydrostatic method. The stone showed a uniaxial optic figure, weak pleochroism, and was inert to both long- and short-wave ultraviolet radiation. These properties all pointed to the rare gem mineral taaffeite as the identity of the cabochon. However, we had never seen a cat's-eye taaffeite before. Since we could only get a spot R.I., and thus no estimate of the birefringence, we decided to analyze the stone on the Raman spectrometer. The Raman spectrum confirmed that the stone was indeed taaffeite.

Microscopic examination did not reveal the parallel needles or growth tubes normally found in a chatoyant stone. Instead, there were parallel reflective planar inclusions with striations (figure 15). These striations, along with the reflectivity of the inclusions, caused the chatoyancy. We have seen similar reflective inclusions as a cause of chatoyancy on at least one other occasion (see “Cat's-eye sapphire,” Summer 1995 Gem Trade Lab Notes, pp. 126–127). *SFM*

PHOTO CREDITS

Maha DeMaggio photographed figures 6, 7, 11, 12, and 14. John Koivula was the photographer for figures 1, 2, 4, 5, 8, 9, 10, and 13. Shane McClure provided figure 15.

Editors ✕ Mary L. Johnson and John I. Koivula

Contributing Editors

Dino DeGhionno and Shane F. McClure,
GIA GTL, Carlsbad, California

Emmanuel Fritsch, IMN, University of Nantes, France

Henry A. HŠnni, SSEF, Basel, Switzerland

Karl Schmetzer, Petershausen, Germany

TUCSON 1999

The 1990s ended with a quietly productive season at the various Tucson gem and mineral shows, where many new items were brought to our attention. The editorial team spent two weeks visiting almost all of the 27 shows. Information was also gathered by GIA Gem Trade Laboratory staff members Philip Owens, Cheryl Wentzell, Dr. Ilene Reinitz, Karin Hurwit, Maha DeMaggio, and contributing editors Dino DeGhionno and Shane McClure, as well as by Phil York and Wendi Mayerson of GIA Education, collection curator Jo Ellen Cole, and *G&G* senior editor Brendan Laurs. Highlights of the information we gathered, and some of the many items seen, are presented here. Additional reports from Tucson '99 will appear in future Gem News sections.

DIAMONDS

Fashioned diamonds from the Ekati mine, Northwest Territories, Canada. Faceted diamonds from Canada's first diamond mine, Ekati (see, e.g., Winter 1998 Gem News, pp. 290–292), were available in the United States for the first time, at the AGTA show. Craig de Gruchy of Sirius Diamonds (at the booth of Barker & Co., Scottsdale, Arizona) showed Dr. Ilene Reinitz several round brilliants. Six of the diamonds, which weighed from 0.75 to 1.01 ct, had been graded by the GIA Gem Trade Laboratory; they ranged in color from E to J, and in clarity from VVS₁ to VS₁ (figure 1). All had been cut by Sirius Diamonds, Vancouver, British Columbia, which is one of the first companies to manufacture Canadian diamonds in that country. According to Mr. de Gruchy, each Ekati diamond faceted by Sirius is laser inscribed with a polar bear logo (figure 2).

Synthetic diamonds widely available. Alex Grizenko of the Russian Colored Stone Co. (RCS), Golden, Colorado, reported that scientists working for RCS have improved their growth processes and quality control over the last year. They can now grow synthetic diamonds with few

inclusions in relatively large sizes—up to 5.5 ct rough. A variety of colors are being produced: yellow, blue, and treated pink, red, orange, and color-change (figure 3), as well as near-colorless material. Yields for fancy shapes, especially rectangles, can be quite high, resulting in fashioned synthetic diamonds up to about 4.5 ct. Faceted goods are sold under the trademark "Ultimate Created Diamonds." The company currently produces 300–400 carats of crystals per month. However, they are poised to increase production at least 10-fold, in about equal amounts of near-colorless and saturated colors.

According to Mr. Grizenko, these synthetic diamonds have the same properties as those GIA has examined in the past (see, e.g., J. E. Shigley et al., "A chart for the sep-

Figure 1. These six diamonds (0.75–1.01 ct) represent some of the early production from the newly opened Ekati mine, Northwest Territories, Canada. They were fashioned in Canada as well. Courtesy of Sirius Diamonds; photo by Maha DeMaggio.





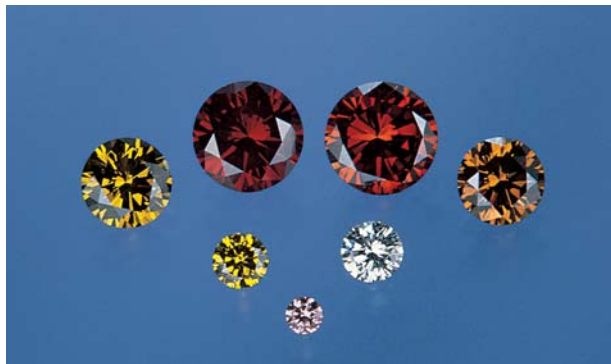
Figure 2. Sirius Diamonds laser inscribes a stylized polar bear on the girdle of each Ekati diamond they facet. This stone weighs about 1 ct; photo © Anthony de Goutière.

aration of natural and synthetic diamonds," Winter 1995 *Gems & Gemology*, pp. 256–264; Spring 1995 Gem Trade Lab Notes, pp. 53–54; and Winter 1998 Gem Trade Lab Notes, pp. 286–287). Dr. Ilene Reinitz, who spoke with Mr. Grizenko at Tucson, confirmed the reported properties. In particular, all of the RCS near-colorless synthetic crystals show phosphorescence after exposure to SWUV, although the strength of the reaction varies greatly from one sample to another.

Dr. Reinitz also spoke to another purveyor of synthetic diamonds, Dr. Leonid Pride of the Morion Co., Brighton, Massachusetts. This company works with crystal growers in the eastern Ukraine. Dr. Pride showed her (predominantly rough) yellow, blue, treated red, and heavily included near-colorless synthetic diamonds, ranging from 0.18 to 1.24 ct.

In addition, Gem News editor John I. Koivula saw a yellow synthetic diamond crystal at the GJX show that had triangular growth hillocks (resembling etched trigons, but raised above the surface of the crystal) on the octahedral faces. These hillocks showed a positive orientation to the host face—that is, the triangles were parallel to the triangular sides of the octahedral crystal face—instead of the negative orientation seen for the etched

Figure 3. These 0.04–1.07 ct round brilliant synthetic diamonds illustrate some of the as-grown and treated colors available this year. Courtesy of Alex Grizenko; photo by Maha DeMaggio.



trigons on natural diamond crystals (a photograph of similar triangular growth hillocks on a synthetic diamond is shown as figure 5 on p. 48 of the Spring 1997 issue of *Gems & Gemology*). In conversations with dealers offering both materials at the show, Mr. Koivula was amused to note that synthetic moissanite was more expensive than synthetic diamond.

COLORED STONES AND ORGANIC MATERIALS ■

Cat's-eye andradite from San Benito County, California.

Although this material is not new (see T. Payne, "The andradites of San Benito County, California," Fall 1981 *Gems & Gemology*, pp. 157–160), recently a lease was activated in the area by Steve Perry Minerals, Davis, California. Mr. Perry was marketing rough and cut material that had been mined at the Yellow Cat claim since November 1998 (figure 4). The deposit is located about 12 km northwest of the Benitoite Gem mine, within the same serpentinite body. The andradite occurs in fractures cutting the serpentinite, together with dark green chlorite (ripidolite) and traces of black perovskite and white apatite.

The deposit produces mineral specimens and limited amounts of cutting rough of the yellow-green to brownish orange variety of andradite. So far, about 300 grams of cat's-eye rough have been extracted, with cutting yields of about 10%–15%. Smaller quantities of facet-grade rough are recovered: Mr. Perry estimates that the year's production will yield about 50 carats of faceted material (see, e.g., figure 5). Of this, about 75% is "honey colored," 10% is orange, and 10% is yellow (all of these hues are sometimes called "topazolite" in the trade);

Figure 4. Small amounts of cat's-eye andradite (shown here, 0.65 and 6.09 ct) are being mined again in San Benito County, California. Courtesy of Steve Perry; photo by Maha DeMaggio.



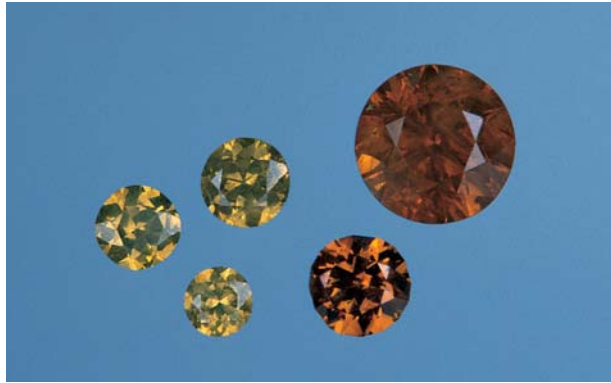


Figure 5. These faceted andradites (0.07–1.10 ct) illustrate the range of color in which the San Benito County material occurs. The greenish yellow stones are typically smaller than those with warmer yellow to orange hues. Courtesy of Steve Perry and Len Pisciotta; photo by Maha DeMaggio.

another 5% is greenish yellow. Eye-clean finished stones are usually smaller than 0.5 ct, and faceted andradite larger than 1 ct from San Benito County is rare. Mr. Perry projects that small amounts of material will continue to be produced.

An “enhydro” emerald from Colombia. Although quartz crystals and agates are the usual hosts for large fluid inclusions with movable gas bubbles—“enhydros”—this rare feature can occur in other materials as well. For instance, enhydro gypsum crystals were seen at Tucson this year, and we reported previously on an enhydro tanzanite crystal (Spring 1997 Gem News, p. 66). At the 1999 AGTA show, Ray Zajicek of Equatorial Imports, Dallas, Texas, loaned us for examination a 20.95 ct doubly terminated emerald crystal (figure 6) he had acquired in Colombia that contained a large fluid inclusion with a movable gas bubble (figure 7). The fluid-and-gas-filled inclusion in the emerald was so large that the specific gravity of the stone was only 2.62 (rather than a more typical 2.72). Additional properties were: refractive indices—1.573–1.580; “Chelsea” color filter reaction—red; and inert to both long- and short-wave UV radiation. The inclusion appeared natural, and we saw no evidence of clarity enhancement in this emerald crystal.

Abundant eudialyte. Eudialyte is an uncommon mineral found in alkali- and zirconium-rich intrusive rocks, such as in Canada, Greenland, and the Kola Peninsula of Russia; it is rarely seen in gem quality. (The gemological properties of a faceted 0.36 ct eudialyte from southwestern Quebec, Canada, were reported in the Winter 1993 Gem News, pp. 287–288.) This year, Bill Gangi of Bill Gangi Multisensory Arts, Tucson, had unusually large quantities of fashioned eudialyte, which he showed contributing editor Shane McClure. Mr. Gangi has purchased the entire mine run of more than 45 kg of brightly colored eudialyte-rich rock from a mine in eastern

Canada. The eudialyte was fashioned into free-form cabochons that incorporated portions of the matrix (figure 8). Other minerals present in this material were feldspar, tourmaline, fluorite, and galena.

New cuts for Oregon sunstone. Although not a new material, Oregon sunstone continues to intrigue cutters and carvers (see, for example, the “watermelon” sunstone carving in Summer 1997 Gem News, p. 145). Klaus Schäfer of Idar-Oberstein, Germany (who was in Tucson at the booth of Bernhard Edelsteinschleiferei, Idar-Oberstein), has faceted this material in a manner that highlights the copper inclusions (figure 9). Schäfer includes matte-finished facets in his fashioned sunstones to direct light through the stone so that some inclusion layers are prominent and others recede. To produce the matte facets, he uses silicon carbide applied with a brush to an iron lap wheel.

Near-colorless forsterite. K. K. Malhotra of K&K International, Falls Church, Virginia, loaned contributing editor Shane McClure a near-colorless 6.20 ct cushion-cut stone (figure 10) from Sri Lanka. The stone appeared

Figure 6. This Colombian emerald crystal (20.39 × 11.62 × 8.76 mm) contains a large fluid inclusion with a movable gas bubble. Specimen courtesy of Ray Zajicek; photo by Maha DeMaggio.



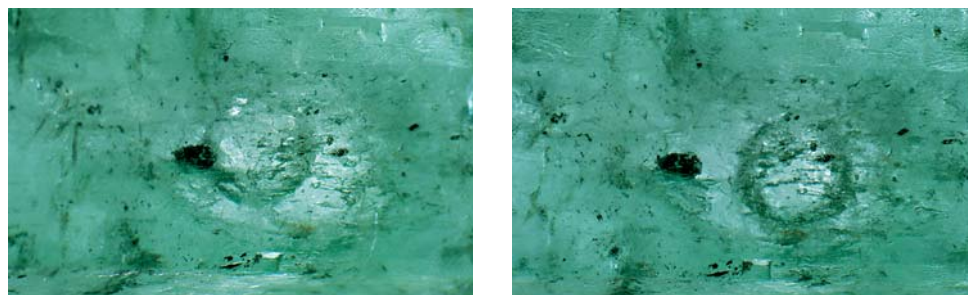


Figure 7. As the emerald is tilted (left, right), the gas bubble moves in the 2.4-mm-long fluid-filled cavity. Photomicrographs by John I. Koivula.

pale green when viewed table-down, but it was essentially colorless when viewed table-up. It had R.I. values of 1.639–1.670 and an S.G. of 3.25. Its absorption spectrum showed only a weak, sharp peak at 495 nm. The stone was inert to both long- and short-wave UV radiation. Microscopic examination revealed numerous parallel strings of whitish clouds. A Raman spectrum had major peaks at 857 and 825 cm^{-1} , and smaller peaks at 968, 919, 608, 434, and 306 cm^{-1} . All of these properties were consistent with olivine that contains little or no iron (i.e., end-member forsterite). EDXRF analysis of the forsterite by GIA Gem Trade Laboratory research associate Sam Muhlmeister revealed major amounts of magnesium and silicon, some iron, minor manganese, and traces of zinc and calcium. The trace elements suggested a natural origin for the stone (see, e.g., K. Nassau, "Synthetic forsterite and synthetic peridot," Summer 1994 *Gems & Gemology*, pp. 102–108).

The most common series in the olivine mineral group is that between forsterite (Mg_2SiO_4) and fayalite (Fe_2SiO_4). The common gem variety of olivine, peridot, is forsterite with about 12 atom percent iron substituting for magnesium (see, e.g., W. A. Deer et al., 1974, *An Introduction to the Rock-Forming Minerals*, Longman Group Ltd., London, pp. 1–7) and R.I. values of 1.654–1.690. This sample of colorless gem-quality forsterite contained only about one-third as much iron as typical peridot (as estimated from the EDXRF data), which would account for its colorless appearance. It was

Figure 8. These five cabochons of eudialyte-rich rock measure about 2–3 cm each. Courtesy of Bill Gangi; photo by Maha DeMaggio.



surprising to see a natural gem forsterite—not a peridot—of this large size.

"Watermelon Garnet." The variety of elbaite tourmaline that has a pink center and green rind is familiar to most people in the gem trade as "watermelon" tourmaline. This form of tourmaline is routinely cut perpendicular to the length of the crystal and sold as polished slices for jewelry applications. Recently, Bill Heher of Rare Earth Mining Co., Trumbull, Connecticut, sent one of the Gem News editors (MLJ) a polished slab and a polished, tapered cabochon that were reminiscent of watermelon tourmaline in color but not pattern (figure 11). According to Mr. Heher, the material was mined in the 1940s in South Africa, and was represented to him as "hydrogrossular garnet" (commonly referred to as "Transvaal Jade"). He was also told that the material had "high concentrations of chromium and manganese."

Refractive index (spot) values of 1.712 were obtained for both the green and pink areas of the cabochon. We did not determine specific gravity because the samples contained a significant amount of matrix. Both the pink and green portions were inert to long- and short-wave UV radiation, but some areas of the matrix showed white fluorescence to long-wave UV.

The absorption spectrum (as seen with a handheld spectroscope) was interesting in that the green end of the cabochon showed a strong single line at 466 nm; howev-

Figure 9. This Oregon sunstone (about 2 cm across) has been fashioned with some matte-finished facets to bring out the appearance of the copper inclusions. Courtesy of Klaus Schäfer; photo by Maha DeMaggio.



er, as the stone was moved from the green to pink portion across the spectroscope, this absorption line gradually became fainter. It completely disappeared in the pink area that was farthest from the green end.

Another interesting characteristic was noted when the cabochon was analyzed along its length with a laser Raman microspectrometer. By comparison with reference spectra, we identified the green end as vesuvianite and the pink end as hydrogrossular, which was consistent with the gemological properties. Raman spectra obtained at spots intermediate between the two ends indicated a mixture of these phases. This gradation in the Raman spectra down the length of the stone supports the observations of the visible-light absorption spectra, since a line at about 466 nm is characteristic of vesuvianite. As the hydrogrossular became the major phase in the mixture, toward the pink end of the cabochon, the 466 nm line faded out.

Because Mr. Heher had been told that the material contained high concentrations of chromium and manganese, we asked Sam Muhlmeister to measure the chemistry using EDXRF spectrometry. An analysis across the entire sample revealed no evidence of Cr. The chemical elements detected were aluminum, calcium, iron, manganese, silicon, strontium, and titanium.

This material presents an interesting nomenclature dilemma. The primary mineral in the green area, vesuvianite, is more familiar to gemologists as idocrase. The pink material is hydroxyl-rich garnet—hibschite, katoite, or hydrous grossular—and usually simply referred to as hydrogrossular. In the samples we saw, there appeared to be a dominance of hydrogrossular (pink) over idocrase (green), so that “hydrogrossular-idocrase” would be an appropriate name to apply to these bicolored, mixed-mineral gemstones. Mr. Heher had several hundred stones in

Figure 10. This 6.20 ct cushion-cut near-colorless stone, reportedly from Sri Lanka, is natural forsterite. Courtesy of K. K. Malhotra; photo by Maha DeMaggio.

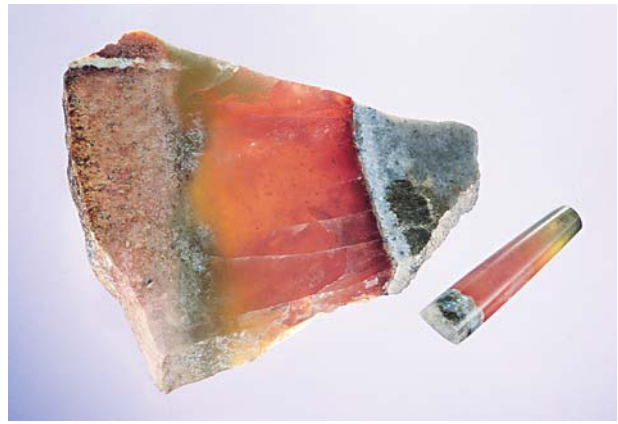


Figure 11. This 8.5 cm polished slab and 25.52 ct cabochon were both cut from hydrogrossular-idocrase rock that was mined in South Africa in the 1940s. Courtesy of Bill Heher; photo by Maha DeMaggio.

Tucson. Because brightly colored bicolored gems are always popular, a consistent supply of good-quality material would create its own market in the areas of designer jewelry and small carvings.

New deposits in India and Nepal. Anil Dohlakia of Anil Dohlakia, Inc., Franklin, North Carolina, had several interesting gems that were recently mined from new deposits in Asia. These included kyanite from Nepal; apatite from Rajasthan, India; and chrysoberyl from Andhra Pradesh, India.

The kyanite (figure 12) was found shortly before the Tucson show. Approximately 500 carats have been faceted from the 5% of the rough that was gem quality. The resulting fashioned stones are somewhat large (to more than 10 ct) and range from medium to dark in tone.

The apatite is also notable for the large pieces recovered; the largest fashioned stone Mr. Dohlakia had (which weighed more than 50 ct) is shown in figure 13. He reported that about 200 kg of apatite were available.

About 500 carats of fashioned cat's-eye chrysoberyl

Figure 12. These kyanite ovals from Nepal weigh 6.07, 7.74, and 10.12 ct. Courtesy of Anil Dohlakia; photo by Maha DeMaggio.



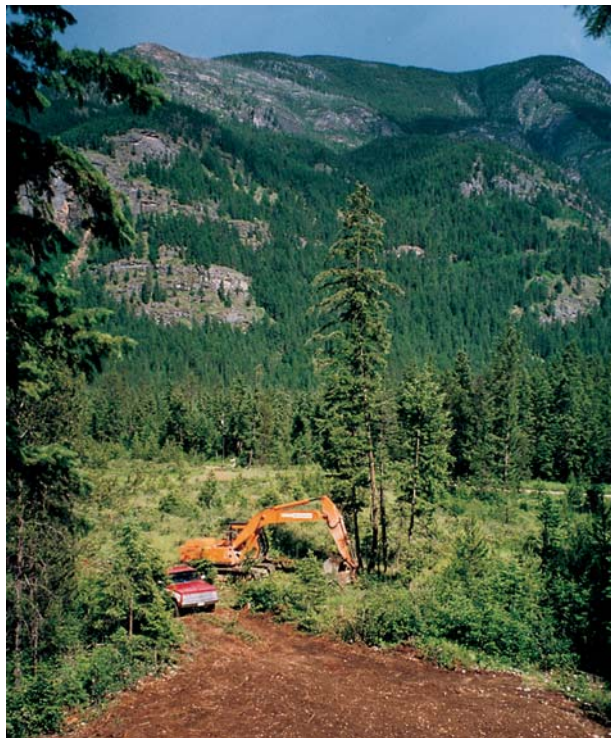


Figure 13. Rajasthan, India, is the source of this faceted apatite, which weighs more than 50 ct and measures 29 x 24 mm. Courtesy of Anil Dohlakia; photo by Maha DeMaggio.

were available from the new find near Vishakhapatnam, Andhra Pradesh State. The cabochons ranged up to 20 ct.

Iolite and other gems from Canada. Canadian mining company Anglo Swiss Resources (Vancouver, British

Figure 14. The Slocan Valley in British Columbia is being explored and mined for several gem minerals by Anglo Swiss Resources. Bulk sampling at the Blu Moon claim is shown here; the Blu Starr claims are visible on the hillside in the background. Photo courtesy of Anglo Swiss Resources.



Columbia) is developing deposits of several colored gem minerals in the Slocan Valley of southeastern British Columbia. The company's claims cover an area of metamorphic host rock that measures 13,000 acres (about 45 km²). The following information is based on discussions with Anglo Swiss president Len Danard—who was showing rough and cut material in Tucson—and information provided by geologist James Laird.

The company began by examining their sapphire prospects, particularly at the Blu Moon and Blu Starr groups of claims (figure 14). Gray-to-black sapphires with good asterism (figure 15) were found in the host rock; Mr. Danard estimates grades of 30 carats of finished cabochons per ton of rock. Heat-treatment experiments produced some improvement in the color, but at the expense of the asterism. Mr. Danard hopes to recover more-profitable goods when they start mining their 1,853 acres of newly permitted placer deposits in the Slocan and Little Slocan Rivers this spring. Bright pinkish red pyrope-almandine garnets (again, see figure 15) were also found in the host rock at the Blu Starr claim. The garnet crystals can exceed 10 cm in diameter, but because they are often highly fractured, the largest stone fashioned to date weighs 3 ct. About 250,000 carats of rough garnet were collected during the 1998 mining season, and yields of 46% were realized from pre-trimmed ore.

In November 1998, iolite (again, see figure 15) was found in the host rock at two separate workings, then known as the Rainbow North and Rainbow South zones. These are believed to be part of one continuous rock unit that extends for more than 2 km along the surface. The largest crystal recovered weighed more than 1,500 ct. However, much of this material is also heavily fractured, so the largest iolite faceted thus far weighs only 0.64 ct. Nevertheless, the material shown to one of the Gem News editors (MLJ) was an attractive deep bluish violet, even in small sizes. The company estimates that about one billion carats can be recovered from the surface layers of the deposit.

Amethyst, light blue beryl, moonstone, titanite, and zircon have also been recovered by Anglo Swiss from the Slocan Valley; as of February 1999, all but the zircon had been faceted. Several varieties of quartz (e.g., smoky, star, rock crystal, and rose) have been recovered, as have Japan-law-twinned quartz crystals for use as mineral specimens. Clearly, this area has the potential to produce a large variety of gem materials.

Jasper “planets.” One of the pleasures of the Tucson experience is finding materials that are reminiscent of other materials. Many of the resulting Gem News entries are cautionary tales, of the “Don’t be fooled by this!” variety. Here is a case where the resemblance is unlikely to cause confusion, however. Two spheres of Mexican jasper (figure 16) were shown to one of the Gem News editors (MLJ) by Jorge A. Vizcarra of OK. Rock’s & Minerals Whole, El Paso, Texas. The spheres are unlikely



Figure 15. Among the gems recovered from the Slocan Valley are star sapphires (upper left; largest stone 18 × 12 mm), pyrope-almandine garnets (upper right; rough 9 mm in diameter), and iolite (left; rough 17 mm long). Courtesy of Len Danard; photos by Jeff Scovil, © Anglo Swiss Resources, Inc.



to be confused with giant planets in the outer solar system, but their colors and markings greatly resemble those of Jupiter and Saturn.

Opal in matrix from Brazil. Carlos Vasconcelos of Vasconcelos Brasil, Governador Valadares, had a few samples of opal with good play-of-color (figure 17) from a new deposit near Tranqueira in Piauí State, northern Brazil. The area lies about 200 km south of previously known opal deposits in Piauí, and was discovered about 5 km southwest of another locality that is being mined for

Figure 16. These are not planets visible in the clear skies of Tucson, but jasper spheres (62.8 and 75.3 mm in diameter) from Mexico. Photo by Maha DeMaggio.



orange opal. The deposit was first found about three years ago, but organized mining is just beginning. About 200 carats of rough have been produced thus far.

White and pastel Chinese freshwater cultured pearls. At the AGTA show, Hussain Rezayee of Freiburg, Germany, and Tetsu Maruyama of C. Link International, Tokyo, showed the *G&G* editors several strands and loose samples of freshwater cultured pearls (figure 18) grown on farms in China. This material has been available in abundance lately, in much larger sizes and far better quality than the “rice pearls” of several years ago. The colors include orange, “lavender,” pink, and white.

According to a company brochure supplied by Mr. Maruyama, the C. Link farms in China have nearly 500,000 pearl oysters each, and the pearls are tissue

Figure 17. This 6 × 5.5 × 2 cm piece of opal in matrix comes from a new deposit in Brazil. Photo courtesy of Carlos Vasconcelos.





Figure 18. These tissue-nucleated freshwater cultured pearls are typical of the better-quality material recently produced in China. The white circled pearls are 11 mm (and larger) in diameter, and the cultured pearls in the other strands range from 9.5 to 11 mm. Courtesy of Hussain Rezayee; photo by Maha DeMaggio.

nucleated rather than bead nucleated. A 9 mm round cultured pearl takes about four years to grow, and those larger than 10 mm require five to seven years. However, 600 tons of 8 mm cultured pearls have been produced (from an unspecified number of farms and an unknown time period). Round tissue-nucleated cultured pearls are rela-

tively rare: Only 3% of the production of 8 mm pearls are considered round by C. Link, and only 5% of this small group are considered top quality.

The largest cultured pearls in this sample measured 12.5 mm in diameter (for rounds) and slightly larger than 15 mm (for button shapes).

Drusy quartz “leaves.” At the booth of Rare Earth Mining Co., Trumbull, Connecticut, Dr. Ilene Reinitz saw many colors of drusy agate that had been carved into leaf shapes by Greg Genovese of Cape May, New Jersey (figure 19). We found these shapes to be an interesting and attractive use of geode material—which was, in this case, reportedly from Rio Grande do Sul, Brazil. The leaves ranged from about 10 × 16 mm to over 7 cm long; Mr. Genovese carved 1,000 such pieces during the five months preceding the show. Colors in the rough were chosen for their resemblance to natural leaves, although some material was dyed blue or black.

Twelve-rayed star quartz from Sri Lanka. Star quartz was reported in *Gems & Gemology* several times in the 1980s. These entries included white and brown stones with six-rayed stars, a blue-gray stone with a 12-rayed star, quartz with one strong band (a cat’s-eye) as well as less prominent rays, and Sri Lankan samples with multiple centers of asterism (see, e.g., Gem Trade Lab Notes: Winter 1982, p. 231; Summer 1984, pp. 110–111; Spring 1985, pp. 45–46; and Spring 1987, pp. 47–48). This year in Tucson, Michael Schramm of Michael Schramm Imports, Boulder, Colorado, showed Dr. Ilene Reinitz a 31.37 ct star quartz from Sri Lanka (figure 20) that had



Figure 19. These five leaf shapes were carved from drusy quartz by Greg Genovese; the large “oak leaf” on the lower right measures 7.2 × 2.8 cm. Courtesy of Rare Earth Mining Co.; photo by Maha DeMaggio.



Figure 20. This 31.37 ct star quartz from Sri Lanka shows many optical effects, including a 12-rayed star, multiple centers of asterism, and one bright band that looked like a cat's eye when the stone was viewed with low-intensity illumination. Courtesy of Michael Schramm; photo by Maha DeMaggio.

many of these optical effects. This stone contained a 12-rayed star, additional off-axis stars, and a bright central band that had the appearance of a cat's-eye when viewed with low-intensity illumination. As mentioned in the Summer 1984 Lab Note, Dr. Edward Gübelin had concluded that sillimanite was responsible for the asterism in Sri Lankan star quartz.

New finds of spessartine in Brazil. At least three dealers had Brazilian spessartines that were reportedly from new sources. James Dzurus of Franklin, North Carolina, had some spectacular orange spessartines from a deposit in Minas Gerais. He showed contributing editor Shane McClure and editor MLJ a 29 gram piece of rough (with dodecahedral and trapezohedral crystal faces), as well as fashioned stones ranging from 9 to 38.58 ct. The rough was mined during the last two years at an unspecified new pegmatite deposit. We hope to have more information about spessartine from this source in a future Gem News item.

Carlos Vasconcelos had mineral specimens of gem-quality spessartine from a new find at Barra de Cuieté, Minas Gerais. Mining of the pegmatite began about two years ago, initially for ceramic-grade feldspar and gem tourmaline. Since October 1998, about 50 kg of spessartine have been recovered, with 2,000 carats fashioned so far. The largest cut stones reportedly weigh more than 20 ct.

Brian Cook (Nature's Geometry, Graton, California) had samples and photos of a new spessartine find in northeastern Brazil that he is mining with partner Dean Webb (Pan-Geo Minerals, Sebastopol, California). The material was recovered from a granitic pegmatite at the



Figure 21. A number of new localities in Brazil have produced fine-quality gem spessartine. These samples, from northeastern Brazil, weigh 70.90 and 5.45 ct (rough) and 2.66 ct (faceted). Courtesy of Brian Cook; photo by Maha DeMaggio.

Mirador mine in Rio Grande do Norte State. About 5 kg of gem rough have been recovered from this pegmatite since January 1999 (figure 21). The find was so recent that only rough was available; however, a 2.66 ct stone was faceted by gem cutter Jacques Vireo (Precision Cutters of Los Angeles, California) while at the Tucson show. Limited amounts of gem-quality gahnite showing a light green color were also recovered with the spessartine.

TREATMENTS

"Blatant" dyed pearls. With the increasing availability of large freshwater cultured pearls, we saw large quantities of inexpensive cultured pearls that were obviously dyed. The strand in figure 22, acquired in Tucson by contributing editor Dino DeGhionno, consists of 71 drilled cultured pearls with a bright, light green color that is only vaguely similar to a color seen in untreated cultured pearls. Dye concentrations were readily apparent with a

Figure 22. Large quantities of dyed freshwater cultured pearls were seen in Tucson this year. The cultured pearls in this strand range from 7 × 5.5 mm to 8 × 6 mm in diameter. Photo by Maha DeMaggio.





Figure 23. This 99.90 ct free-form promoted as “cultured snow quartz” is actually fused silica glass with a high density of gas bubbles. It makes a convincing imitation of quartzite. Photo by Maha DeMaggio.

microscope. According to David Federman, in the March 1999 issue of *Modern Jeweler* (“Triple Crown,” p. 38), Chinese freshwater cultured pearls are commonly bleached during processing. The “rejects” from the bleaching process are dyed “silver” or “pistachio.”

SYNTHETICS AND SIMULANTS

Fused silica glass, sold as “cultured snow quartz.” Fine-grained quartzite is sometimes tumbled or even fashioned into cabochons, but it is not a gem material that we would expect to see imitated. Nevertheless, Gems Galore of Mountain View, California, was marketing matte-finished tumbled pieces of so-called “snow quartz” (figure 23). According to their literature, the material was produced by “fusing quartz” and then rapidly cooling it to a “quasi-amorphous state.” The sample we acquired was composed of two eye-visible layers. Magnification revealed that both layers contained dense

Figure 24. This 338.6 ct piece of rough and 8.92 ct cabochon are manufactured slag glass from central Sweden. Photo by Maha DeMaggio.



concentrations of round bubbles of various sizes, and the boundary between the layers was simply a demarcation between different densities of bubbles. The sample had an R.I. of 1.46, and EDXRF analysis revealed only silicon. Although we could not discern any individual grains, the sample gave an aggregate reaction in the polariscope, probably because of scattering of light by the gas bubbles. On the basis of these properties, especially the low R.I. value and characteristic inclusions, we concluded that this material was silica glass.

Blue slag glass from Sweden, resembling opal. Slag glass is a material that seems to be particularly confusing to the amateur field collector. Over the past five years, we have seen several misidentifications of slag as meteorites, emeralds, and obsidian (see, e.g., “Obsidian imitation,” Winter 1998 Gem News, p. 301). Still another controversial identity was claimed for a probable slag (manufactured) glass available at Tucson this year: CSD, or “Crash Site Debris,” which supposedly had come from the site of a UFO impact at St. Joseph, Missouri, in 1947 (“UFO tale is rocky but rare: ‘Alien’ debris is just slag, skeptic says,” *Arizona Daily Star*, February 5, 1999, pp. 1A, 6A).

It was, therefore, a pleasure to observe a dealer representing slag glass for what it actually is. We acquired a 17.48 × 13.46 × 4.75 mm (8.92 ct) cabochon and a 338.6 ct chunk of rough (figure 24) from Gun Kemperyd Olson of Ingeborgs Stenar AB, Stockholm, Sweden. According to Ms. Olson, this manufactured glass came from the Bergslogen region in central Sweden, where iron has been mined and processed since the 1600s. The cabochon was transparent yellowish green in transmitted light, but appeared milky blue in reflected light. With the microscope, we saw round gas bubbles, linear flow banding, and fluffy-looking aggregates of opaque particles with a metallic luster. The chunk of rough was opaque light blue and showed conchoidal fracture; the fractured surface cut through some of the gas bubbles. Although at first glance this material resembles blue opal (such as that mined in Peru), its microscopic features are distinctive.

The Materials Handbook (G.S. Brady and H.R. Clauser, McGraw-Hill, New York, 1986) defines slag as “molten material that is drawn from the surface of iron in the blast furnace. Slag is formed from the earthy materials in the ore and from the flux. Slags are produced from the melting of other metals, but iron blast-furnace slag is usually meant by the term.” The *Handbook* gives a composition of 32[wt.]% SiO₂, 14% Al₂O₃, 47% CaO, 2% MgO, and small amounts of other elements, although there is considerable variation depending on the ore.

Imitation “Chinese freshwater” cultured pearls. Jack Lynch of Sea Hunt Pearls, San Francisco, California, loaned us four samples (figure 25) that had been represented to him as Chinese freshwater cultured pearls. The beads were purchased at a pearl farm about six hours’ drive from Shanghai, China; they were supposedly natu-



Figure 25. This grayish purple bead (12.5 mm in diameter) resembles certain Chinese freshwater cultured pearls currently in the marketplace, but it proved to be an imitation consisting of a coated round bead. Photo by Maha DeMaggio.

ral-color freshwater cultured pearls that had been processed to make them round after extraction, and all in the parcel shown to Mr. Lynch were the same color.

The greater availability and wide range of colors of freshwater cultured pearls from China were described in *G&G* in Fall 1998, in both the Gem Trade Lab Notes (pp. 216–217) and Gem News (pp. 224–225) sections. The former entry noted sizes up to 13 × 15 mm for oval cultured freshwater pearls; the latter mentioned treated-color blue-to-gray Chinese freshwater cultured pearls (similar to Tahitian products), as well as “pink, orange, and purple” color varieties. So on that basis, these 12.5-mm-diameter grayish purple round beads were somewhat plausible.

However, microscopic examination revealed a surface texture of many small, flattened bubbles on a uniform background (figure 26), resembling the effects of aerosol painting on a smooth surface, and very unlike the appearance of actual cultured pearls. The perfectly round shape of these undrilled samples was also suspicious. Mr. Lynch kindly gave us permission to slice one open. This revealed a painted shell over a featureless white bead.

Synthetic zincite possibly represented as sphalerite.

Although we cannot confirm or refute every rumor that we hear in Tucson, one that came to us from two sources seems worth a comment. At Tucson this year, David and Maria Atkinson of Terra in Sedona, Arizona, mentioned a bright orange material that was being represented as sphalerite from northern Pakistan. They suspected that this material was Polish synthetic zincite, which is being distributed through Russia. Another dealer showed us a faceted oval of synthetic zincite, which was from a parcel of “collector” gems acquired in Sri Lanka.

Synthetic zincite was abundant at Tucson this year, as it has been in recent years, so there is quite a lot of material available for deceptive purposes. To prevent possible misidentifications in the trade, we felt it worthwhile to mention the properties that distinguish orange synthetic zincite from natural sphalerite. The simplest distinctions are: the singly refractive (sphalerite) versus doubly refrac-

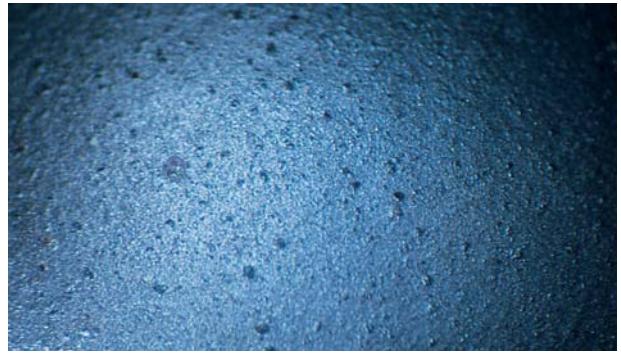


Figure 26. The surface texture of the imitation pearls shown in figure 25 did not resemble that of either natural or cultured pearls. Photomicrograph by John I. Koivula; magnified 15×.

tive (zincite) optic character; inclusions (fluid inclusions and sulfide crystals in sphalerite; dislocations, clouds of small particles, and small acicular crystals in synthetic zincite); and S.G. (4.09 for sphalerite, 5.70 ± 0.02 for synthetic zincite, although both are heavier than typical heavy liquids). For more on synthetic zincite, see the Spring 1995 Gem News, pp. 70–71, and R. C. Kammerling and M. L. Johnson, “An examination of ‘serendipitous’ synthetic zincite,” *Journal of Gemmology*, Vol. 24, No. 8, 1995, pp. 563–568.

MISCELLANEOUS

Drill holes as design elements: Michael M. Dyber and “Luminaires.” American gem carver Michael M. Dyber

Figure 27. This 22.20 ct bicolored African tourmaline was carved by Michael M. Dyber. The carved light tubes, or “luminaires,” reflect the stone’s color in interesting ways. Photo by Robert Weldon, © Michael M. Dyber.



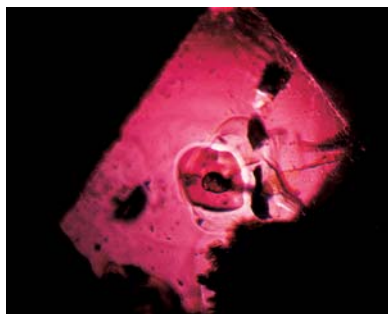


Figure 28. In shadowed transmitted light, a bright Becke line appeared like a halo surrounding the darker red 0.3 mm core (left) in this 0.19 ct spinel octahedron from Myanmar. As the objective was raised (right), the Becke line moved into the core, proving that it has a higher R.I. than the surrounding crystal. Photomicrographs by John I. Koivula.

of Rumney, New Hampshire, has been winning awards for his innovative designs for more than a decade. In the past, he has developed carved gems with “optic dishes”—concave polished curved facets—that reflect and refract light into interesting patterns. This year at Tucson, he introduced gems fashioned with polished cylindrical channels, for which he has trademarked the name “Luminaire.” These particular manufactured “inclusions” (figure 27) might be mistaken at first glance for natural etch tubes, or even prismatic mineral inclusions; however, their polished cylindrical shape demonstrates their manufactured nature.

Using mineralogical techniques to solve gemological problems, part 1: Internal “Becke lines” in spinel. In the Winter 1998 Gem Trade Lab Notes section (pp. 288–289), Gem News editor John Koivula reported on a parcel of spinels from Myanmar that contained cores with higher refractive indices than the surrounding crystal. The relative R.I. values were observed using the Becke line method. The Becke line is a narrow band or

rim of light that is visible along the boundary between materials with different refractive indices when they are examined with intermediate to high magnification (typically, at least 40×). As the distance between the sample and the objective lens of the microscope is increased (i.e., by raising the microscope objective), the Becke line moves into the region with the higher R.I. The Becke line can sometimes be enhanced by shadowing or other techniques (see, e.g., J. I. Koivula, “Shadowing: A new method of image enhancement for gemological microscopy,” Fall 1982 *Gems & Gemology*, pp. 160–164).

The relative R.I. values in the zoned spinel crystals were determined by first focusing sharply on the darker core portion (figure 28, left), and then raising the microscope objective while watching the movement of the Becke line. In both of the samples examined, the Becke line moved into the darker red core (figure 28, right), thus proving that the core had a higher R.I. than the surrounding crystal.

Using mineralogical techniques to solve gemological problems, part 2: “Plato lines” and growth structures in synthetic corundum. During the recent examination of a rectangular block of flame-fusion pink synthetic sapphire belonging to contributing editor Dino DeGhionno, we observed a most unusual anomaly in polarized light. The 60.49 ct block (15.83 × 14.90 × 13.60 mm), which he had

Figure 29. This 60.49 ct block of pink flame-fusion synthetic sapphire was cut to emphasize dichroism. Photo by Maha DeMaggio.

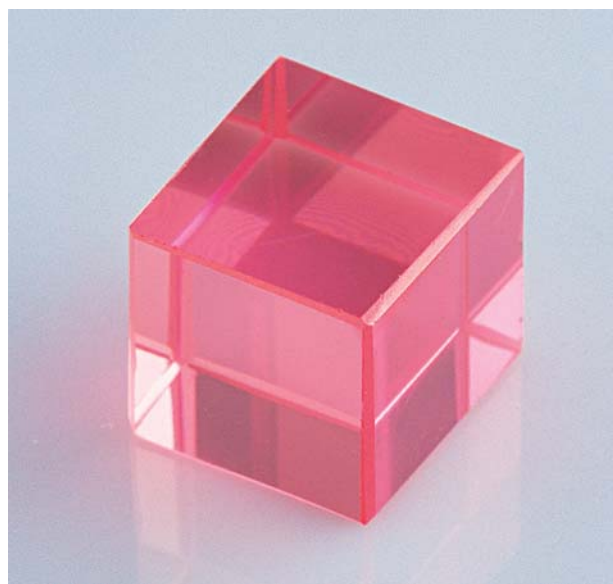


Figure 30. Colorful “Plato lines” are observed in the synthetic sapphire block when it is viewed down the optic-axis direction in cross-polarized light. Photomicrograph by John I. Koivula; magnified 10×.





Figure 31. The subtle mosaic structure becomes visible when the synthetic sapphire block is rotated 90° from the optic-axis direction (left). As the microscope's analyzer is rotated, some of the blocks in the mosaic pattern become dark, while others appear lighter (right). Photomicrographs by John I. Koivula; magnified 10x.

purchased for classroom demonstrations, was oriented to display dichroism dramatically (figure 29). However, it also shows the colorful, strain-related “Plato lines” (Sandmeier-Plato striations; figure 30) that are often observed in flame-fusion synthetic corundum when it is viewed nearly parallel to the optic axis in cross-polarized light (see, e.g., W. F. Eppler, “Polysynthetic twinning in synthetic corundum” Summer 1964 *Gems & Gemology*, pp. 169–174, 191).

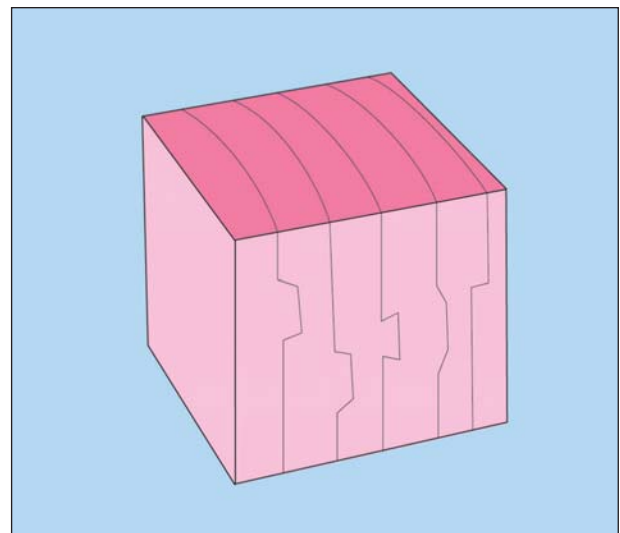
What was curious about this piece, however, is that in addition to the characteristic Plato lines, it shows a very distinctive, yet subtle, form of structurally induced optical activity. In polarized light, this activity appears as relatively thick, interconnected blocks with rectangular edges that, in some areas, give the appearance of a jigsaw puzzle (figure 31, left). When the analyzer of the microscope is rotated, some of the structural blocks in this pattern visibly darken, while others get lighter (figure 31, right). This puzzle-like pattern is crystallographically oriented at about 90° to the optic-axis direction and the Plato lines. Because the pattern is in direct rotational alignment with the long direction of the much more visible Plato lines, when the Plato lines are located—and the block is turned in the direction that they “point”—the next polished face that comes into view is the face that displays the more subtle puzzle-like pattern (figure 32).

This puzzle-like pattern is probably a form of what is known in X-ray crystallography as a mosaic structure; crystals containing such individual “pieces” are referred to as mosaic crystals. As explained by A. Taylor in *X-Ray Metallography* (John Wiley & Sons, New York, 1961, p. 233), mosaic crystals develop when “the lattice takes on the character of a mosaic, in which, without destroying the essential continuity, the mosaic blocks are tilted a few seconds or minutes of arc with respect to each other.” This structural misalignment produces strain in the host crystal. In the case of the synthetic corundum, this strain is easily visible with cross-polarized light as the bright interference colors seen in the optic-axis direction, that is, the Plato lines. It therefore appears that the mosaic structure is the actual cause of Plato lines in flame-fusion synthetic corundum. This relationship was overlooked in the past because the visual effect is quite subtle, and gemologists do not usually work with oriented, polished blocks.

ANNOUNCEMENTS

Nature of Diamonds at the San Diego Natural History Museum. The *Nature of Diamonds* exhibit, which debuted in New York at the American Museum of Natural History in 1997, is now in San Diego, California, through September 7, 1999. The comprehensive exhibit demonstrates many aspects of diamond, from its geologic origins to its place in history, art, and adornment, and its various uses in modern technology. Visitors will find a variety of displays ranging from world-famous gems and jewelry to unusual specimens and diamonds in their natural state. A walk-through mine tunnel, a dramatic walk-in vault, and computer animation enhance the interactive experience. Attendees of GIA's 3rd International Gemological Symposium will enjoy a special gala evening viewing at the museum Tuesday, June 22. Contact the San Diego Natural History Museum at 619-232-3821, or visit their Web site at <http://www.sdnhm.org>, for more information.

Figure 32. This drawing shows the orientation between the mosaic structure in the synthetic sapphire block and the strain-related Plato lines. The optic axis is perpendicular to the top of the cube.



New exhibit at the Royal Ontario Museum. The Inco Gallery of Earth Sciences, an interactive exhibit that explores the Earth's evolution and processes, is scheduled to open May 30, 1999, at the Royal Ontario Museum in Toronto, Canada. One of the exhibit's four main sections is *Treasures of the Earth*, which explains the formation and characteristics of minerals. This section will include the S. R. Perren Gem and Gold Room, which originally opened in 1993 and contains over 1,000 gems. For more details, contact Nikki Mitchell at 416-586-5565, or e-mail nikkim@rom.on.ca.

International Colored Gemstone Association Congress. ICA will hold its next Congress on May 16–19, 1999, in Abano Terme, Italy. Presentations, panels, and workshops will be complemented by a variety of social events. Contact the ICA office in New York at 212-688-8452 for more details.

International Gemological Symposium. The 3rd International Gemological Symposium (hosted by GIA) will take place June 21–24, 1999, at the Hyatt Regency Hotel in San Diego, California. The event, which is held only once every 8–10 years, is known as the "world summit" for the gem and jewelry industry. A distinguished lineup of trade and scientific leaders will speak on the major issues in the industry. Panel discussions, all-new "War Room" sessions, and dozens of poster presentations round out the academic portion of Symposium. To register, contact GIA's Symposium Office at 760-603-4406 (toll-free in the U.S. and Canada, call 800-421-7250, ext. 4406), or register online at <http://www.gia.edu>.

International Society of Appraisers conference. ISA will hold its 20th annual International Conference on Personal Property Appraising on May 2–5, 1999, in Troy, Michigan. There will be a wide array of lectures, seminars (including "Gemstone Enhancement: Effects on Pricing"), panel discussions, and social activities. For additional information, contact the ISA headquarters at their Web site at <http://www.isa-appraisers.org>, or call them at 888-472-4732.

Gemstones in upcoming scientific meetings. Special sections on diamonds and/or colored stones will be incorporated into several upcoming meetings on geology, mineral exploration, and advanced analytical techniques:

- The theme of the 4th Annual Penn State Mineral Symposium (May 21–23, 1999) will be *The Mineralogy of Gems and Precious Metals*. For more information, call Andrew Sicree at 814-865-6427, or write Penn State Mineral Museum, 122 Steidle Building, University Park, PA 16802.
- The Joint Annual Meeting of the Geological Association of Canada and the Mineralogical Association of

Canada (GAC-MAC) will occur May 26–28, 1999, in Sudbury, Ontario, Canada. Special sessions will focus on the genesis of gemstone deposits and diamond exploration using kimberlite indicator minerals. A one-day short course for nonspecialists will review geophysical exploration techniques for several resources, including gold and diamonds. A separate field trip to the Wawa area in Ontario will focus on exploring for rare-element pegmatites and kimberlites using glacial till and modern alluvium. For more information, contact Laurentian University at 705-673-6572 (phone), 705-673-6508 (fax), or you can visit their Web site at <http://www.laurentian.ca/www/geology/1STCIRC.htm>.

- GEORAMAN'99: The 4th International Conference on Raman Spectroscopy Applied to the Earth Sciences will be held June 9–11, 1999, in Valladolid, Spain. Applications of Raman spectroscopy to gemology (and other disciplines) will be discussed. Further information can be accessed at <http://www.iq.cie.uva.es/~javier/georaman/geoeng.html>.

ERRATA:

1. In the Fall 1998 *Gem News* item "Rossmanite, a new variety of tourmaline" (p. 230), *rossmanite* should have been described as a new species of the *tourmaline* group.
2. On page 274 of the Sunagawa et al. article "Fingerprinting of Two Diamonds Cut from the Same Rough" (Winter 1998), figures 6 and 7 are mislabeled. The labels for the a_1 and a_2 directions in the right-hand photo of each figure should be reversed.
3. On pages 264–265 of the Nassau et al. article "Synthetic moissanite: A new diamond substitute" (Winter 1997), the thermal inertia data were printed incorrectly. The sentence at the bottom of page 264 should read: "Because the thermal conductivity ranges of diamond (1.6–4.8 cal/cm °C sec) and moissanite (0.55–1.17 cal/cm °C sec) nearly overlap. . . ." The table below presents the correct data for both thermal conductivity and thermal inertia of diamond and moissanite.

	Thermal conductivity (cal/cm °C sec) (W/cm K)		Thermal inertia (cal/cm ² °C sec ^{1/2})
Diamond	1.6 – 4.8	6.6 – 20.0	0.82 – 1.42
Moissanite-6H	0.55 – 1.17	2.3 – 4.9	0.30 – 0.63

4. The announcement on page 302 of the Winter 1998 *Gem News* that the synthetic moissanite article had received an ASAE award should have mentioned Shane Elen as one of the authors.

Gems *vs* Gemology

Challenge



The following 25 questions are based on information from the four 1998 issues of *Gems vs Gemology*. Refer to the feature articles and "Notes and New Techniques" in those issues to find the single best answer for each question; then mark your choice on the response card provided between pages 46 and 47 of this issue (sorry, no photocopies or facsimiles will be accepted; contact the Subscriptions Department if you wish to purchase additional copies of the issue). Mail the card so that we receive it no later than Monday, July 12, 1999. Please include your name and address. All entries will be acknowledged after that date with a letter and an answer key.

Score 75% or better, and you will receive a GIA Continuing Education Certificate. If you are a member of GIA Alumni and Associates, you will earn 5 Carat Points toward GIA's new Alumni Circle of Achievement. (Be sure to include your GIA Alumni membership number on your answer card and submit your Carat card for credit.) Earn a perfect score, and your name will also be featured in the Fall 1999 issue of *Gems vs Gemology*. Good luck!

Note: Questions are taken from the four 1998 issues. Choose the single **best** answer for each question.

- When using laser Raman microspectrometry to identify gem materials, the operator must be aware that the spectrum can vary according to
 - the size of the sample.
 - the orientation of the sample.
 - the fragility of the sample.
 - the metal in which the sample is set.
- Russian synthetic pink quartz can sometimes be distinguished from natural pink quartz on the basis of its
 - microscopic features.
 - UV-visible absorption spectrum.
 - refractive index.
 - birefringence.
- In GIA's diamond cut model, weighted light return (WLR)
 - is calculated using the two-dimensional path of light rays.
 - excludes the dispersion of light rays as they move through the virtual diamond.
 - places equal emphasis on all light returned from the diamond's crown.
 - places the greatest emphasis on light rays that emerge straight up from the crown.
- To manufacture a blue diamond with a stronger, more evenly colored face-up appearance, a cutter could use
 - a French culet.
 - no culet.
 - 24 pavilion facets.
 - a thick girdle.
- The Raman identification of inclusions in fluorite as barite was further supported by the
 - blocky form of the barite.
 - color change of the barite.
 - presence of barite in the Illinois fluorite deposits.
 - deprecation halos in the fluorite host.
- The model developed for GIA's diamond brilliance study

- A. can only be used to evaluate diamonds weighing more than 1 ct.
 B. assumed that the diamond is perfectly symmetrical and perfectly polished.
 C. used a focused light source that originated above the diamond.
 D. took into account minor inclusions and cavities.
7. The following bonding agent was used by the creator of "Leigha" because of its strength and transparency:
 A. cyanoacrylate adhesive.
 B. epoxy.
 C. UV-curing cement.
 D. natural resin.
8. EDXRF can be used most reliably to
 A. determine the manufacturer of a synthetic ruby.
 B. determine the locality of a ruby.
 C. separate natural from synthetic rubies.
 D. measure the R.I. of faceted rubies.
9. In estimating the weights of mounted colored gemstones, the greatest challenge lies in correcting for
 A. specific gravity.
 B. measurement precision.
 C. rounding errors.
 D. proportion variations.
10. The yield (percentage of original weight retained after cutting) for diamonds cut in India
 A. is about 45%, the same as for well-formed diamonds cut elsewhere.
 B. has been approximately 15%–23% since 1980.
 C. averages only about 4%.
 D. cannot be estimated because of the absence of official statistics.
11. The identification of two diamonds as coming from the same rough is based on their
 A. mineral inclusions.
 B. color and clarity grades.
 C. growth histories.
 D. infrared absorption spectra.
12. Some of the world's largest ruby deposits, such as those found in Cambodia and Thailand, are
 A. metasomatic.
 B. marble-hosted.
 C. metamorphic.
 D. basalt-hosted.
13. The topaz recovered from Klein Spitzkoppe, Namibia, is usually
 A. colorless.
 B. brown.
 C. pale blue.
 D. pale yellow.
14. The preferred nucleus for the culture of abalone blister pearls is in the form of a
 A. sphere.
 B. marquise shape.
 C. flattened hemisphere.
 D. high-domed hemisphere.
15. Images obtained by X-ray topography are distorted according to the
 A. size of the sample.
 B. density of the sample.
 C. intensity of the X-ray beam.
 D. direction of reflection of the X-ray beam.
16. Most diamonds cut in India are
 A. smaller than 7 pts and of low quality.
 B. between 2 and 7 pts and of SI₂ or better clarity.
 C. comparable in size and quality to those cut in Antwerp and Israel.
 D. variable in size but always of good clarity (SI₂ or better).
17. Rubies formed in marble generally contain relatively
 A. low amounts of vanadium.
 B. low amounts of iron.
 C. high amounts of iron.
 D. high amounts of manganese.
18. Which one of the following materials was not identified in the two historical objects from the Basel Cathedral?
 A. Doublets
 B. Rubies
 C. Glass
 D. Quartz
19. The vivid color and iridescence of the nacre of abalone "mabés" from New Zealand is enhanced by
 A. the orientation of microscopic aragonite crystals.
 B. a thick conchiolin layer underneath the nacre.
 C. the presence of a blue polymer coating.
 D. organic dyes.
20. The fact that blue diamonds generally have high clarity is related to their
 A. diamond type.
 B. color.
 C. size.
 D. facet style.
21. Today the percentage of the world's diamonds that are cut in India is about
 A. 70% by weight/70% by wholesale value.
 B. 70% by weight/35% by wholesale value.
 C. 50% by weight/35% by retail value.
 D. 50% by weight/20% by retail value.
22. The coloration of synthetic pink quartz is probably related to the presence of
 A. aluminum.
 B. iron.
 C. phosphorus.
 D. manganese.
23. Which of the following materials cannot be studied by Raman analysis?
 A. Synthetic gem materials
 B. Fluorescent minerals
 C. Metals and alloys
 D. Crystalline inclusions in gems
24. In the GIA analysis of brilliance for round brilliant diamonds, moderately high to high WLR values were calculated
 A. for only one particular pavilion angle.
 B. for many combinations of crown angle, pavilion angle, and table size.
 C. only for table sizes up to 58%.
 D. only for star facets longer than 50%.
25. With respect to the color appearance of type IIb blue diamonds,
 A. each hue transitions smoothly into the neighboring color hues.
 B. the saturation range is compressed compared to yellow diamonds.
 C. subtle hue shifts are seen throughout their color range.
 D. there is little variation in tone.

Book Reviews

Susan B. Johnson & Jana E. Miyahira, Editors

ARAB ROOTS OF GEMOLOGY—Ahmad ibn Yusuf al Tifaschi's *Best Thoughts on the Best of Stones*
Translated with comments by Samar Najm Abul Huda, 271 pp., illus., publ. by Scarecrow Press, Lanham, MD, 1998. US\$45.00.

One important aspect of gemology is the history of gemstones. Unfortunately, a wealth of early works have been lost to modern gemologists, as evidenced by the number of gem references cited in Pliny's first-century encyclopedia that have disappeared without a trace. Although much of the knowledge possessed by ancient Greece and Rome was preserved by Arabic writers, for the most part such works have remained inaccessible to all but the very few western scholars who have learned Arabic.

This compilation offers a fascinating glimpse at ancient gemology, according to the book *Best Thoughts on the Best of Stones*, by Ahmad ibn Yusuf al Tifaschi (1184–1254). Its translation marks the first time that early Arab gemological literature has been studied by a modern Arab gemologist. Mrs. Huda is a competent translator who has endeavored to make the contents of this pioneering work easily accessible to English-speaking readers. She aimed the book at "all readers interested in geology, gemology, mineralogy, jewelry, history, Arab heritage, Islamic art, and the history of science." In the reviewers' opinion, she has accomplished her goals with great success. The book is clearly written in a straightforward manner that is easily understood, even by those readers for whom English is a second language.

After an introduction by Dr. John Sinkankas and a foreword by Eric Bruton, the book opens with a general introductory chapter that briefly discusses early Arabic works on gemstones. This part includes a glossary of gem names in English with their ancient and modern Arabic names and phonetic (English) equivalents. Mrs. Huda places al Tifaschi's work in context by describing the era in which he wrote and the nature of the Arabic literature on gems from the eighth to the 13th centuries. She provides a two-page table of the gemological terms used in the 13th century and explains the monetary terms, weights, and measures employed at that time.

Next, a photocopy of the manuscript in Arabic is provided, followed by Mrs. Huda's English translation of al Tifaschi's survey of 25 gemstones. The organization is very consistent throughout. For each gemstone, al Tifaschi briefly describes how the gem is formed; its localities, qualities, characteristics, benefits (mostly medicinal and talismanic), and prices; and, in some cases, its lapidary treatment. Each section closes with a discussion by Mrs. Huda, which makes al Tifaschi's text understandable for the nongemologist and provides rich grazing for the serious gemologist.

The book is sturdy, measures 14 × 22 cm (5½ × 8½ inches), and is clearly printed on good-quality paper. There are only two illustrations: black-and-white photos of a turquoise Mamluk ring and an almandine garnet mounted in gold. Neither is vital to the usefulness of the book.

The book is remarkably free of typos or errors. After diligent search, we found only one specific error,

probably a typo. On page 229, *azurmalachite* is defined by Mrs. Huda as "malachite intergrown with lazurite." The term *azurmalachite* was coined by George F. Kunz in 1907 for a banded mixture of *azurite* and malachite.

The reviewers consider this an important and unique addition to the gemological literature that deserves a place on the shelf of every serious gemologist.

SI and ANN FRAZIER
Lapidary Journal Correspondents
El Cerrito, California

L'ÉMERAUDE: CONNAISSANCES ACTUELLES ET PROSPECTIVES
[The Emerald: Current and Prospective Knowledge]
Edited by Didier Giard, 235 pp., illus., publ. by Association Française de Gemmologie [gemmes@animasoft.fr], Paris, 1998 (softbound; in French, with partial English translations). 350.00 FF (about US\$57.00).

This attractive, lavishly illustrated volume is a collection of 35 articles and essays from 52 authors worldwide. Emphasized are developments in the study of emerald in the closing years of the millennium. The book's editor has collected articles on history/culture (8), geochemistry (1), inclusions (2), enhancement (3), synthesis (2), geology/mineralogy (3), specific deposits (10—including Afghanistan, Australia, Brazil, Colombia, India,

**This book is available for purchase through the GIA Bookstore, 5345 Armada Drive, Carlsbad, CA 92008. Telephone: (800) 421-7250, ext. 4200; outside the U.S. (760) 603-4200. Fax: (760) 603-4266.*

Madagascar, Pakistan, Zambia, and Zimbabwe), optics (1), and lapidary/jewelry (2), along with a bibliography of 1990s works and abstracts of recent contributions. An extensive table giving the gemological properties of emeralds from various deposits and the principal types of synthetic emerald completes the text. There is no overall index.

Of particular value are articles on the use of infrared spectroscopy and laser Raman microspectrometry, and the use of oxygen isotopes for characterizing emeralds from specific sources. Also useful are articles on the common practice of "oiling" or otherwise filling fractures with liquids or polymers. Other valuable articles provide updated information on the geology and origin, and mining, of the world's major deposits. Many other articles make for highly interesting and informative reading. Unfortunately, those on cutting emeralds and setting them into jewelry offer little of value, having been covered already in far more thorough publications.

A "retrospective bibliography" for the years 1990–1997 appears near the end of the book but erroneously lists the GIA Bookstore as the publisher for several books (see, for example, the listing for Bowersox and Chamberlin, 1995). The bibliography is apparently intended to provide an update on recent works. However, this reviewer would have liked to see such valuable sources of information on the emerald and its literature as R. A. Dominguez's *Historia de las Esmeraldas de Colombia* (1965), I. A. Mumme's *The Emerald* (1982), G. O. Muñoz and A. M. Barriga Villalba's *Esmeralda de Colombia* (1948), A. Santos Munsuri's *La Esmeralda, Las Gemas, y Otras Materias Preciosas* (1868), and J. Sinkankas's *Emerald and Other Beryls* (1981) mentioned in some sort of preliminary bibliography.

As is often the case with books assembled from articles by a number of contributors, there is some unevenness in presentation. Also,

several articles on geochemistry, advanced identification techniques, and geology are beyond the comprehension of readers not formally educated in those sciences. Nevertheless, the whole hangs together very well, and provides a wealth of up-to-date information that is not readily available in any other single current publication.

As a final note concerning this important and valuable compilation, the addition of English summaries and translations of most of the articles is a welcome feature, but a final inspection by an English-language editor could have prevented certain awkward phrasings and spellings.

L'Émeraude is made from high-quality materials. Although a hardcover version is not available, the book is encased in a stiff paper cover, with a matching black dust jacket.

JOHN SINKANKAS
Peri Lithon Books
San Diego, California

OTHER BOOKS RECEIVED

The Great Encyclopedia of Precious and Decorative Stones, by *Nikodem Sobczak and Tomasz Sobczak*, 422 pp., illus., publ. by *National Science Publishers, Warsaw*, 1998 (in Polish), US\$20. This reference text describes "precious" and decorative stones, their imitations and synthetic counterparts, as well as artificial products that are used in decorative arts and jewelry. The opening section provides a 56-page background on crystallography and the gemological and physical properties of gem materials. Next, nearly 350 pages cover specific gems and decorative materials in alphabetical order. Complete listings of characteristics are provided for the most important stones, along with localities of origin. The authors used academic theses and periodicals published through the end of 1996 to write this encyclopedia, which contains 264 color

photographs. They plan to publish an English edition.

STUART D. OVERLIN
Gemological Institute of America
Carlsbad, California

Larousse des Pierres Précieuses, by *Pierre Bariand and Jean-Paul Poirot*, 287 pp., illus., publ. by *Larousse-Bordas, Paris*, 1998 (in French), 250.00 FF (about US\$42.00).* Updated and expanded (see the Spring 1986 *Gems & Gemology*, pp. 65–66, for a review of the first edition), this *Larousse* is intended for a general audience. Its opening section, History and Qualities of Gems, is a 60-page overview of gem history, symbolism, origins, sources, properties, imitations and synthetics, identification techniques, and classification. At the heart of this *Larousse* is its Dictionary section, where the reader will find more than 200 entries on gemstones and other gem materials, in different levels of detail, accompanied by dozens of excellent color photographs by Nelly Bariand. The remaining portion is an Appendix that contains a glossary, a comprehensive bibliography, a listing of museums with major gem collections, and a table of gem characteristics. SDO

Standards & Applications for Diamond Report/Gemstone Report/Test Report, by *SSEF Swiss Gemmological Institute*, 118 pp., illus., publ. by *SSEF, Basel, Switzerland*, 1998, US\$65.00. This monograph was written to clarify the SSEF Swiss Gemmological Institute's full gem treatment disclosure policy. It provides several examples of the Institute's various test reports and describes how different gem treatments are evaluated. The first section, an overall statement of the laboratory's policy and standards, is followed by two chapters devoted to colorless and colored diamonds, respectively. Subsequent chapters summarize ruby, sapphire, and emerald individually, while chapter 8 discusses other gemstones. The manual closes with a chapter on pearls and cultured pearls. SDO

Gemological



ABSTRACTS

EDITOR

A. A. Levinson
*University of Calgary, Calgary,
Alberta, Canada*

REVIEW BOARD

Anne M. Blumer
Bloomington, Illinois

Peter R. Buerki
GIA Research, Carlsbad

Jo Ellen Cole
GIA Museum Services, Carlsbad

Maha DeMaggio
GIA Gem Trade Laboratory, Carlsbad

Michael Gray
Coast to Coast, Missoula, Montana

R. A. Howie
Royal Holloway, University of London

Mary L. Johnson
GIA Gem Trade Laboratory, Carlsbad

Jeff Lewis
GIA Gem Trade Laboratory, Carlsbad

Margot McLaren
Richard T. Liddicoat Library, Carlsbad

Elise Misiorowski
Los Angeles, California

Jana E. Miyahira-Smith
GIA Education, Carlsbad

Carol M. Stockton
Alexandria, Virginia

Rolf Tatje
Duisburg University, Germany

Sharon Wakefield
Northwest Gem Lab, Boise, Idaho

June York
GIA Gem Trade Laboratory, Carlsbad

COLORED STONES AND ORGANIC MATERIALS

Black is beautiful. A. Lohr, *Hawaii Business*, Vol. 43, No. 9, March 1998, pp. 68–69.

Several Hawaiian jewelry companies are reaping the benefits of the current upswing in U.S. consumer demand for Tahitian black pearl jewelry. According to many in the trade, this demand is fueled by the successful advertising campaign for Elizabeth Taylor's "Black Pearls" perfume.

One company, Steven Lee Designs, struggled to increase market share until the company's namesake began incorporating black pearls into his jewelry designs. The first year after this change, the company's sales more than doubled. Now, Lee says, about 80% of his company's business is black pearl jewelry.

Another company that has experienced a dramatic sales increase is Tahitian Midnight Pearls. Although this wholesale pearl supply company is based in Tahiti, its sales office is located in Hawaii. The president of the U.S. division states that his company experienced a 13-fold increase in pearl sales between 1995 and 1997. The company currently sells about 70% of its pearl inventory to the U.S. market.

This same story is repeated for many successful Hawaiian jewelry companies that have turned to black pearls to expand their market and attract new customers.

SW

This section is designed to provide as complete a record as practical of the recent literature on gems and gemology. Articles are selected for abstracting solely at the discretion of the section editor and his reviewers, and space limitations may require that we include only those articles that we feel will be of greatest interest to our readership.

Requests for reprints of articles abstracted must be addressed to the author or publisher of the original material.

The reviewer of each article is identified by his or her initials at the end of each abstract. Guest reviewers are identified by their full names. Opinions expressed in an abstract belong to the abstractor and in no way reflect the position of Gems & Gemology or GIA.

© 1999 Gemological Institute of America

Emerald chemistry from different deposits: An electron microprobe study. I. I. Moroz and I. Z. Eliezri, *Australian Gemmologist*, Vol. 20, No. 2, 1998, pp. 64–69.

Twenty-six natural emeralds—from 11 mining districts in nine countries—and three hydrothermally grown synthetic emeralds were analyzed nondestructively with an electron microprobe. Multiple analyses were obtained, particularly for color-zoned crystals, resulting in a total of 219 analyses for 16 elements.

The emeralds from “schist-type” occurrences in Australia, Brazil, Mozambique, Russia, Tanzania, and Zambia showed relatively high concentrations of magnesium (0.7–3.1 wt.% MgO), iron (0.3–1.8 wt.% FeO), and sodium (0.2–2.8 wt.% Na₂O). In contrast, Colombian and Nigerian emeralds showed low contents of magnesium (<0.76 wt.% MgO) and sodium (<0.67 wt.% Na₂O). The synthetic emeralds had chemical characteristics similar to those of natural stones from Colombia and Nigeria.

Kyaw Soe Moe

Indonesian Pearl Report. *Jewellery News Asia*, No. 171, November 1998, pp. 50–68 passim.

This compilation of seven short articles concerns the state of pearl production in Indonesia. It provides insight into the country that may challenge Australia’s position in the global South Seas pearl market in the new millennium. Indonesia produced about 200–220 kan—equal to approximately 30% of the world’s white South Sea pearls—in 1998 [1 momme = 3.75 g; 1000 momme = 1 kan]. The expected annual growth is about 15%.

Currently, the Indonesian pearl industry is profiting from low labor costs for unskilled workers, which are about one-tenth of those in Australia (skilled employees are paid salaries comparable to those in other countries). Also aiding the Indonesian expansion is the fact that there are few restrictions on investing in the pearl industry. This has encouraged pearl companies from other countries to invest, and set up farms, in Indonesia. With such rapid growth, the Indonesian Pearl Culture Association has suggested a system to regulate new pearling licenses to prevent overcrowding and pollution. The report includes overviews on several companies that are currently culturing pearls in Indonesia. *JEM-S*

Opal report. C. Dang, *Jewellery News Asia*, No. 171, November 1998, pp. 74, 76–77, 80, 82–86.

The three articles in this report are based on interviews with several opal manufacturers and suppliers, and present a picture of the global market for loose opals and opal jewelry; information on manufacturing of Peruvian opal is also supplied.

According to opal suppliers, sales of calibrated opal under \$300 have increased in the U.S., where demand is high for black opal and boulder opal with blue and green play-of-color. This type of opal sells best in the 3–10 ct

category, for stones under \$100 each. Also popular is fire opal, which wholesales for \$10 to \$20 per carat, and calibrated white opal, which wholesales for under \$300 per carat. Demand in Europe is mostly for black and boulder opal in ovals and freeforms from 1 to 5 ct, priced between \$100 and \$300 each. In Asia, demand is mainly from Japan, Taiwan, and Singapore for calibrated stones priced between \$2 and \$5 per carat; there is also some demand, mainly in Japan, for top-quality stones up to \$90,000 each. The Olympic Games scheduled for 2000 in Sydney, Australia, are expected to increase sales of opal in that country, because the Australian government is promoting opal as the national gemstone.

Opal jewelry suppliers report that sales of opal jewelry are growing in the U.S., Europe, and Asia. In the U.S., demand is strong for 9–18K gold earrings, rings, bracelets, and pendants that are set with black opal or boulder opal; wholesale prices for these items range from \$200 to \$2,000. In Europe, most popular are black opal and boulder opal (in oval and freeform shapes), set in yellow and white gold and platinum; prices range from \$200 to \$10,000 depending on size and quality. The largest market for opal jewelry in Asia remains Japan, even after an approximately 40% drop in sales in 1998 compared with 1997. Leading the demand are pieces with black, boulder, white, or fire opal in prices under \$500, as well as much more expensive pieces from \$50,000 to \$60,000. Some manufacturers report increased sales of opal doublets and triplets. For example, demand is high in the U.S. for pendants, earrings, rings, and bracelets in 14K gold with 1–4 ct doublets, particularly with a green play of color, at prices below \$100.

Peruvian opal has recently been introduced by Gallant Gems, Hong Kong, and is being marketed in the U.S., Germany, Switzerland, and Japan. Polished stones in freeform shapes, cabochons, and beads of various sizes wholesale from \$0.50 to \$3,000 per carat depending on quality. Gallant, which supplies Peruvian opal in pink, green, or blue, has developed a special cutting technique for the material, which has a different hardness from opal mined elsewhere. *MD*

Pearl identification. S. J. Kennedy, *Australian Gemmologist*, Vol. 20, No. 1, 1998, pp. 2–19.

Pearl identification and testing is a specialized discipline that requires sophisticated instrumentation and considerable experience. This well-illustrated article describes the equipment and procedures used at the Gem Testing Laboratory of Great Britain in London. After providing definitions of many pearl terms (e.g., *natural pearls*, *nacre*, *conchiolin*, *orient*, *nucleated cultured pearls*, *non-nucleated cultured pearls*), the author describes the laboratory’s pearl-testing procedures. Visual examination is used to determine external features (e.g., color, luster, shape, and surface characteristics), as well as internal features seen within drill holes. When examined with 10×

magnification, imitations are easily detected by their grainy surface texture. All pearls (including necklaces) submitted to the laboratory are also checked with X-radiography for details of their internal structure (e.g., the presence or absence of a bead nucleus) that, when combined with visual observations, are necessary for determining whether a pearl is natural or cultured. X-ray luminescence and X-ray diffraction techniques are employed for special situations.

The article contains much useful information. For example, natural pearl necklaces are almost always graduated; if a cultured pearl necklace is graduated, the color match between pearls is usually much better than in a natural pearl necklace. The greatest challenge in pearl testing is differentiating natural pearls from tissue-nucleated cultured pearls. When this situation arises, two X-radiographs are taken in mutually perpendicular directions. If growth lines are present within the gray area in the center of the sample, the pearl is probably natural. An even, or somewhat patchy, center that is a slightly darker gray indicates the presence of a cavity. If that cavity is irregular in shape and relatively small, then the sample is a tissue-nucleated cultured pearl; however, if the outline of the cavity roughly follows the contours of the external shape of the sample, it is probably a natural pearl.

MD

Pearls in the making. A. Mercier and J.-F. Hamel, *Islands Business*, Vol. 24, No. 4, April 1998, pp. 16–17.

A pearl project was recently established in the Solomon Islands (South Pacific Ocean), to (1) assess the potential for pearl culturing in this venue and (2) study the biology of the blacklip pearl oyster (*Pinctada margaritifera*) in order to protect the remaining natural stocks. The project is a collaborative venture between the International Centre for Living Aquatic Resources Management (ICLARM) and the Solomon Islands Fisheries Division.

The center of this intensive study was the seeding of nearly 2,000 blacklip oysters in September 1997 at a research facility located on the small island of Nusa Tupe. Harvesting of this first batch of cultured pearls was scheduled for March 1999.

Researchers indicate that prospects for establishing a profitable pearl-culturing industry in the Western Province of the Solomon Islands are promising. SW

Rossmanite, $\square(\text{LiAl}_2)\text{Al}_6(\text{Si}_6\text{O}_{18})(\text{BO}_3)_3(\text{OH})_4$, a new alkali-deficient tourmaline: Description and crystal structure. J. B. Selway, M. Novák, F. C. Hawthorne, P. Černý, L. Ottolini, and T. K. Kyser, *American Mineralogist*, Vol. 83, No. 7–8, 1998, pp. 896–900.

Rossmanite is a new tourmaline species, the type locality being the Hradisko quarry of the Rožná pegmatite, western Moravia, Czech Republic. This is also the type locality for lepidolite, which was first discovered over 200 years ago, in 1792. Chemically, rossmanite is classified as

a lithium-aluminum tourmaline, along with elbaite and liddicoatite. The distinction between the three species is based on the element occupancy in the "X" site: sodium for elbaite, calcium for liddicoatite, and predominantly vacant (i.e., alkali-deficient, represented by " \square " in the chemical formula) for rossmanite. It occurs as pink columnar crystals with striations on the prism faces parallel to the c-axis. Indices of refraction are $\omega = 1.645$ and $\epsilon = 1.624$, and the specific gravity is 3.06.

Rossmanite is indistinguishable from elbaite, the most important gem tourmaline species, by standard gemological techniques; it can be identified only by chemical analysis. The species is named after Professor George R. Rossman of the California Institute of Technology, Pasadena, in recognition of his wide-ranging contributions to mineralogy in general, and to the tourmaline group of minerals in particular. [*Abstracter's note:* Rossmanite is now known from other pegmatites in the Czech Republic, Canada, Italy, and Sweden; see Gem News, Fall 1998 *Gems & Gemology*, p. 230.] AAL

Special emerald report. W. Lau, *Jewellery News Asia*, No. 167, July 1998, pp. 43–52 passim; No. 168, August 1998, pp. 56–70 passim; No. 169, September 1998, pp. 157–168 passim.

The worldwide emerald industry is suffering primarily for two reasons: a slowdown in the Asian economy and confusion over emerald treatments. About 60%–65% of the world's emerald rough comes from Colombia. In June 1998, a new organization, PSICEJ (Promotional Society for the International Center for Emeralds and Jewelry) was established by the Colombian government and trade groups to revitalize exports and improve the image of emeralds to the trade. The description of this organization, its objectives, and its support for a proposed "emerald center" in Bogotá (which would include a bourse, a gemological laboratory, lapidaries, and educational and conference facilities) sets the stage for this three-part collection of articles covering the entire industry from mining to retailing. Most of the emphasis is on the industry as seen from the Colombian perspective, but some attention is also paid to new deposits in Brazil and to the positive implications of Zambia's recent liberalization of mining regulations.

The various articles contain a wealth of information (but with some inconsistencies from one entry to the next) about the Colombian industry. For example, an estimated 500,000 workers are employed in all aspects of the industry; the finest gem material comes from Muzo and Chivor, but Cosquez presently has the greatest (77% by weight) production; and of the total 1997 exports, rough emeralds accounted for 85% by weight but only 1.7% by value, whereas polished emeralds accounted for 15% by weight and 98.3% by value.

Emerald wholesalers from several countries give insight into their businesses, including the qualities and sizes in which they specialize, the efforts they use to

restore consumer confidence, and the latest market trends for the countries in which they deal. Another highlight is the nature of emerald fillings (e.g., resins, Opticon, and cedarwood oil), and the advanced analytical methods by which these fillings are identified by the SSEF Swiss Gemmological Institute in Basel. Overall, these articles are realistic with respect to the present state of the world's emerald trade and decidedly positive about the future. *MM*

Sweet Home rhodochrosite—What makes it so cherry red? K. J. Wenrich, *Mineralogical Record*, Vol. 29, No. 4, 1998, pp. 123–127.

Rhodochrosite (MnCO_3) crystals from the Sweet Home mine, Colorado, were analyzed to ascertain the differences between the pink rims and the “gemmy” red cores. Microscopic observation revealed that the red cores are transparent, while the pink rims contain numerous solid and fluid inclusions. Crystal and inclusion relationships suggest that the transparent red core formed first, at a higher temperature than the pink rim that subsequently overgrew it.

Electron microprobe analyses were conducted on 127 specimens to measure 28 chemical elements. The results for Fe+Mg+Ca, which can substitute for Mn in the crystal structure of rhodochrosite, are most important. Fe+Mg+Ca make up <1 atomic percent in the red (transparent) rhodochrosite, compared to 2–7 atomic percent in the pink rims. Relatively high Fe contents are responsible for the coloration of lower-quality pink rhodochrosite. Gem-quality red rhodochrosite from the Sweet Home mine is chemically the “purest” on record. These results will help narrow the search for gem quality crystals to those areas in the mine with low Fe+Mg+Ca geochemical signatures. [*Editor's note:* For more information on rhodochrosite from this locality, see K. Knox and B. K. Lees, “Gem rhodochrosite from the Sweet Home mine, Colorado,” Summer 1997 *Gems & Gemology*, pp. 122–133.] *JL*

Troubled waters. D. Ladra, *Colored Stone*, Vol. 11, No. 4, July-August 1998, pp. 14–19.

Analysis of trade figures for the period 1992–1996 indicates that there is a healthy consumer demand for pearls, as the value of world consumption was US\$3.7 billion over this five-year period. However, world production during this time amounted to US\$2.5 billion, so supply is not keeping up with demand. This is due to the dwindling supply of natural pearls, as well as to the decline in cultured pearl production in Japan (where widespread oyster deaths are being attributed to a parasitic infection or virus). Although there are pearl fisheries throughout the world, Asian countries supplied 96.1% of the unworked cultured pearls, 78.6% of the worked cultured pearls, and 53.7% of the natural pearls that entered the world markets in the 1992–1996 period; cultured pearls accounted for at least 90% of the total production. Of the

Asian producers, Japan, Australia, China, and Indonesia were the biggest suppliers of cultured pearls, while India provided 15% of the world's natural pearls. Interesting details, including statistics, are given for the industries in Japan, China, and the South Seas (mainly Australia and the Philippines).

Projections to the year 2001 indicate dramatic increases (on the order of 150% in US\$ terms) in the worldwide production of cultured pearls over 1997, but a decline of 40% for natural pearls. Nevertheless, the imbalance between supply and demand is expected to grow, creating ample opportunity for investment in pearl culture. *AMB*

Turquoise: Blue sky . . . Blue stone. B. Jones, *Rock & Gem*, Vol. 28, No. 6, June 1998, pp. 13–15.

This article is concerned primarily with turquoise from the Southwestern United States, where it has been revered since ancient times by Native Americans, as evidenced by the large amounts found at diggings at Chaco Canyon (New Mexico) and elsewhere. It is found in gravesites and is known to have been traded with coastal tribes. Today, it has worldwide appeal.

Geologically, turquoise is a secondary mineral that forms in a weathering environment; its occurrence is due to the availability of essential aluminum (from feldspars) and phosphorus (from apatite), and it is commonly associated with weathered copper deposits. The beautiful sky-blue color is modified toward a less desirable green color with the incorporation of iron into the crystal structure. However, when iron occurs as black-to-red infillings of iron oxide, the popular “spiderweb” pattern results.

As gem-grade turquoise supplies have dwindled, the price for the finest material has sharply increased. Also, lower-quality material has been routinely treated to enhance its durability and/or color. One stabilization process, developed by Colbaugh Processing Co. in the 1950s, brings out the natural color of lower-grade turquoise while giving it sufficient hardness and strength to survive lapidary treatment. The turquoise is dried by intense and prolonged heating, infused under pressure with epoxy, sealed in small metal containers, and cooled very slowly; the entire process takes months.

Turquoise was once easily obtained from copper deposits by amateurs, since it had no ore value. Today, however, most turquoise mined in the U.S. is obtained by contractors who have arrangements with the large copper companies operating open pit mines in Arizona. Rarely can an individual collect good rough on his or her own. *MD*

DIAMONDS

Argyle's tale: The making of a mine. M. Hart, *Rapaport Diamond Report*, Vol. 21, No. 30, August 7, 1998, pp. 30, 32.

Although a few alluvial diamonds were found in the

Pilbara district of Western Australia in the 1890s, it was not until October 2, 1979, that the huge AK1 pipe, which would become the Argyle mine, was discovered in the far north region of Western Australia. The AK1 pipe measures 2 km long, ranges from 150 to 500 m in width, and covers 45 hectares (about 111 acres). The mine is owned and operated by Argyle Diamond Mines Pty. Ltd. (owned 57% by Rio Tinto plc of London, 38% by Ashton Mining Ltd., and 5% by WA Diamond Trust). Although the deposit is massive, its diamonds are generally small and of low value (average about \$7 per carat), but these factors are offset by its high grade (6 carats/ton of ore when production started in 1986); it currently produces about 40 million carats annually. Future production will depend on the grade of the ore and the mine's ability to maintain efficient production. Argyle operates an in-house diamond-sorting facility, and nonunion work is farmed out to subcontractors, thus avoiding the characteristic labor pitfalls of many mines. MM

Argyle extends open pit. *Diamond International*, No. 54, July-August 1998, pp. 15-16.

Rio Tinto and Ashton Mining, the owners (together with the Australian government) of the Argyle diamond mine in Western Australia, have approved the expansion of the AK1 open pit mine, and the work has already begun. To access an additional 17.6 million tonnes of open-pit ore at an average grade of 2.58 carats per tonne, pre-stripping of around 100 million tonnes of waste is required. The mining reserve at AK1 is estimated at 64 million tonnes. Underground development of the mine still remains a possibility at a later date. MM

Argyle succeeds selling full annual production: No inventory growth. *Mazal U'Bracha*, Vol. 15, No. 197, November-December 1998, pp. 48-49.

Whereas the world market for more-expensive diamond jewelry has been hampered by the present state of the Asian economies, the demand for cheaper polished goods cut in India has remained steady. Australia's Argyle mine, a major supplier of rough to the Indian cutting centers, sees a continuing trend to "trade down" as consumers search for value. With the greater demand for jewelry with diamonds of lower quality, the Argyle product constitutes a growing market niche. For the first half of 1998, Argyle saw stronger prices and record sales for its rough; there was no growth in inventory. The alliance between Argyle and the Indian diamond industry is pivotal to Argyle's success. Argyle supports all efforts, including signed agreements with its Indian customers, to prevent the use of child labor in diamond manufacturing.

The United States and Japan are the major consumer markets for Argyle-type (i.e., low-quality "Indian goods") diamonds. On a weight basis, such diamonds account for 62% and 68%, respectively, of these countries' sales of stones smaller than 0.17 ct. AAL

The diamond pipeline into the third millennium: A multi-channel system from the mine to the consumer. M. Sevdemish, A. R. Miciak, and A. A. Levinson, *Geoscience Canada*, Vol. 25, No. 2, 1998, pp. 71-84.

Canada is poised to become one of the world's significant producers of gem-quality diamonds. It is anticipated that, by 2002, Canada will produce about 10% (by weight) of the world's rough diamonds. This new resource requires that Canada develop expertise in various economic aspects of the diamond industry, particularly in marketing the rough. This article explores the dynamics of the "diamond pipeline" for distributing and marketing diamonds in the late 1990s.

Historically, the majority of diamond rough proceeded from mine to consumer via a single-channel pipeline controlled by the Central Selling Organisation (CSO), a wholly owned company of De Beers Consolidated Mines, Ltd. The CSO's mission is to maintain equilibrium between supply and demand, which then translates to price stability. Two recent events significantly affected this balance. After the dissolution of the Soviet Union in the early 1990s, the Russians began selling significant quantities of their diamond rough outside the CSO pipeline. Then, in 1996, the Argyle mine in Australia did not renew its contract with De Beers and began marketing all of its production independently.

These departures from the traditional distribution and marketing strategy have led to the current multi-channel diamond pipeline, which consists of three parallel channels for distribution and marketing: the Traditional Gem Channel, the Indian Channel, and the emerging Russian Channel. The Traditional Gem Channel consists of the generally higher-value production that remains in the former single-channel system. The authors estimate that about 50% of the world's retail diamond jewelry sales result from this channel. The Indian Channel is the conduit for small and low-quality diamonds. Production that enters this channel originates both with the CSO and from the open market, including Argyle and Russian stones. About 50% of the diamond jewelry sold at retail worldwide contains stones that have traversed this channel.

The authors also postulate the existence of a discernible Russian Channel. This channel, though, is still evolving through conflicting economic and political interests. Approximately 25% of the world's diamonds are mined in Russia, but at present only a small portion of these stones are routed through the Russian Channel. The impact of these changes on the traditional marketing of rough diamonds provides additional options for Canada's emerging diamond industry. SW

A gem of a mine. *South African Mining, Coal, Gold & Base Minerals*, May 1, 1998, pp. 10, 15, 17.

This relatively short article gives a good general overview of the De Beers Finsch diamond mine in the northern part

of Cape Province, South Africa, from the original prospectors looking for asbestos in 1957 through plans for block caving in 2003.

Finsch Diamonds was established in 1961, and mining began soon after. In 1978, after bench mining in the open pit to a depth of 423 m, underground mining commenced. By 1990, work in the open pit had stopped completely. To date, the plant has treated more than 95 million tons of ore, yielding about 78 million carats of diamonds. The mine had a recovered grade of 58 carats per hundred tons in 1997. Among South African diamond mines, the Finsch pipe—at about 500 m in diameter and 18 hectares (44 acres) in surface area—is second in size only to the Premier pipe.

The kimberlite is mined using a modified blast hole, open stoping method. At the treatment plant, the ore gets scrubbed, crushed, washed, and screened to size the material. A dense media separation is followed by X-ray separation of the diamonds, which are then sent to a sorting facility. The article is illustrated with an informative flow chart of the treatment plant and a graphic model that explains block caving.

Thomas Gelb

India bounces back. *Diamond International*, No. 55, September–November 1998, pp. 57–60, 62.

After two years of decline, Indian exports of cut and polished diamonds for 1997–98 (financial year ending March 31) jumped 6% over the previous year in terms of both value (to \$4.493 billion) and weight (to 20.6 million carats). Thus, India's share of the global trade in polished diamonds is 40% in terms of value and 80% in terms of weight, the highest ever. Much of this is a reflection of reduced sales of better-quality rough by De Beers and thus a decline in more-expensive diamonds on the world market. Import of diamond rough amounted to a staggering 115 million carats—about equal to the total current world rough production. The euphoria is not without its pressures, however. For example, the average price realized for Indian-cut diamonds (i.e., predominantly near-gems) has declined 31% from its 1990–91 peak (the average was \$218 per carat in 1997–98). There is also concern about a steady supply for rough diamonds in the current multi-channel pipeline. Extended credit demands (up to 150–160 days) by overseas buyers, meanwhile, have had detrimental effects on cash flow.

Nevertheless, the Indian diamond industry is optimistic. It feels that new technology, continued government cooperation (e.g., simplified customs and banking procedures), and increased exports of diamond-set jewelry (which already accounts for 15% of the country's gem and jewelry exports) will enable the industry to continue its expansion. Government estimates show a 12% increase in exports per annum through 2002. This is consistent with the prediction by one diamantaire that within 10 years India—in addition to its monopoly in near-gem stones—will process 50%–75% of the goods in the

“medium” range and 10%–20% of gem-quality diamonds. At this level, India would command 60% (by value) of the global trade in polished diamonds.

AAL

India's GJEPC claims negligible level of child labor in Indian diamond industry. *Mazal U'Bracha*, Vol. 15, No. 106, October–November 1998, pp. 67–70.

The illegal use of child labor in underdeveloped countries is a highly sensitive and significant issue; in the past, some components of India's diamond industry have been implicated in this tragedy. India's Gem and Jewellery Export Promotion Council (GJEPC) is concerned about this matter, not only from a humanitarian perspective, but also because of the negative effects of what it considers adverse and exaggerated press reports. Since 1995, GJEPC has been intensifying its anti-child-labor campaign with success.

An independent survey conducted in June 1998 showed that the incidence of child labor (i.e., workers younger than 14 years old) in the Indian diamond industry has declined significantly from 1994–95, when the last survey was conducted. Presently, child labor represents 0.16% of the work force in the “organized sector” (i.e., larger, better-equipped factories, and generally good working conditions), and 1.47% in the “semi-organized sector” (i.e., medium to low technology, and satisfactory to poor working conditions). The wages for these categories are US\$59–\$95 per month and \$35–\$71 per month, respectively. On the basis of statistics from 659,550 workers, the child labor rate for the entire diamond industry in India is 0.89% (compared to 3.18% during 1994–95). GJEPC's goal is to bring this down to zero.

AAL

Nucleation environment of diamonds from Yakutian kimberlites. G. P. Bulanova, W. L. Griffin, and C. G. Ryan, *Mineralogical Magazine*, Vol. 62, No. 3, 1998, pp. 409–419.

A detailed study of mineral inclusions in the genetic center [nucleation point] of single crystals of Yakutian diamonds, which was undertaken to gain insight into the growth environment of diamond crystals, shows that most of the diamonds nucleated on mineral “seeds.” In peridotitic diamonds, the most common central inclusion is Mg-rich olivine; in eclogitic diamonds, pyrrhotite and omphacite (a clinopyroxene) are most abundant. The minerals identified as the central inclusions of Yakutian diamonds indicate that the diamonds grew in a reduced environment, with fO_2 [oxygen fugacity] controlled by the iron-wüstite equilibrium. The data imply that diamond nucleation took place in the presence of a fluid, possibly a volatile-rich silicate melt, that was highly enriched in large-ion lithophile elements (e.g., K, Ba, Rb, and Sr) and high field-strength elements (e.g., Nb, Ti, and Zr). This fluid also carried immiscible Fe-Ni-sulfide melts, and possibly a carbonatitic component.

RAH

An oscillating visible light optical center in some natural green to yellow diamonds. I. M. Reinitz, E. Fritsch, and J. E. Shigley, *Diamonds and Related Materials*, Vol. 7, 1998, pp. 313–316.

Most natural- and treated-color green diamonds are colored by exposure to ionizing radiation, which manifests itself as an absorption peak at 741 nm (associated with the GR1 center). Of the [approximately 3,000] colored diamonds seen by GIA researchers in the last decade, 10 green-to-yellow stones—which would be expected to produce a GR1-related absorption spectrum—instead showed many peaks in their UV-visible absorption spectrum when chilled to liquid nitrogen temperatures. The authors list 38 peaks between 543 and 761 nm, which can be divided into two series: one centered around 620 nm with 202 cm^{-1} spacing between the peaks, and the other centered around 700 nm with 169 cm^{-1} spacing.

All 10 stones showed weak nitrogen-related features in the mid-infrared, including those related to single substitutional nitrogen, as well as features related to hydrogen impurities in the diamonds. The authors believe that the unique structure of the UV-visible absorption pattern is related to a molecule or molecular ion impurity, with more than one energetically accessible state at liquid nitrogen temperature. However, the absorption peaks do not match those for any known simple molecule (or ion) containing carbon, nitrogen, and/or hydrogen. This low-temperature absorption spectrum has only been seen in natural-color diamonds. *MLJ*

Trace element composition and cathodoluminescence properties of southern African kimberlitic zircons. E. A. Belousova, W. L. Griffin, and N. J. Pearson, *Mineralogical Magazine*, Vol. 62, No. 3, 1998, pp. 355–366.

Zircon (ZrSiO_4) commonly occurs in felsic granitoid crustal rocks, and more rarely in mafic rocks such as kimberlite pipes (which are of mantle origin). Individual zircon crystals are geologically long-lived in alluvial environments. This study assesses whether or not kimberlitic zircons exhibit unique characteristics that can aid prospectors in the search for diamondiferous pipes. Fifty-one zircons (0.5–6 mm) were taken from 12 southern African pipes. The authors used cathodoluminescence (CL) to observe the crystal structure and laser ablation inductively coupled plasma-source mass spectrometry (ICPMS) to examine the chemistry of the zircons. With CL, the kimberlitic zircons appeared dominantly blue, in contrast to crustal zircons, which (in the authors' experience) are yellow. The authors suggest that higher concentrations of trace elements in crustal zircons lead to more crystal lattice defects, which cause the dominance of yellow CL hues. This hypothesis is supported by the ICPMS data, which showed a concentration difference between yellow and blue CL zircons of up to two or three orders of magnitude for some trace elements. When the zircons are

plotted on trace-element discrimination diagrams, the kimberlite and crustal zircons each plot in their own distinct groups. The authors conclude that the distinctive CL and geochemical characteristics of the kimberlite zircons allow their use as prospecting tools. *JL*

GEM LOCALITIES

Application of graphite as a geothermometer in hydrothermally altered metamorphic rocks of the Merelani-Lelatema area, Mozambique Belt, north-eastern Tanzania. E. P. Malisa, *Journal of African Earth Sciences*, Vol. 26, No. 2, 1998, pp. 313–316.

In the Merelani-Lelatema tanzanian and green garnet mining area in Tanzania, the graphite-bearing host rocks underwent regional high-temperature metamorphism, followed by hydrothermal alteration. Since the formation of graphite in metamorphic rocks is mainly a function of temperature, this study sought to use graphite to determine the highest temperatures reached during the regional metamorphic event.

X-ray diffraction analyses of the graphite were applied to a preexisting temperature calibration curve. Regionally, the metamorphic temperatures for the graphite ranged from 523°C to 880°C. Graphite samples specifically from tanzanite-bearing hydrothermal deposits yielded a temperature range of 690°C–715°C. This range is higher than that estimated from fluid inclusions in the tanzanite (390°C–444°C), and supports previous observations that the tanzanite did not coexist with the graphite during the high-temperature regional metamorphism. Rather, the tanzanite was introduced later by hydrothermal solutions through fault zones. *JL*

Gemstone bonanza at Yogo Gulch. S. Voynick, *Wild West*, Vol. 11, No. 1, June 1998, pp. 36–41, 81.

This article describes the historical events and fascinating people involved in sapphire mining at Yogo Gulch, Montana. It travels in time from Jake Hoover's discovery of the translucent blue stones at Yogo Creek in 1895, through the mine's numerous British and American owners, to the current owner, Roncor Inc. Dr. George F. Kunz, of Tiffany & Co., originally confirmed the identity of the blue pebbles from Jake Hoover's sluice box as "sapphires of unusual quality." Jake Hoover stayed involved, eventually taking on partners, until 1897, when he sold his quarter share to his partners for \$5,000 so he could join the Alaskan gold rush. Two months later, British interests purchased his share for \$100,000.

Production at Yogo started in 1896 and continued almost without interruption until July 1923, when a flash flood destroyed the mine infrastructure. From 1898 through 1923, the Yogo dike yielded 16 million carats of rough sapphire, resulting in 675,000 carats of fine blue cut sapphire worth \$25 million. Charles T. Gadsden, appointed mine supervisor in 1902, resided at Yogo from 1903

until his death in 1954, even though the mine (locally known as the English mine) had been inactive for more than 30 years.

In 1956, Yogo returned to American ownership. Since then there has been only minor, intermittent production, by a variety of American owners and lessees, none of which has had significant success. While mining has never progressed deeper than 250 feet (about 77 m), it is believed that the dike exceeds a mile (1.6 km) in depth and contains reserves estimated at 40 million carats of gem-quality rough sapphire. [Editor's note: For further details, see K. A. Mychaluk, "The Yogo sapphire deposit," Spring 1995 *Gems & Gemology*, pp. 28–41.]

Kim Thorup

Geological evolution of selected granitic pegmatites in Myanmar (Burma): Constraints from regional setting, lithology, and fluid-inclusion studies. K. Zaw, *International Geology Review*, Vol. 40, No. 7, 1998, pp. 647–662.

Pegmatite veins and dikes 2–5 m wide and 30–150 m long commonly occur along a 1,500-km-long, north-to-south trending belt of tungsten- and tin-bearing granitoids in Myanmar (Burma). Five pegmatites (Sakangyi, Gu Taung, Payangazu, Taunggwa, and Sinnakhwa) are described in detail. Gem minerals found in these pegmatites include tourmaline, beryl (aquamarine), and topaz. The pegmatites show distinct internal mineralogic zoning, with felsic minerals (e.g., feldspar and muscovite) more abundant in the core, and quartz and schorl tourmaline more abundant in the outer zones. As determined by fluid-inclusion microthermometry, the pegmatites formed at 230°C–410°C. The Na/K ratio of fluid inclusions indicates the presence of substantial potassium in the pegmatite-forming fluids; no evidence was observed for phase separation of these fluids.

Troy Blodgett

Geological setting and petrogenesis of symmetrically zoned, miarolitic granitic pegmatites at Stak Nala, Nanga Parbat-Haramosh Massif, Northern Pakistan. B. M. Laurs, J. D. Dilles, Y. Wairach, A. B. Kausar, and L. W. Snee. *Canadian Mineralogist*, Vol. 36, Part 1, 1998, pp. 1–47.

In the early 1980s, bi- and tri-colored tourmalines up to 10 cm in length were discovered in "pockets" (miarolitic cavities) in granitic pegmatites in the Stak Valley of northern Pakistan. Of the nine pegmatites in this area, only one has been mined economically, from which tens of thousands of crystals have been recovered; at present, production has dwindled. Because the well-crystallized tourmalines have cracks and inclusions, they have greater value as specimens than as cut gemstones. The schorl-elbaite crystals are typically color zoned, from black at the base to green, locally pink, and colorless or (rarely) pale blue at the termination.

The pegmatites are flat lying, 1–3 m thick, and 30–120 m long; they are zoned both texturally and chemically.

The crystallization sequence produced a narrow outer zone, followed by a coarser wall zone, and finally a coarse core zone characterized by an enrichment in minerals containing H₂O, F, B, and Li (e.g., tourmaline, lepidolite, and topaz), along with a decrease in other elements such as Fe. The valuable tourmaline occurs in the miarolitic cavities with albite, quartz, K-feldspar, muscovite/lepidolite, topaz, and other minerals. The origin of the cavities, which are concentrated along the crest of a broad antiform in the pegmatites, is explained by an increase in vapor pressure during the final stages of magma crystallization. Late rupturing of the cavities permitted the removal of residual fluids that otherwise would have caused etching or alteration of the pocket minerals. The pegmatites are believed to have formed about 5 million years ago, on the basis of age dating (⁴⁰Ar/³⁹Ar geochronology) of the lepidolite. These are among the youngest gem-bearing pegmatites in the world; they were exposed by rapid uplift due to the collision of the Indian and Asian plates.

AAL

The geology, mineralogy, and history of the Himalaya mine, Mesa Grande, San Diego County, California.

J. Fisher, E. E. Foord, and G. A. Bricker, *Rocks & Minerals*, Vol. 73, No. 3, May-June 1998, pp. 156–180.

The Himalaya mine, located on Gem Hill in the Mesa Grande pegmatite district of Southern California, has been North America's largest producer of gem and specimen-grade tourmaline since its discovery 100 years ago. During the first period of mining, pink and red tourmaline was very popular with the Dowager Empress of Imperial China, and large amounts of tourmaline were shipped to China for carving. The boom ended in 1911, when the Chinese aristocracy was overthrown during the Boxer Rebellion. Production of tourmaline from the mine is estimated at over 100 tons, which is remarkable since the dike averages less than one meter thick! In addition to tourmaline, the mine has produced many fine crystals of other pegmatite minerals and gemstones, including morganite and goshenite beryl, apatite, quartz, and microcline; numerous specimens are found in museums and private collections. Mining has been sporadic, driven by the price of tourmaline. The periods of greatest activity have been 1898–1912, 1952–1963, and 1977 to the present.

There have been more than 20 mineralogical and geological studies of the Himalaya dike system. There are two main dikes in the mine, referred to as the upper and lower dikes. Both contain gem-bearing pockets, but most of the work has been done on the upper dike because it produces the valuable pink tourmaline, while the lower dike produces green tourmaline. Recent work has produced an extensive honeycomb of tunnels inside Gem Hill, and it remains to be seen if the mine will continue to produce in the years to come.

Jim Means

Madagascar rubies debut. G. Roskin, *Jewelers' Circular-Keystone*, Vol. 169, No. 8, August 1998, pp. 40, 42.

Strongly saturated, slightly purplish red rubies that have yielded cut stones up to 3 ct have been found recently in Madagascar. Characteristic inclusions are rounded transparent crystals, "treacle" type graining, and nests of short, flat, acicular 60° needles. The rubies contain uneven, strong, parallel growth lines and fingerprint-like veils, similar to those seen in both Burmese and Thai material. The color is somewhat dark in tone, and the ruby fluoresces moderate red to long-wave UV radiation. A dealer in Pittsburgh, Pennsylvania, is distributing the faceted material in the U.S. MM

A recent find of kunzite at the historic Katerina mine, Pala District, San Diego County, California. J. Fisher, *Mineral News*, Vol. 15, No. 1, January 1999, pp. 1, 6-7.

This article reports on the reopening of the Katerina mine in Southern California, historically one of the larger producers of kunzite in the region. Lilac-colored material from this mine was first identified as spodumene by George F. Kunz early in the 20th century; subsequently, this gem material was named kunzite in his honor. Following a short history of the mine, details are given on the development work being done by the current owners, O. Komarek and B. Weege. A condensed geological overview is also presented. Although the specimens found in late 1998 are of modest quality, the mine has produced significant amounts of attractive gem material in the past. MG

Update on ruby output in Kenya. *Jewellery News Asia*, No. 170, October 1998, p. 63.

About 50%–60% of the rough ruby produced at the mine near Kasigau in southern Kenya is of marketable quality. The mine, which has been producing commercially since 1995, is located in Tsavo National Park, 500 km from Nairobi, Kenya. The top two grades of ruby rough account for 4%–5% of the overall output. Ruby reserves are expected to last 20 years. The rough material, which must be heat treated to improve clarity and color, is sold through auctions and then fashioned into beads, cabochons, and faceted stones. Prices of polished stones range from \$15/ct for low-quality to \$5,000/ct for top-quality material. Other colored gems found in the area include kornerupine, red spinel, rhodolite and tsavorite garnet, sapphire, tanzanite, and tourmaline. MM

INSTRUMENTS AND TECHNIQUES

The application of ground-penetrating radar to mineral specimen mining. B. K. Lees, *Mineralogical Record*, Vol. 29, No. 4, 1998, pp. 145–153.

Ground-penetrating radar (GPR) is a shallow-depth geophysical exploration method based on detecting the electrical properties of rocks as they are produced by radar

waves. Through interpretation of the GPR data, structures in the rock are inferred. This method is commonly applied to environmental waste and archaeological problems. After explaining the technique, Mr. Lees describes his use of GPR to locate rhodochrosite-bearing cavities at the Sweet Home mine in Colorado.

Both the depth of penetration of radar waves into the rock and the resolution of the resulting data are a function of the wave frequency. A 100 MHz antenna, with a signal that penetrated about 25 feet (7–8 m) into the rock, yielded a reliable resolution down to about 1 to 2 feet. The technique allowed the miners to visualize structural characteristics that influence the location of cavities, as well as the cavities themselves, but the data could not be used to tell if the cavities actually contained rhodochrosite crystals. Twelve cavities were discovered, one of with a signal that produced \$40,000 worth of specimen and gem material. The total cost of the GPR survey was \$13,000. The author suggests that GPR will become more viable in the future for near-surface mineral specimen exploration as better software is developed and the cost of the system decreases. JL

JEWELRY MANUFACTURING AND GEM CUTTING

Automatic bruting. J. Lawrence, *Diamond International*, No. 52, March-April 1998, pp. 67–69.

Semi-automatic bruting is a technical and economic success in the diamond industry. It is superior to traditional hand bruting for several reasons: (1) yield is typically 3% greater, resulting in 5% added value; (2) there are essentially no broken stones, whereas 1%–2% broken stones is considered normal for traditional methods; and (3) it produces better roundness and proportions. In addition, salaries are lower with semi-automatic bruting, because the operators are typically younger and less experienced. (This is offset, though, by the fact that experienced bruters are more productive on a volume basis.) The limitations of automated bruting are two-fold: (1) cements used to bond the stone to the stone holder have limited strength; and (2) perfect roundness cannot be achieved, as the software programs currently available do not center the stone perfectly in the machines. Nevertheless, the author implies that within a decade economic considerations will justify the expense of developing a fully automated bruting machine. AAL

The case for CAD/CAM. J. Thornton, *American Jewelry Manufacturer*, Vol. 43, No. 1, January 1998, pp. 62–65.

Computer-aided design (CAD) and computer-aided manufacturing (CAM) have evolved from engineering applications to the creation of elegant jewelry designs, sculptured forms, and engravings. Cameos, medallions, rings, earrings, and pendants are being created by scanning, digitizing, and adding colors and relief. The computer programs

enable manufacturers to merge images quickly to create jewelry to customers' precise specifications. Pendants are copied in minutes, and the copy can be reduced and mirrored to make matching earrings. From creation to completion, manufacturers maintain control over their products, since outside engravers are no longer needed.

The positive experiences of two manufacturing jewelry companies using CAD/CAM are described, and examples of some unexpected benefits of the new methods are given. For example, gold and silver are used in smaller quantities, because thinner pieces with flatter relief can be produced. The engraving software has also greatly reduced the risk of the die cracking, and individual pieces can be produced with one press stroke instead of several. According to die maker Jed Fournier of Bliss Tooling, Rhode Island, "this may only save us 15 to 30 seconds on each piece but, on a thousand pieces, it adds up."

MD

Cutters on quartz. S. E. Thompson, *Lapidary Journal*, Vol. 52, No. 4, July 1998, pp. 21–27.

Quartz is one of the most common minerals in the world, and it is also the gem material that is most available to lapidaries. The author interviewed five lapidaries, who share the intricacies of cutting crystalline and cryptocrystalline quartz, the tools they use, and the dangers (to the stone) that can be experienced during cutting and polishing. One of the lapidaries is photographer Harold Van Pelt, who provided photographs of his many splendid *objets d'art* and of some of the tools and machinery he used to create them.

MG

Electroformed objects for jewelry: Secondary ion mass spectrometry characterization of Au films from CN-free electrolytes. M. Fabrizio, C. Piccirillo, and S. Daolio, *Rapid Communication in Mass Spectrometry*, Vol. 12, No. 13, 1998, pp. 857–863.

Electroforming of gold jewelry yields pieces that have a high volume/weight ratio, and can attain fine detailing equal to the more commonly used method of investment casting. However, electroforming is more expensive because of equipment costs and expenses associated with handling the chemical solutions involved in the process. In this study, relatively inexpensive cyanide-free chemical baths normally used in the electronics industry were tested for jewelry use. Different cathodes—on which the gold film is deposited—were also tested. The researchers examined the gold films using secondary ion mass spectrometry (SIMS) in order to identify the different chemical species and complexes involved with electrodeposition in each chemical bath. Hardening agents such as nanoscopic diamond and rutile were detected, as was the brightening agent arsenic oxide. Of the chemical solutions tested, the ethylenediamine tetra acetic acid (EDTA) bath proved the best for jewelry forming because of the rate of gold deposition, the concentration range, and the service life of the solution.

JL

Faceting angles. G. L. Wykoff, *Rock & Gem*, Vol. 28, No. 3, March 1998, pp. 52–56, 58.

The most important thing to know when faceting a gemstone is not necessarily how to grind and polish, but which angles produce the brightest, most brilliant gem. The author explains some of the recent developments in factoring these angles and the unique cutting styles that have resulted. The most pertinent point is that angles are but a guide to making a brilliant stone and faceters should experiment on their own; such experiments have resulted in very innovative, and now even somewhat mainstream, styles. Although this article is a little technical in places, for the most part it is highly enjoyable and thought provoking.

MG

JEWELRY RETAILING

How to sell to today's bride and groom. D. O' Donoghue, *National Jeweler*, Vol. 42, No. 13, July 1, 1998, pp. 34, 38.

Approximately 2.4 million couples marry each year in the U.S., and these couples spend nearly \$3.3 billion on jewelry. Today's couples are older and more sophisticated, and they are willing to pay more to get exactly what they want in engagement and wedding rings. Statistics show that nine out of 10 brides wear earrings on their wedding day, 65% give jewelry as thank-you gifts to members of the wedding party, and 44% of brides and grooms choose jewelry as a wedding present to each other. The author, who is beauty director of *Bride's* magazine, lists tips on selling engagement rings and wedding-related jewelry gifts.

Some of the new trends dictated by this generation of buyers include a rising demand for platinum in wedding and engagement rings, the growing popularity of freshwater and South Sea pearls, and a resurgence of antique-inspired filigree rings. Diamonds remain the most desirable gems for wedding rings. Retailers are encouraged to build a lasting relationship with their bridal customers, from determining the best purchase within their budget to rendering services after the purchase is made. Retailers should also keep apprised of the latest trends in the marketplace, and offer flexible payments and unconditional guarantees to make the buying process less intimidating.

MD

Selling treated gemstones. R. Weldon, *Professional Jeweler*, Vol. 1, No. 5, June 1998 et seq.

This ongoing series of informative articles helps retail jewelers and their sales associates explain gemstone treatments or enhancements to customers "in an honest and positive manner." The first article, "Emerald Education," appeared in the June 1998 issue (pp. 171–172). Other treated gem materials discussed to date include: heated ruby (July 1998, pp. 123–124), heated sapphire (August 1998, pp. 133–134), dyed or irradiated cultured pearls

(September 1998, pp. 125–126), heated aquamarine (October 1998, pp. 145–146), heated amethyst and citrine (November 1998, pp. 101–102), laser-drilled diamonds (January 1999, pp. 107–108), and fissure-filled rubies (February 1999, pp. 161–162). These articles not only provide valuable information on the various types of treatments used to enhance a gem's appearance, but they also give methods for detecting such treatments. In addition, Mr. Weldon includes tips on caring for treated or enhanced gems and legal considerations. *MM*

When a cert can hurt. G. Roskin, *Jewelers' Circular-Keystone*, Vol. 169, No. 10, October 1998, pp. 98–101.

"Comments" on a diamond grading report, which are often innocuous, may sound ominous to a customer if they are not properly communicated, which could lead to the loss of a sale. Examples are given of comments found on a GIA certificate that may be perceived to have negative connotations but are actually of minor significance (e.g., "crown angles greater than 35°" and "surface graining not shown"). Comments that are cited as being most damaging to a diamond sale include references to proportion details and minor blemishes. The problem is compounded when several comments are listed on the same report. The comments on proportion details can sometimes be eliminated if the diamond is recut. However, this is time consuming and expensive, and it involves elements of risk such as excessive weight loss and chipping. Fluorescence reported as moderate or strong also can hurt a sale.

The article advises jewelers to communicate their knowledge of the report process to their clients, so that they clearly understand the reason for the comments. It is particularly important to explain whether the particular characteristic mentioned in the report affects the diamond's beauty or durability. *JEC*

PRECIOUS METALS

Consumption of silver in 1997 exceeds supply. *Jewellery News Asia*, No. 168, August 1998, p. 36.

The Silver Institute's *World Silver Survey 1998* reported that demand for silver exceeded supply (from mine production and the recycling of scrap) by 198 million ounces in 1997. Consumption reached a record total of 863.4 million ounces, a growth of 6.1% over 1996. The demand for silver in jewelry and silverware fabrication rose 5.3% to 280.2 million ounces, following a growth of 15.6% in 1996. Italy's silver consumption rose 10.5% to 44.8 million ounces, and India's rose 3.2% to 95.2 million ounces (with 66.6% of the total Indian demand used in jewelry, silverware, and gift items). There was also surging industrial demand for silver in the United States. This is the ninth consecutive year in which conventional supply failed to keep up with silver demand. *MM*

A slippery standard for gold prices. K. Clark, *U.S. News & World Report*, Vol. 125, No. 19, November 16, 1998, pp. 84–85.

Gold prices are down 25% from 1996, to about the level of 1979. However, this decrease is not generally reflected in the retail prices of finished jewelry—at least not in the United States, where, for example, raw gold constitutes about 25% of the price of a typical store-bought necklace. This article suggests three ways of obtaining the most value when purchasing gold jewelry at retail: (1) Buy plain classic pieces of jewelry, where price comparisons can be made; (2) comparison shop the malls (negotiate prices), wholesale clubs, on-line sites, and television shopping shows; and (3) buy used pieces. Rather than being purchased as an investment, gold jewelry should be bought to be worn and enjoyed. *AMB*

SYNTHETICS AND SIMULANTS

Laboratory-created gems grow acceptance at retail. C. Fenelle, *National Jeweler*, Vol. 42, No. 14, July 16, 1998, pp. 74, 76, 78, 80, 82.

Laboratory-created (also called *synthetic*, *man-made*, *created*, or *laboratory-grown*) gemstones have gradually and steadily gained acceptance in the trade. The most popular created stones, according to some jewelers, are synthetic alexandrite, emerald, and ruby, which can be sold for a fraction of the cost of natural stones. The market has seen an increase in the number of synthetic stone suppliers, of manufacturers designing jewelry with synthetic gems, and of synthetic gems being displayed in retailers' "fine jewelry" cases. Consumers are showing an increased awareness and acceptance of synthetic gems, since these materials allow greater accessibility to normally extravagant jewelry items.

While the created-gemstone industry has experienced stable pricing in the last couple of years, there is concern about the increasing number of gem growers and the variable quality of synthetic gems being released on the market. Another concern among retail jewelers is that synthetic gemstones are becoming exceedingly difficult to distinguish from their natural counterparts. Because synthetics have been fraudulently sold as natural stones, retailers are exercising caution when choosing their suppliers. Retailers and suppliers alike are confident that laboratory-created stones will continue to rise in popularity with growing consumer acceptance. *MD*

TREATMENTS

Discrimination of a treated jadeite (class B)—judged from the colloidal fillings. W. Su, F. Lu, X. Gu, Y. Wu, J. Zhang, J. Cai, and P. Zhuang, *Journal of Chengdu University of Technology*, Vol. 25, No. 2, 1998, pp. 349–353 [in Chinese with English abstract].

The identification of "B jade" (i.e., jade that has been bleached and then polymer impregnated) is an important

matter in the jade trade, and this article describes efforts to do this with microscopic observation. The first step is to identify which, if any, of three types of materials are filling the interstitial areas in the jadeite: (1) natural minerals formed by geologic processes during or after the formation of the jadeite, (2) very fine grit and/or wax emplaced during the cutting and waxing processes, and (3) colloidal (polymer) filling materials that are introduced during the "B jade" treatment process. Once such materials have been located in the sample, their hardness is determined with a needle probe under magnification. If it is suspected that the filling material is a polymer, this can be confirmed by infrared spectroscopy. *Taijin Lu*

Fracture healing/filling of Möng Hsu ruby. R. W. Hughes and O. Galibert, *Australian Gemmologist*, Vol. 20, No. 2, 1998, pp. 70–74.

Rubies from the Mong Hsu deposit in Shan State, north-east of Taunggyi, Myanmar, present two problems as gem materials. The first is their dense "silk" clouds and the strong purplish color caused by their unusual blue cores. Ordinary heat treatment can be used to eliminate both phenomena; the market generally accepts such heat-treated stones. The second problem lies in the fact that Mong Hsu rubies are typically heavily fractured. These fractures are commonly "healed" by heat treatment of the stones with borax and other chemicals, which causes the surface of the stone to melt and to be redeposited in the fractures; undigested material cools as pockets of a flux glass. This treatment, which is permanent and irreversible, improves a stone's durability. In the past, such fracture healing/filling was neither reported nor detected. Now that it is a known practice, however, the trade must decide how to deal with it [see, e.g., the following abstract], especially because many dealers (particularly

those in the Japanese market) reject such filled goods. Without such treatment, many of the Mong Hsu rubies would have little gem value. *RAH*

Thais launch ruby disclosure system. M. Elmore, *Colored Stone*, Vol. 11, No. 6, November-December 1998, pp. 1, 30–33.

After four years of discussions between the Thai Gem and Jewelry Traders Association (TGJTA) and the Japan Jewellery Association over the glass filling of rubies, a new classification (for stones ≥ 1 ct) has been adopted to give Thai dealers a common language for disclosing ruby treatments. The TGJTA's classification has three categories for treated stones:

- A. *Natural Ruby*: The ruby has been enhanced by heat, but at 10 \times magnification no residue from the heating process is visible on or within the stone.
- B. *Heat Enhanced Natural Ruby*: The ruby has been enhanced by heat, and at 10 \times magnification some residue from the heating process is visible within the stone.
- C. *Heat Treated Natural Ruby with Foreign Substances Present*: The ruby has been enhanced by heat, and at 10 \times magnification some residue from the heating process is visible on the surface of the stone and within the stone.

Unheated Natural Ruby is a classification used for rubies that have not been enhanced in any way.

While Thai dealers consider the classification system adequate, some are skeptical that the disclosure program will be successful, as it is voluntary. The TGJTA has no enforcement mechanism, and some think a change in industry practice will come only when consumers begin to require disclosure. *MD*

1998 Manuscript Reviewers

Gems & Gemology requires that all articles undergo the peer-review process, in which each manuscript is reviewed by at least three experts in the field. This process is vital to the accuracy and readability of the published article, but it is also time-consuming for the reviewer. Because members of our Editorial Review Board cannot have expertise in every area, we sometimes call on others in our community to share their intellect and insight. In addition to the members of our Review Board, we extend a heartfelt thanks to the following individuals who reviewed manuscripts for *G&G* in 1998:

Mr. David Atlas
Dr. Grahame Brown
Mr. Derek Cropp
Mr. Israel Eliezri
Mr. Al Gilbertson
Mr. Mike Gray
Dr. Edward J. Gübelin
Mr. Hertz Hasenfeld

Dr. Donald B. Hoover
Mr. Mark Johnson
Mr. George Kaplan
Mr. Sheldon Kwiat
Mr. Shane F. McClure
Ms. Elise Misiorowski
Ms. Danusia Niklewicz
Mr. Glen Nord

Mr. Dale Perelman
Dr. Ilene Reinitz
Mr. Jeremy Richdale
Mr. Russell Shor
Dr. Sergey Smirnov
Mr. Basil Watermeyer
Dr. Christopher Welbourn
Mr. Lazar Wolfe